Research And Development In Engineering Technology

(Volume-1)

Edited By:

Dr. Rakesh Kumar Yadav

Dr. S.S. Pawar

Dr. Amit Kumar Mishra

Dr. Rakesh Kumar Bhujade

2021 EDITION

AGPH **Books**

Research And Development In Engineering Technology

Dr. Rakesh Kumar Yadav
Assistant Professor, Department of Computer Science & Engineering, IFTM University, Uttar Pradesh, India.

Dr. Shyam Sundar Pawar
Associate professor, Department of Mechanical Engineering
Sarvepalli Radhakrishnan University Bhopal (M.P.)

Dr. Amit Kumar Mishra
Senior Faculty, Department of Information and Technology, iNurture Education Solutions Private Limited, Bengaluru, Karnataka

Dr. Rakesh Kumar Bhujade
HOD Department of Information Technology, Government Polytechnic, Daman

AG PH Books

2021

First Edition: 2021

ISBN: 978-81-953278-9-8

Published by:

Academic Guru Publishing House,

B-6, Shopping Complex, Ground Floor, Hoshangabad Rd, behind Indian Oil Petrol Pump, Vidya Nagar, Bhopal, Madhya Pradesh 462026

Website: https://www.agphbooks.com

About the Author

Dr. Rakesh Kumar Yadav pursed Bachelor of Technology from Uttar Pradesh Technical University, UP, and Master of Technology from Singhaniya University, Rajasthan and Ph.D. from IFTM University, UP. He has worked in many reputed institutes. He is currently working as an Assistant Professor in Department of Computer Science & Engineering, IFTM University, UP. He has published more than 25+ research papers in reputed international journals and conferences. He has been reviewed many research papers of journals and conferences. He has published many Patents. He has guided various M.Tech and PhD students. He has written many books and examination series also. He has also taken many guest lectures. His main research work focuses on Machine Learning, Biometric, Image Processing, Computer Vision, Soft Computing and Artificial Intelligence. He has 14+ years of teaching experience in higher education.

Dr. Shyam Sundar Pawar is currently designated as an Associate professor at Sarvepalli Radhakrishnan University Bhopal (M.P.). With an ambition of enhancing the technical world, he completed his BE from Govt. Engineering college, Ujjain (M.P.) Affiliated from Vikram University, Ujjain (M.P.) and M.Tech from MANIT, Bhopal followed by Ph.D. at RGPV, Bhopal (M.P.). Embedded with his academic skills, Dr. Pawar has reviewed numerous papers and has also made various published researches of his own in several national and international journals. He is also recognized for his amazing teaching skills. He has also supervised various Ph.D. Scholars during his academic Career. There are hundreds of students who were guided by him and completed their M.Tech successfully. He has been guest lecturer at various important events.

Dr. Amit Kumar Mishra earned his PhD from Banasthali Vidyapeeth in Tonk, Rajasthan, and was awarded best paper in COVID-19 by MPCOST Bhopal (Govt Of MP). iNurture Education Solutions Private Limited, Bengaluru, Karnataka, currently employs me as a Senior Faculty, IT Academics. He has attended several international conferences and international workshops worldwide. Several book chapters were published by Taylor & Francis, CRC Press, and John Wiley & Sons, Inc. He has published more than 25 research papers in reputed journals indexed by Scopus and the Web of Science and more than 60 papers at international conferences. Several students have done M.Tech under his guidance. Invited lectures were given at national and international events. He has published one international and three national papers in the fields of machine learning and IOT.

Dr. Rakesh Kumar Bhujade completed Ph.D. in Artificial Intelligence in 2016, cracked UPSC and currently working as Head of the Information Technology Department in Government Polytechnic, Daman. He has published 01 Philippines Patent, 02 Australian Government Patents (Grants), 05 Indian Patents, 03 Books, 02 AWS Global Certifications, 01 Research Grant and more than 30 papers in Scopus Indexed International Journal/Conferences. He also acted as Advisory/Reviewer Board member in many International Journals and Conferences. Dr. Rakesh is expertise in Neural Network, Soft Computing, Artificial Intelligence and Machine Learning.

Preface

We are delighted to publish our book entitled " Research and Development in Engineering Technology ". This book is the compilation of esteemed articles of acknowledged experts in the fields of technological advancements.

This book is published in the hopes of introducing the modern technology and their recent advancements to our readers. Technology has grown to become an essential part of our daily life but new modern features remain unknown until a long time. This book provides our readers with a better understanding of the advancements that are made in the field of technology.

The articles in the book have been contributed by eminent scientists, academicians and research scholars. Our special thanks and appreciation go to experts and research workers whose contributions have enriched this book. We thank our publisher AGPH BOOKS (Academic Guru Publishing House), India for taking pains in bringing out the book.

Finally, we will always remain a debtor to all our well-wishers for their blessings, without which this book would not have come into existence.

- Editorial Team

Research and Development in Engineering Technology

(ISBN: 978-81-953278-9-8)

CONTENT

Academic Guru Publication House

Research and Development In Engineering Technology
Volume 1
Year: 2021

AG PH Books

FAULT CHARACTERISTICS AND PROTECTION OF DISTRIBUTED SOLAR GENERATION

Badal Bisen[1*]

[1]*Junior Engineer, Electric Loco shed/Ajni Central Railway, Nagpur*

Abstract

Low current defect, insignificant negative, and zero series currents are the characteristics of inverter-based distributed energy sources (DERs). Knowledge of the fault characteristics of DER is required for the investigation and protection of relays. For the most part, no studies have been done to examine how faults affect the DER model. This article focuses on Dominion Energy's flaws. Of illustrate that the real reaction to DER mistakes may be different than previously thought, stopper defects are studied. It was necessary to model any possible MATLAB-related impact on this study using an advanced simulation environment. There must be a way for the simulation results to be compared to other published results. There is still a lot of work that has to be done to completely test the ideas created using real-world networks so that this thesis may be thoroughly analysed.

Keywords: Inverter-based distributed energy sources, Relay, Dominion Energy, fault properties, null series currents.

1. INTRODUCTION

Traditional feeders are radial systems of which the user is the key fault point. Mainstream mistake detection schemes are used. When the measured value crosses the default value momentarily or time lag,

* ISBN No. 978-81-953278-9-8

an over-current device operates in schemes that overflow. The duration between major and backup defensive systems is matched in order to allow the first to safely clear a malfunction before the least disruption. They are another cause of loss, as energy distributions Resources (DER), as they are put on delivery circuits. The DER fault current partially compensates for the tool's current charge, which tends to slow relay operations. Therefore, a detailed definition of the characteristics of DER fault is necessary with the impact of DER on the current fault analysis and safety relay environment. [1]

1.1. Distributed Generation Background

As a whole, the phrase "distributed or distributed generation" refers to any technique for generating electric power that is applied to distribution networks. Conventional central power generating systems, in which power is generated and transferred to clients through transmission and distribution lines, provide a direct comparison to the DG concept. Although central power networks remain crucial to the worldwide energy supply, their flexibility has been reduced in order to meet the needs of the ever-changing global power market. Large capital-intensive power plants and the T&D system for energy distribution form the core of central power.[2]

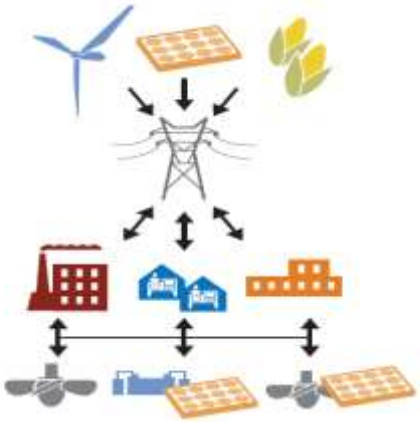

Figure 1: A Distributed Electricity System

In addition, few experiments were carried out to examine the behavior of DER faults during real fault events despite the abundance of work on DER modeling. In this study, Dominion Energy will examine recorded fault events. Dominion Energy obtained fault case reports at points of interconnection (POI). There are seven fault events analyzed at three solar DER locations. Temporary and irreversible fault answers can be captured. The study would rely on steady states in which relays are conducted. [3]

1.2. Research Objective

The following are the objectives of this thesis:

- To study the Inverter-based distributed energy sources (DERs) by using MATLAB Simulink Software.

- Implementation of Circuit breaker with counter set recloser over current relay by replacing overcurrent relay
- Comparison of no relay model, over current relay and Circuit breaker with counter set recloser over current relay.
- Triggering pulses, PVA voltages and Sequence currents are analyzed in this study.

2. LITERATURE REVIEW

Analysis of distributed solar production faults, the safety gaps in old solutions and current techniques for failure detection and classification are discussed in this chapter. The merits and disadvantages of the various existing approaches are also discussed and contrasted.

(Kuna et al., 2020) [4] Dominion Energy has been blamed for a number of incidents in the past. Low current loss is a property of the power supply used by inverters, DERs, and the Zero negative and 0-series. The understanding of DER fault attributes is essential in the case of fault analysis and secure relay implementation. The vast majority of the DER modelling effort was focused on DER performance.

(Alsafasfeh *et al.*, 2019) [5] Useful capability maximisation concerns are addressed by developing the core node-system and power-system analysis principles of the IEEE for photovoltaic energy sources with voltage fluctuation limits. The MATLAB R2017B simulator is used for performance review and evaluation of the job done. The 33-node IEEE system is used to simulate the integration spectrum of PV electric power, and the total integration potential of PV power is assessed at each node, providing a logical decision-making system for preparing the integration of distributed PV energy into a constrained power grid.

(Adnan, Yusoff and Hashim, 2018) [6] The transmission of electrical power generated from renewable sources and located close to customers or loads is known as "Distributed Generation." In addition to increasing voltage and energy efficiency, distributed generating installations may also reduce stress slumps and congestion while also supplying more competitive renewable energy resources electricity. High levels of distributed generation in the existing national grid system may have a number of negative repercussions, including failure rates and the effectiveness of power protection systems, for example.

(Bangash, Farrag and Osman, 2017) [7] Explores the effect on the security of distribution networks of the growing degree of Distributed Generation (DG). Studies have started to minimize the impact on the device failure stage of small-scale embedded generation (SSEG). The penetration level of Residential DG is modular on the Low Voltage (LV) network common in the UK, taking into account the stability of the faults. The loading and discharge, according to the regular charging period, are determined by the penetration level of DG energy storage in the shape of a battery bench.

(sudhakar, Malaji and Sarvesh, 2014) [8] Addresses a simple understanding of how these power flows can impact the power system efficiency and reliability of a photovoltaic (PV) injection power system-dependent distributed generation. The harmonic currents injected into the energy grid can be of significant concern since they may result in undesirable deformity, power reversal, and voltage control.

(Camacho *et al.*, 2007b) [9] Gives a survey of the various advanced automotive control methods used in the last 25 years in the control of solar plant outlet temperature using dispersed collectors. The key characteristics of each technique are explained in a classification of the modeling and control methods mentioned in the first part of this survey. The techniques covered differ from traditional advanced control to those that have little industrial implementations.

3. METHODOLOGY

3-phase transmission line: one of the core elements of an electrical power grid is the power transmission line. It primarily transmits electrical energy from energy sources to charging centers, normally separated by long distances, with limited losses. Three-phase electricity is the standard way to produce, transfer, and deliver electricity in alternating current. For power transmission, it's the most popular method used by electric grids globally and a kind of polyphase system. It is also used for driving big and other heavy engines. A three-wire, three-phase circuit is normally more economical to transfer a specified quantity of energy than an analogous two-wire single-phase circuit at the same line of the ground voltage. [10]

DER is steadily adding to the energy efficiency and reliability of the economy today. DER may also play a vital role, as a result of concentrations of consumer influence, in preventing dysfunctions in dynamic markets for electricity. The newly formed independent grid operators are starting to engage in demand control projects to better handle summer's peak loads. The DER Interconnection Mechanism consists of every device that forms a physical connection between the DER and the EPS, typically the local electrical distribution network (hardware and software). Since the interconnection mechanism is an electrical connection between the DER device and the EPS, it governs energy movement in one or both directions and is capable of providing separate and foundational functions to benefit EPS as well as DER operations.

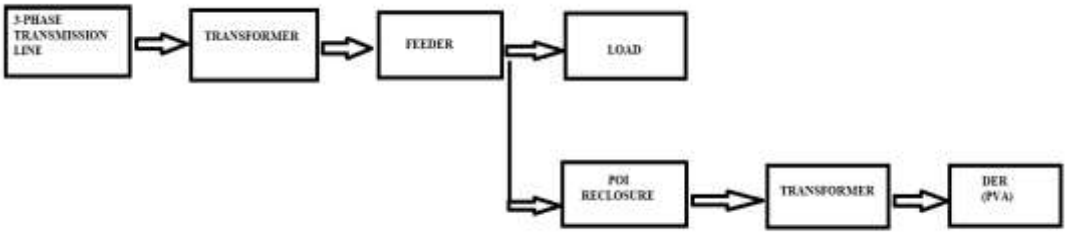

Figure 2: Different components used in proposed methodology

4. SIMULATION RESULTS AND DISCUSSION

Algorithm development is carried out in MATLAB (R2016). It is possible to utilise the signal processing toolbox in MATLAB Library functions for various techniques, including windows, rotation and scaling.

4.1. Simulation Parameter

Sim Power System Toolbox is also used to construct the project for this test. The table below displays different parameters used in this analysis, and their values will also appear in the table. Several parameters include the voltage supplied, energy, transformer step-up, frequency, temperature, capacitor, resistance, etc. For this study, Simulation is done using MATLAB.

Table 1 Different simulation parameters

Name of parameter	Unit and Value
Supply Voltage	132KV
Power	2500KVA
Step-up down Transformer	132KV/34.5KV
Power rating of step-up transformer	47MVA
Frequency	50Hz
Phase to phase voltage	34.5KV
Active Power	100KW
Reactive Power	50KVAR
Circuit Breaker Resistance	0.01 Ohm
Solar irradiation	1000 W/m^2
Temperature	35 Degree
Duty Cycle	0.5
Capacitor	1000 Micro Farad
Resistance	0.005 Ohm
Inductor	5Mh

4.2. Simulation result and discussion

The studied faults are located on feeder and outside of a solar farm. Data on faults are obtained by the POI recorder, which calculates DER inverters' fault current contribution. Figure shown below depicts the components of a coordinated control system, which include sensors, equipment controllers, data input devices, and systems. Sites that had power outages weren't running at full capacity.

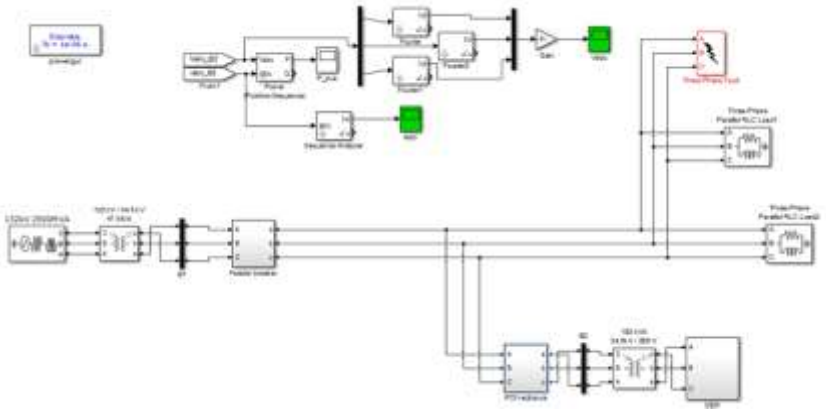

Figure 3: Simulation model without relay

Devices that protect low-voltage circuits or single home appliances up to huge switchgear that regulates high-voltage circuits feeding a whole area are all forms of breakers. Circuit breakers and fuses are sometimes referred to as OCPDs because of their ability to automatically disconnect power from an improper device.

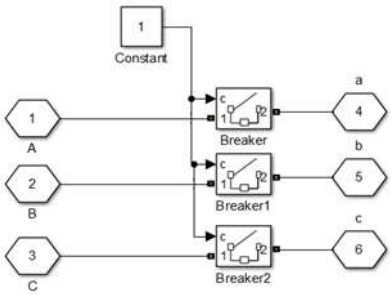

Figure 4: Circuit breaker with no relay protection system

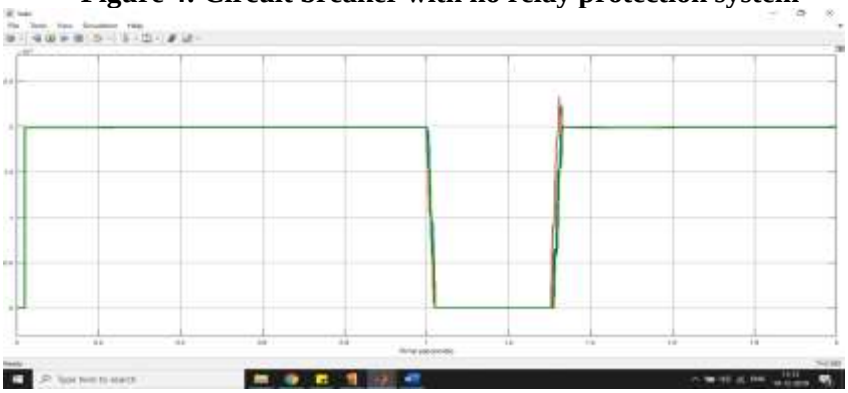

Figure 5: PVA voltages with no relay protection with fault from 1 to 1.3sec

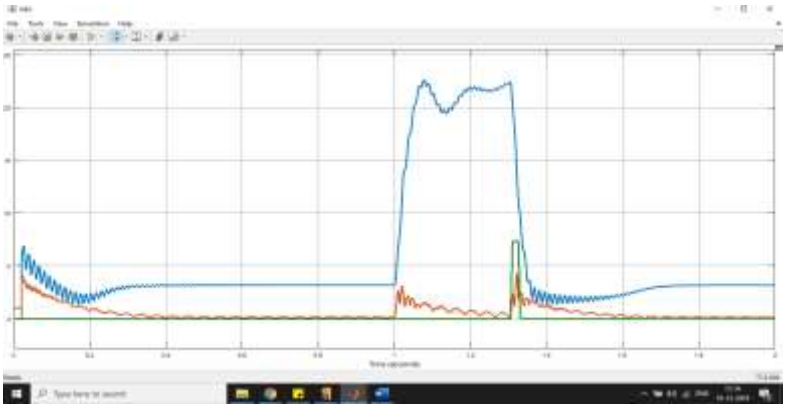

Figure 6: Sequence currents with no relay protection with fault from 1 to 1.3sec

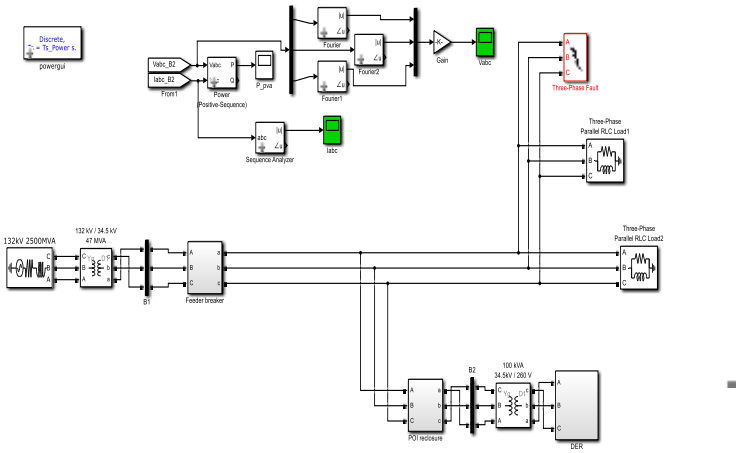

Figure 7: Simulation model with over current relay

The over-current relay is an important relay for the security of feeders, transformers, bus couplers, etc. It may be used for the security of main or backup relays. In the research into the effects of network parameters and configurations on the performance of these relays, the modeling of overcurrent relays and other safety relays is relevant. The present relay using the MatLab/Simulink program is explored in this study shows in the image. The simulation model over the current relay shown above shows the simulation model.

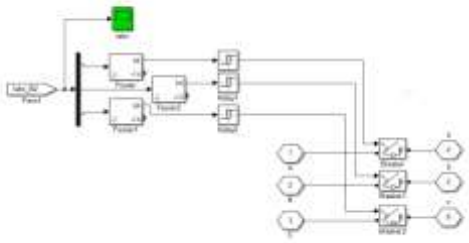

Figure 8: Circuit breaker with over current relay

Circuit breaking is a mechanical system composed of two functions that are open, defective or pathological, and closed connections with regular or stable circumstances in compliance with normal and abnormal conditions. The Circuit Breaker works automatically via the relays and sends a travel signal to the circuit breaker when the relay coil is activated. And the operative unit such as the engine, generator, transformer, and light electronic equipment or devices with circuit breaker contacts is open and secure.

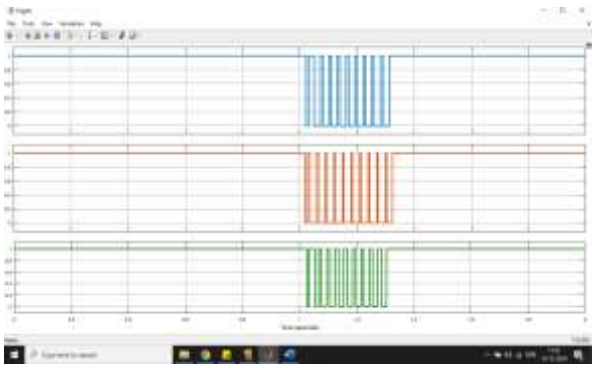

Figure 9: Triggering pulses of over current relay

The number of triggers is very high as the fault is persistent the relay cannot eliminate the fault permanently.

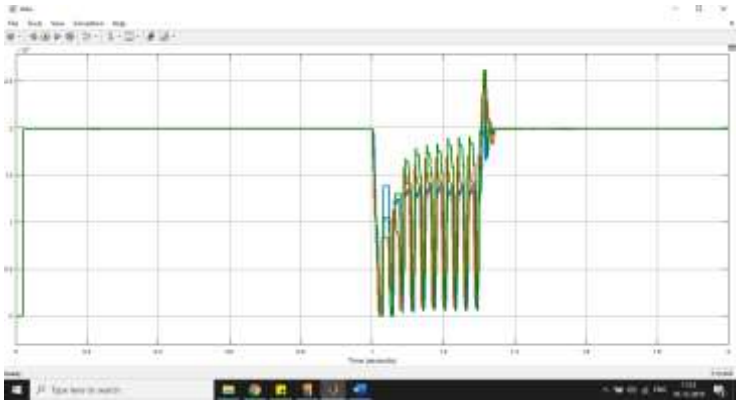

Figure 10: PVA voltages with over current relay protection with fault from 1 to 1.3sec

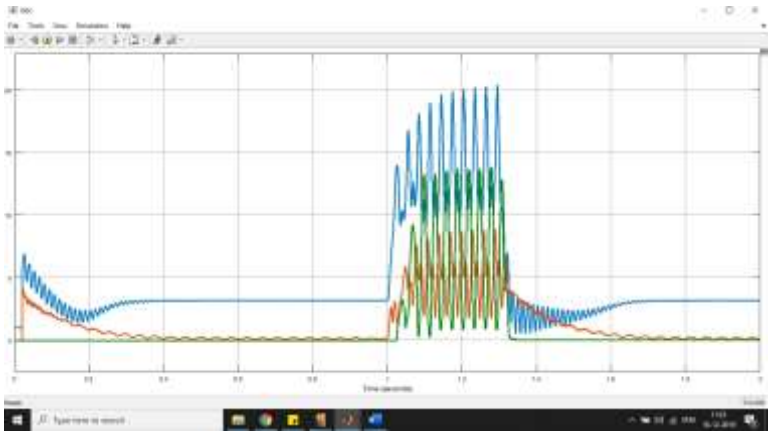

Figure 11: Sequence currents with over current relay protection with fault from 1 to 1.3sec

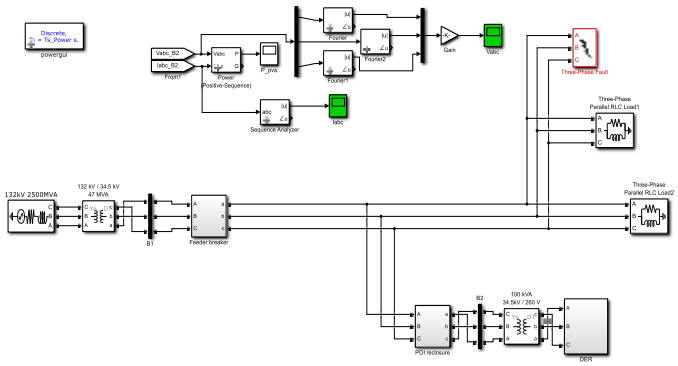

Figure 12: Proposed simulation model of counter set reclosure over current relay

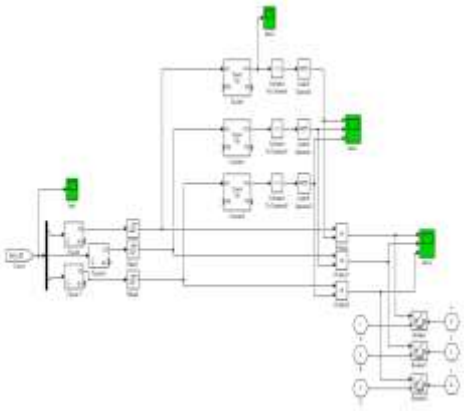

Figure 13: Circuit breaker with counter set reclosure over current relay

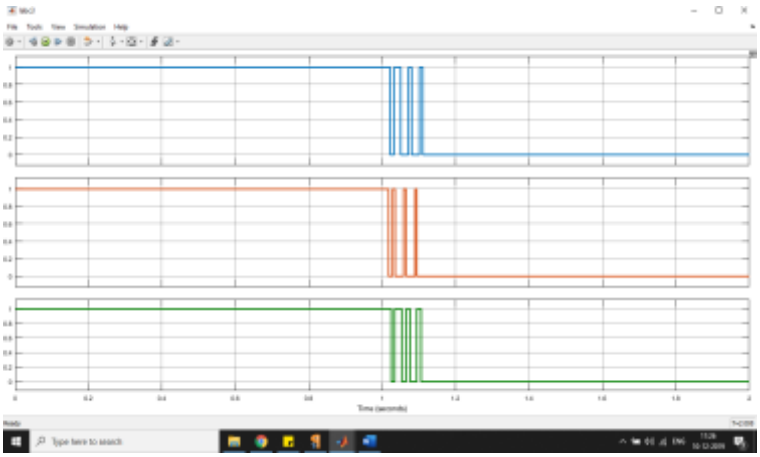

Figure 14: Triggering pulses of over current relay

Three times is the maximum number of times the relay may be set to trigger OFF and remove the defect from DER.

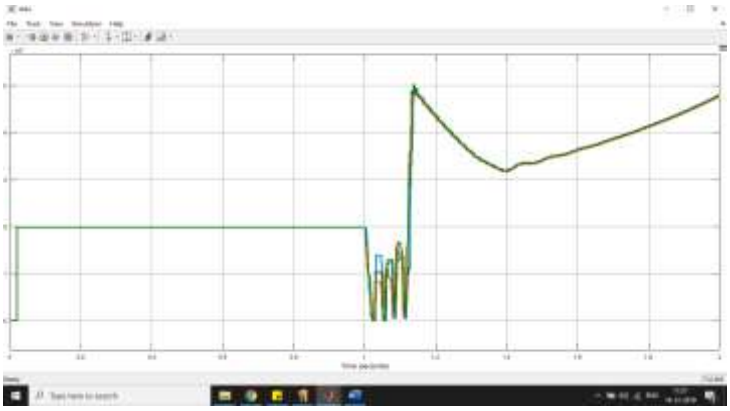

Figure 15: PVA voltages with over current relay protection with fault from 1 to 1.3sec

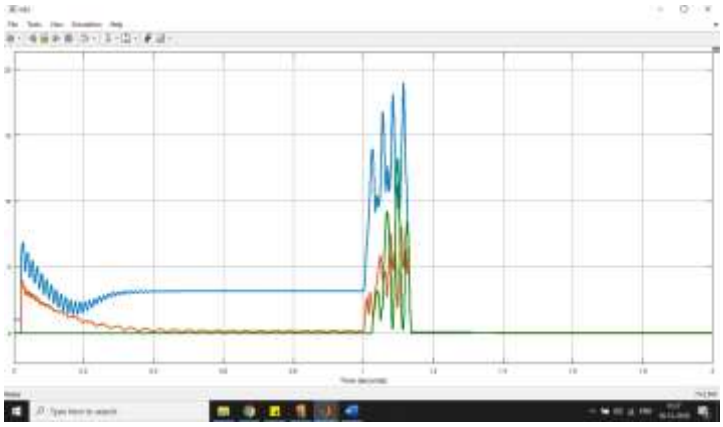

Figure 16: Sequence currents with over current relay protection with fault from 1 to 1.3sec

In figure, the number of constraints is seen with the counter set reclosure over the current relay to three cycles, which activates the circuit breaker OFF entirely while the loss persists beyond three recloser times.

5. CONCLUSION

Distributed generation in the coming decades, especially close to the low-voltage consumer side, is expected to play a greater role in power generation. Power users are increasingly interested in building their own generation capacity in order to benefit from versatile DG technology to generate electricity in desirable times, increase energy efficiency and quality, or provide heating/cooling. The variety of DG technologies, as well as their diversity in scale, efficiency, and appropriate applications suggests that in

many different manufacturing, commercial and residential environments, DG may provide energy supply solutions. This will improve the reliability of the power supply that DG contributes.

References

[1] G. Kou, L. Chen, P. Vansant, F. Velez-Cedeno, and Y. Liu, "Fault Characteristics of Distributed Solar Generation," *IEEE Trans. Power Deliv.*, vol. 35, no. 2, pp. 1062–1064, 2020, doi: 10.1109/TPWRD.2019.2907462.

[2] Z. Cheng, Z. Li, J. Liang, J. Si, L. Dong, and J. Gao, "Distributed coordination control strategy for multiple residential solar PV systems in distribution networks," *Int. J. Electr. Power Energy Syst.*, vol. 117, no. September 2019, p. 105660, 2020, doi: 10.1016/j.ijepes.2019.105660.

[3] M. H. Athari, Z. Wang, and S. H. Eylas, "Time-series analysis of photovoltaic distributed generation impacts on a local distributed network," *2017 IEEE Manchester PowerTech, Powertech 2017*, 2017, doi: 10.1109/PTC.2017.7980908.

[4] S. Kuna, K. Nandini, N. V. N. Reddy, and K. H. Reddy, "Simulation and Analysis of Fault Characteristics of Distributed Solar Generation," *Int. J. Innov. Technol. Explor. Eng.*, vol. 9, no. 8, pp. 305–310, 2020, doi: 10.35940/ijitee.h6350.069820.

[5] Q. Alsafasfeh, O. A. Saraereh, I. Khan, and S. Kim, "Solar PV grid power flow analysis," *Sustain.*, vol. 11, no. 6, pp. 1–25, 2019, doi: 10.3390/su11061744.

[6] A. Z. Adnan, M. E. Yusoff, and H. Hashim, "Analysis on the impact of renewable energy to power system fault level," *Indones. J. Electr. Eng. Comput. Sci.*, vol. 11, no. 2, pp. 652–657, 2018, doi: 10.11591/ijeecs.v11.i2.pp652-657.

[7] K. N. Bangash, M. E. A. Farrag, and A. H. Osman, "Impact of energy storage systems on the management of fault current at LV network with high penetration of distributed generation," *Int. J. Smart Grid Clean Energy*, vol. 6, no. 3, pp. 195–206, 2017, doi: 10.12720/sgce.6.3.195-206.

[8] P. sudhakar, D. S. Malaji, and D. . Sarvesh, "Protection issues of Power Systems with PV Systems Based Distributed Generation," *IOSR J. Electr. Electron. Eng.*, vol. 9, no. 3, pp. 18–27, 2014, doi: 10.9790/1676-09351827.

[9] E. F. Camacho, F. R. Rubio, M. Berenguel, and L. Valenzuela, "A survey on control schemes for distributed solar collector fields. Part II: Advanced control approaches," *Sol. Energy*, vol. 81, no. 10, pp. 1252–1272, 2007, doi: 10.1016/j.solener.2007.01.001.

[10] R. Cleber da Silva and S. Kurokawa, "Model of Three-Phase Transmission Line with the Theory of Modal Decomposition Implied," *Energy Power Eng.*, vol. 05, no. 04, pp. 1139–1146, 2013, doi: 10.4236/epe.2013.54b217.

Academic Guru Publication House

Research and Development
In Engineering Technology
Volume 1
Year: 2021

AG PH Books

SENTIMENT ANALYSIS OF USER YOUTUBE COMMENTS USING CLASSIFIER ALGORITHM

Shivani Wadhwani[1*]

[1]*M.Tech in Computer Science Engineering, Technocrats Institute of Technology, Bhopal (M.P.)*

Abstract

"Sentiment Analysis" is the process of extracting other people's (speaker or writer) opinions from a given original source (text) utilizing natural language processing (NLP), linguistics computing, & data mining. In sentiment analysis, sentiment classification of various parameters such as comments, reviews and products has become a significant application. For the interpretation of meaning of each and every comment, "text mining approach" is used. For understanding the meaningfulness of any content, it is important to classify them into positive and negative comments on the basis of user opinion.

In the present study, researcher has performed sentiment analysis on YouTube comments on the most popular topics nowadays by using Classifier techniques.

Keywords: Machine Learning, Support Vector Machine, Data mining, Sentiment analysis.

1. INTRODUCTION

Opinion mining is the other name used for sentiment analysis. "Sentiment analysis" is the procedure used to determine the emotional tone behind the series of words. It is also used to understand the opinions, emotions, attitude expressed on the online platform. In social media monitoring, sentiment

* ISBN No. 978-81-953278-9-8

analysis is mainly used to obtain the overview of wider public opinion regarding particular topic. Sentiment analysis can be used in broad and powerful way. All around the world, organizations are using the ability to extract insights from the social data. The correlation of shift in stock market is shown by the shifts in sentiment on social media. Sentiment analysis can rapidly understand the consumer attitude as well as it can react accordingly but it does not mean that it is a perfect science at all. Human languages are considered to be the complex language. It is important to make a machine learn the various grammatical nuances, slangs, misspellings which occur online are not an easy way. It is also not easy to make the machine learn the way context can affect the tone. For example, a sentence is considered here: "My flight's been delayed. Brilliant!‖". Some people will think that the person might be sarcastic. As we know people do not have good experience on having a delayed flight. So, on this particular sentence by applying the contextual understanding as negative, the sentiments can be analyzed. Machine can easily analyze the word brilliant‖ and it can be observed as positive. This is comparable to how a linguist specialist would educate a machine how to perform basic sentiment classification. The dictionary that robots use to understand emotions will grow as language changes. Language is evolving faster with the usage of social media. 140 character constraints, the urge to be brief and other dominant memes have affected the ways people interact with each other online. Many challenges are coming up with the course. Human beings apply criteria to all words and expressions that indicate positive or negative sentiments, taking into account how circumstance may impact the tone of the information. The software can tell that the first statement below is positive as well as the second is negative thanks to well defined rules.

After studying the above example, the limitations of the sentiment analysis are also observed as it is not exactly used as the 100percent accurate marker. A human eye is always needed to watch it as it is prone to human errors. The extraction of the attitude or mood represented in a block of unstructured data in connection to the subject of the document being studied is called "sentiment extraction (SE)". There are various steps taken for the extraction as follows: Adjectives and adverbs are used which determines the polarity of the sentence at the very first level. Some of the positive words which can be used as rating are: good‖, ‖awesome‖, ‖excellent‖ and soon. On the other hand, some of the negative words are: ―bad‖, ―poor‖, ―abomination‖ and so on.

1. Humans have contextual polarity of the rating word at the very next level, which takes into consideration local modifiers that come before or after the rating word.
2. Such rating words are tied to some entity, usually the topic of some conversation, at the greatest degree. For instance, in the line "The gouda was awful," the entity is "gouda," as well as a negative feeling is conveyed against it.

1.1. Why Sentiment Analysis?

The utilization of "natural language processing", identification through computational linguistics, text analysis and extraction of subjective information is defined as sentiment analysis. The other name used for Sentiment analysis is opinion mining. The main application of sentiment analysis is in reviews & social media sites. It is used from marketing to customer service. The attitude of the speaker or the writer can be easily determined through sentiment analysis for some particular topics or complete contextual

polarity of the document. Attitude can be defined as the affective state, emotional state, evaluation of his or her judgement or emotional communication. Social networking sites, blogs on World Wide Web are creating huge amount of data every day.

Essential information & data regarding business profits and other important factors of scientific and commercial industries is contained in sentiment analysis. “Sentiment analysis” is needed because it is not possible to extract the information or keep manual tracking on them. Sentiments or opinion of the users on a particular product, subject or area are expressed which is known as Sentiment Analysis. Computational linguistics, natural language processings and also the text analytics are using sentiment analysis for identification of subjective data from the base or primary data. The sentiments are divided into categories such as: positive or negative. So, the general attitude is determined of the speaker or writer according to the topic.

1.2. Objectives of Research

- Acquisitions of raw youtube data and converts into standard datasets.
- To analyze the content from youtube.
- Prediction of content from youtube.
- Content Classification and build the opinions of particular events.
- Develop Sentiment Analysis Tool

2. LITERATURE REVIEW

For different aspects of “youtube video features”, several researches have been performed [1]. Decision is made on the basis of one of the important comment among several comments on any specific video [2]. The video objects are annotated by these comments [3, 4]. The behaviour of the user is also analyzed through the comments and it can be used to find the troll users [5]. The sentiments can be analyzed for the comments and the positivity & negativity of the sentiments can also be analyzed [6]. The videos are categorized into different categories on the basis of comments on particular videos [7].

Sentiment Analysis is a methodology for analysing information in the form of text and determining the substance of thoughts from the content. Emotion mining or feeling mining are the other name given to Sentiment Analysis. YouTube, Facebook and Twitter are some of the social media platforms which are also known as “On-line communication channels” and nowadays these channels are creating so much interest in human life. [8] On these social media channels, people share their thoughts, feeling etc. We share similar on opinion mining or feeling evaluation, which is an area of web machine learning and Data Mining, in this research report.

It is important for airline operators to get feedback from their customers particularly for operational planning and strategic planning. To get such type of feedbacks, social media sites are becoming trending. On the other hand, social media sites are not trivial task for the analysis, categorization and generation of useful data. The capabilities of “Naïve Bayes classifier” are investigated in the present study for the

sentiment analysis of "airline image branding". The impact of data size is also examined in the present study on the accuracy of the classifier. For some online conversations, the data is collected according to the incident for airline's security operations which are managed by the passengers in a case study. A loss of $1 billion was observed about the incident for the company's corporate value. From Twitter, the data was collected and it was processed & analyzed through "Naïve Bayes Classifier". [9]

"Multi-label text classification" method is used for sentiment analysis of Hinglish comments on YouTube using Deep learning. Different parameters were used with "Multi-layer perceptron (MLP)" to investigate several sentiments in the comments. MLP has been modelled and estimated by making variations in optimizers, neurons, activation functions and several other engineering techniques. Some of the other engineering methods are: customized embedding, pre-trained embedding, tf-idf and count vectorizer. [10] Two different datasets were used for performing these experiments such as: "Nisha Madhulika's dataset" and "Kabita's Kitchen dataset". From the results, it was observed that 98.53percent of accuracy was observed in Kabita's Kitchen and 98.48percent accuracy was observed for Nisha Madhulika in MLP. During the present study, careful tests were performed for the evaluation of the experiment.

3. METHODOLOGY

3.1. Machine learning techniques

Machine learning (ML) is a data analytics technique which acquires knowledge from the previous practice and provides information directly to the systems without being programmed explicitly. Definition says "a computer program is said to learn from experience E with respect to some task T and some performance measure P, if its performance on T, as measured by P, improves with experience E". ML has become a key technique for solving problem and for making better decisions and predictions. Mainly we used machine learning techniques every day to make significant decisions in stock trading, medical diagnosis, weather forecasting, and many more. Although the term Machine Learning (ML) was developed by author [26], its advancement and expansion has never been more instrumental than it is today. The prospect of using machine learning for decision making in numerous fields has a important function in the upliftment of the people. Though specialized techniques of machine learning such as NN and SVM are already established, a great deal of effort is being put by the researchers to cater the rising needs of citizens.

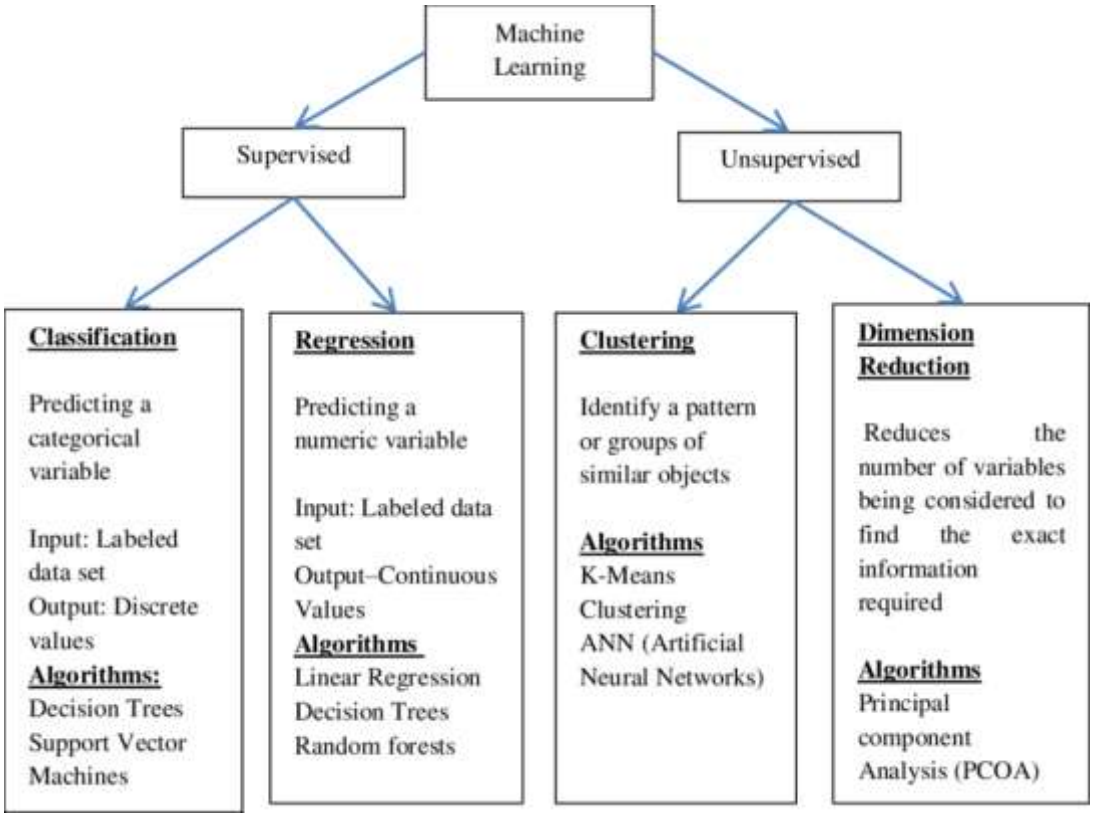

Figure 1: Different machine learning algorithms

Unsupervised learning concepts don't have any target or outcome variable in the training datasets to draw inferences. Since the samples given to the learner are unlabeled, there is no evaluation of the accuracy of the output by the relevant algorithm. It is commonly used for clustering problems.. Some of the examples that come under this category are Apriori Algorithm and K-Means. Reinforcement learning algorithms uses previous practice to acquire the best knowledge and convert it in taking appropriate decisions in business. In this example, the machine has been introduced to a training environment that uses trial and error to determine which action would offer the highest reward. "Markov Decision Process" is the example of reinforcement learning. However, there are number of techniques present for machine learning and they can be categorized on the basis of applicability to the problems belonging to different domains.

Machine learning techniques such as: classification, clustering and regression can be used to address the categories of problems. On the basis of supervised learning, regression and classification can be categorized on the other hand; clustering is defined as the unsupervised learning. Forecasting outcome is considered as regression if it is continuous. Boolean type is used to represent the forecasting output. In the same groups, clustering is defined as the arrangement alike attributes.

The authors [27] explained basically data analytics, which is also called analysis of data, may be categorized into the following four types, also shown in Figure 3.3, considering complexity and value addition.

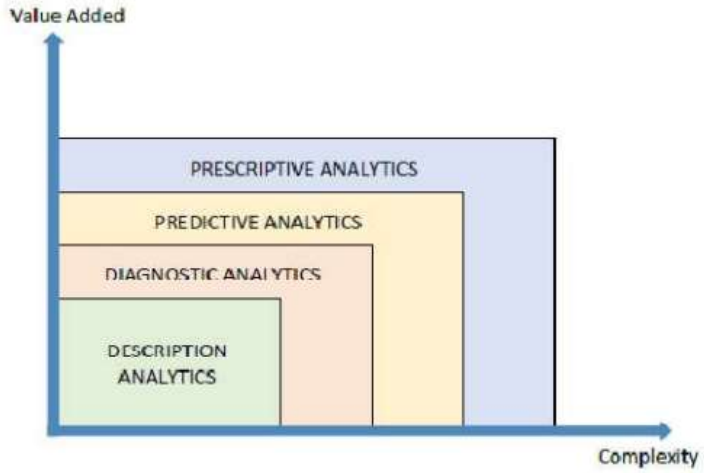

Figure 2: Types of data analytics

Descriptive analytics juggles raw historical data to draw conclusion about past and the output is represented by using only right or wrong without stating the reason. It basically handles quarries of type "what happened".

Diagnostic analytics tries to locate interdependencies and classify the patterns. It handles the question of type "why something happened", historical data are measured against other data.

Predictive analytics applies the conclusion drawn from above two categories for identifying about the trends and behaviour of data and predicts the future.

Prescriptive analytics is based on the concept of optimization that helps to understand the uncertainties to make better decisions and achieve the best outcomes.

4. RESULT AND DISCUSSION

Architecture is getting comments from youtube API and directly importing to CSV _le .Data cleaning and stop words are extracted from comments so that each word of sentiment calculated and printed their sentiment scores on the graph.

Library Used

Library (devtools)
Library (vosonSML)
Library (magrittr)
Library (tuber)
Library (dplyr)

Library (ggplot2)
Library ("tm")
Library ("SnowballC")
Library ("wordcloud")
Library ("RColorBrewer")
Library (tidytext)
Library (tidyverse)
Library (httr)
Library (SocialMediaLab)
Library (syuzhet)
Library (psych)
Total video comments extracted: 6846

- Getting Youtube comments from youtube Api with the help of api key.
- Deriving the sentiment of each comment: Sentiment was calculated for each comment using the sentiment score of the terms in the comment. A comment's sentiment is equivalent to the total of the sentiment scores for each of the terms in the comment. The _le nrc . containing a list of pre-computed sentiment scores was used to determine term score in each tweet.
- Deriving the sentiment of new terms: The sentiment for the terms that do not appear in the file nrc was computed based on the overall tweet sentiment deduced in step 2.
- Computing term frequency: Frequency of each term was calculated as of occurrences of the term in all comments]/[of occurrences of allterms in all comments].

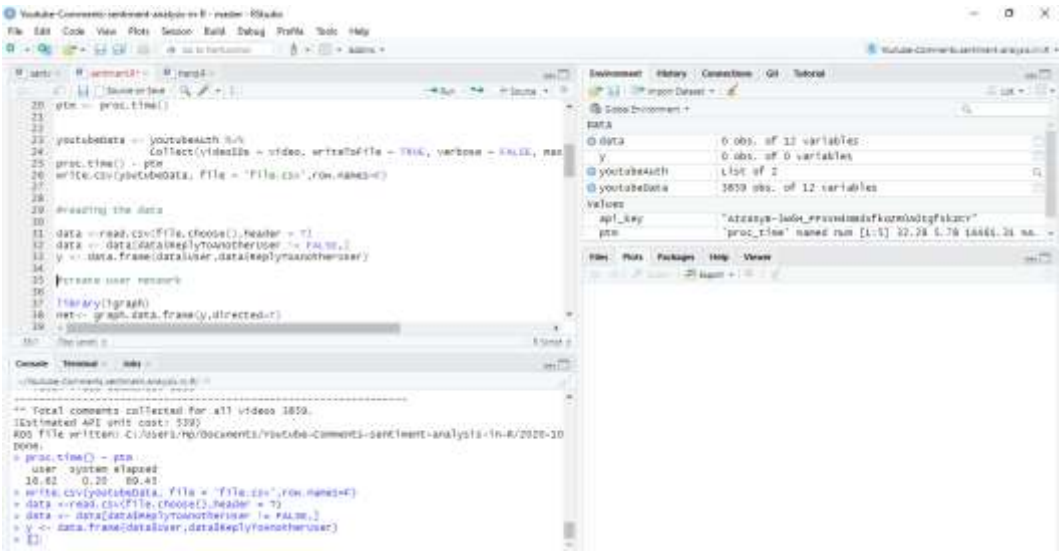

Figure 3: Architecture of R language

	Comment
686	Krugersagt:don't get infected and don't infect others People...
797	7:58 Americans: "tHe GoVeRnMeNt ArE tRyInG tO cOntRol U...
730	I am form the future and let me say this is a fast pandemic a...
765	Me and my classmates had to watch this video for an assign...
792	OKAY NOW MAKE A CURE:)
445	Think we have a fast pandemic
820	Dude this is sad
056	If it were a bio weapon it's not a very good one, considering...

Figure 4: Extracted comments from Youtube into CSV formate.

 # Google developer API key

```
api_key <-"********************"
youtubeAuth <- Authenticate("youtube", apiKey = api_key)
#Video ID
video <- (c("BtN-goy9VOY"))
```

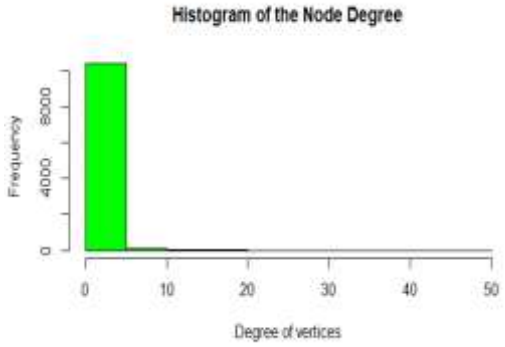

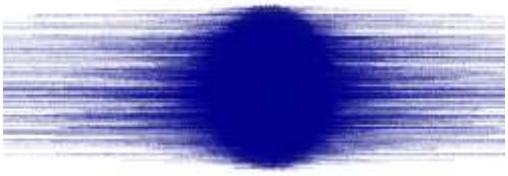

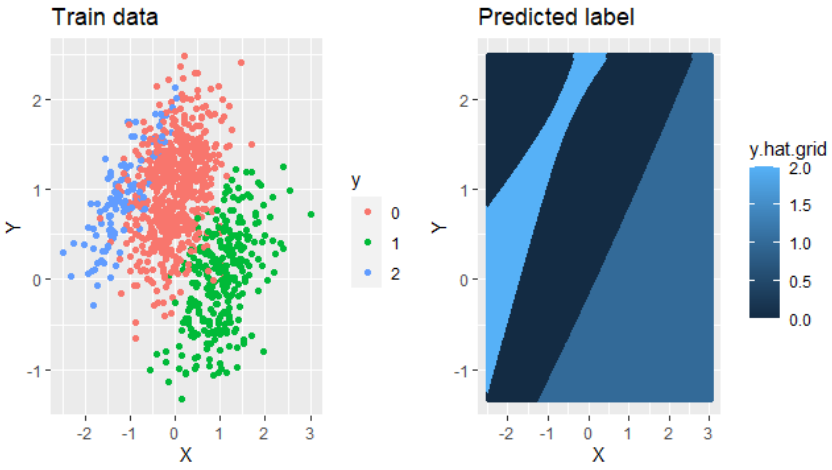

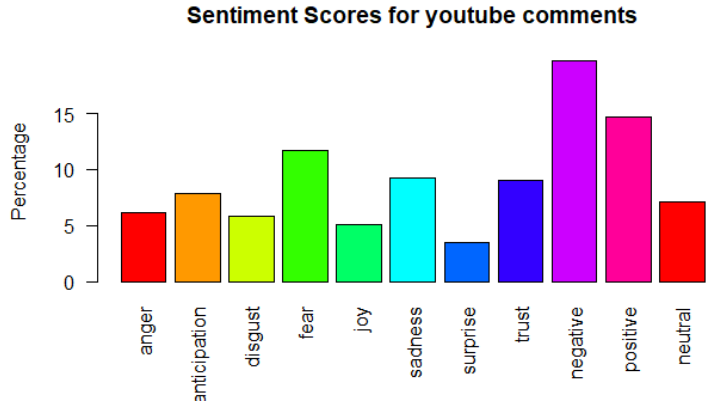

4.1. Network Analysis

Network analysis is becoming a widely used tool for scholars specially to deal with the complexities of interrelation between actors as well as all sorts. Instead of seeing actors as isolated entities, Network analysis provides a placement of significant on the relationship among the actors. For network analysis, there are numerous applications and the network graph is also created for example: cytoscape and gephi. In network analysis, R has been developed as the powerful tool; however it is not particularly designed for the same. In comparison with the "strength of R", the stand-alone network analysis software is a threefold. Reproducible research is enabled by R at first which is not possible with GUI. Robust tools are provided by the data analysis power of R for the manipulation of data especially for network analysis. R is transformed into a complete network analysis tool with the ever growing range of packages designed. Statement suite of igraph and packages are included in the essential network analysis packages for R.

4.2. Nodes and Edges

"Multitude of separate entities" as well as their connection is the two essential aspects of the network. In this, the vocabulary used might be inconsistent and even technical among the packages, softwares and disciplines. Either nodes or vertices, the entities are considered for the graph and the connections are performed as links or edges. Nomenclature of edges and nodes are mainly used here except the discussed packages which were using different vocabulary. The data must be in particular way in the network analysis packages so that special type of objects can be created which are utilized in each package. Adjacency matrices, sometimes termed as socio matrices, are used to create the object classes network, igraph, and tidygraph.

4.3. Edge and node lists

In 1585, Daniel van der Meulen received letters to form a network object from the database. In the present study, the researcher also making both edge list & node list. The data frame of letters is manipulated through the necessitated use of the dplyr package which was sent to Daniel and was divided into two different fragments consisting of structure of edge and node lists.

4.4. Network Objects

Tidygraphy and igraph are closely related with the network object classes. It is not difficult to translate in between the igraph object and network object. It is important to keep both the packages and objects separately. It will be best if only one package loaded at one time because capabilities of network can overlap the igraph.

Performance Measures

Precision, accuracy and recall performance evaluation are used for the analysis of accuracy value of the SVM method's results compared with the confusion matrix method. Confusion Matrix is used for the evaluation which includes False Negative Rate (FN rate), True Positive Rate (TP rate), False Positive Rate (FP Rate) and True Negative Rate (TN Rate). These are the indicators used here. For positive class, TP rate is used and for negative class TN rate is used. FP rate is classified as positive class however it is class negative. FN rate is classified as the negative class however it is a class positive. [28]

In performance measures discuss the performance evaluative measures to youtube datasets. Following are the evaluative measures of classifiers. These evaluative measures find the goodness of classifier and suitability of data.

True Positives (TP): TP are the predicted values here which means that value of actual class is YES as well as the value of predicted class is also YES. For example: If the same thing is indicated by actual class and the predicted class that this passenger survived.

True Negatives (TN): TN are the predicted values here which means that value of actual class is NO as well as the value of predicted class is also NO. For example: Actual class and predicted class will say

the same thing such as passenger did not survive. When actual class contradicts with the predicted class then false positive and false negatives are obtained.

False Positives (FP): FP are the predicted values here which means that value of actual class is NO and the value of predicted class is YES. For example: Passenger did not survive according to actual class, but passenger will survive according to predicted class.

False Negatives (FN): FN are the predicted values here which means that value of actual class is YES and the value of predicted class is NO. If actual class value indicates that the passenger survived and the predicted class states that passenger will die.

The following section describes the parameters for the calculation of Accuracy, Precision and Recall.

Accuracy: Accuracy is the ratio of correctly predicted observation and the total observations. It is considered as the most intuitive performance measure. People might think that if they got high accuracy then their model is best. And yes accuracy is the great measure but only one condition when values of false positive and values of false negatives are almost same. So, it is important to evaluate the performance of the model by taking other parameters also in consideration.

$$\text{Accuracy} = TP+TN/TP+FP+FN+TN$$

Precision - The ratio of correctly observed positive observations of predicted class and the total number of observations of predicted class is defined as Precision. The challenge that this measure answers is how many of the passengers who were identified as having survived obviously did. The low false positive rate is related to high precision.

$$\text{Precision} = TP/TP+FP$$

Recall (Sensitivity) - The ratio between the predicted positive observations and the observations in actual class are defined as Recall. The answers provided by recall are: All the passengers who really survived and how many of them were labelled.

$$\text{Recall} = TP/TP+FN$$

Table 1: Accuracy Performance Measure

Methodology	**Accuracy (%)**
Existing work [29]	81%
Proposed work	89.3%

5. CONCLUSION

YouTube is defined as the source of comprehensive video information on the web. In all the social media sites, YouTube is one of the most popular sites. As on this site, users can directly interact with rating, sharing and commenting on videos.

Sentiment analysis model is proposed here for YouTube video comments. Naïve Baise Algorithm is also used here. The “neural network's output” is a categorization of negative, positive, or neutral sentiments.

However, it is still challenging for the researchers to classify the general events as well as detection of the sentiment polarities for the comments of the users. On this, huge work has been performed but still there is still a long way to overcome such issues.

Following are the problems emphasized in the present work to identify the polarity of the comments given by the YOUTUBE users.

- Challenges in present sentiment dictionaries
- Users are using informal language.
- On the basis of community-created terms, sentiments are estimated.
- Proper labels must be assigned to the events.
- To attain satisfactory classification performances
- Challenges involved in "social media sentiment analysis".

In comparison with the statistical model, the results showed that this model achieved better accuracy. The range of classification accuracy is in between 70percent to 89percent.

References

1. S. Siersdorfer, S. Chelaru, J. S. Pedro, I. S. Altingovde and W. Nejdl, "Analyzing and mining comments and comment ratings on the social web," ACM Transactions on the Web (TWEB), 8(3), 2014, pp. 1-39.
2. S. Siersdorfer, S. Chelaru, W. Nejdl and J. San Pedro, "How useful are your comments? analyzing and predicting youtube comments and comment ratings," In Proceedings of the 19th international conference on World wide web (ACM), 2010, pp. 891-900.
3. E. Momeni, C. Cardie and M. Ott, "Properties, Prediction, and Prevalence of Useful User-Generated Comments for Descriptive Annotation of Social Media Objects," In Proceedings of ICWSM, 2013.
4. O. Uryupina, B. Plank, A. Severyn, A. Rotondi and A. Moschitti, "SenTube: A Corpus for Sentiment Analysis on YouTube Social Media," In LREC, 2014, pp. 4244-4249.
5. E. Momeni, B. Haslhofer, K. Tao and G. J. Houben, "Sifting useful comments from Flickr Commons and YouTube," International Journal on Digital Libraries, 16(2), 2015, pp.161-179.
6. H. Lee, Y. Han, Y. Kim and K. Kim, "Sentiment analysis on online social network using probability Model," In Proceedings of the Sixth International Conference on Advances in Future Internet, 2014, pp. 14-19.
7. K. Filippova and K. B. Hall, "Improved video categorization from text metadata and user comments," In Proceedings of the 34th international ACM SIGIR conference on Research and development in Information Retrieval, 2011, pp. 835-842.
8. Mehta, P., & Pandya, S. (2020). A Review On Sentiment Analysis Methodologies , Practices And Applications. *INTERNATIONAL JOURNAL OF SCIENTIFIC & TECHNOLOGY RESEARCH*, *9*(02), 601–609.

9. Odim, M. O., Ogunde, A. O., Oguntunde, B. O., & Phillips, S. A. (2020). Exploring the Performance Characteristics of the Naïve Bayes Classifier in the Sentiment Analysis of an Airline ' s Social Media Data. *Advances in Science, Technology and Engineering Systems Journal*, *5*(4), 266–272.
10. Donthula, S. K. (2019). Man is What He Eats : A Research on Hinglish Sentiments of YouTube Cookery Channels Using Deep learning. *International Journal of Recent Technology and Engineering (IJRTE)*, *2*, 930–937. https://doi.org/10.35940/ijrte.B1153.0982S1119

Academic Guru Publication House

Research and Development
In Engineering Technology
Volume 1
Year: 2021

AG PH Books

ESTIMATION OF FLOOD VULNERABILITY BY DEA: A CASE STUDY OF NARMADA RIVER

Adarsh Sahu[1*]

[1]*Research Scholar, Department of Civil Engineerimg, Maulana Azad National Institute of Technology , Bhopal*

Abstract

The aim of this study is to analyze the situation, the background, the factors, risk circumstances, the magnitude and consequences of the flood, to record the danger and vulnerability, as well as the community's numerous implications; to analyze local awareness, traditions, and beliefs; and to develop community-based flood mitigation and disaster prevention strategies. The development of right flood control strategies necessitates a thorough understanding of the risk mechanism. Several interventions can be used at the catchments, drains, and floodplains under socioeconomic and environmental restrictions. The present study is conducted to assess the flood vulnerability of all the 22 districts in the Narmada river basin of India. This report will explore flood mitigation and prevention strategies. To proceed with a risk-based flood management strategy, its essential understand the floodplain's risk features first and afterwards identify the major element to reduce the risk.

Keywords: Vulnerability, Narmada River, DEA, Disaster, hazards.

1. Introduction

In developing countries, the negative effects of natural disasters as well as climate change are observed on the livelihoods risk of people living in such regions or countries. As the intensity increases of such

* ISBN No. 978-81-953278-9-8

events, it create hurdle in the strain of poverty reduction strategies. Throughout this framework, it's extremely important to keep in mind that natural disasters have the ability to derail several development programmes directed at accomplishing sustainable growth in the country, as certain areas are more prone to natural hazards than others. As in India, major section of the society is engaged in agricultural sector which mainly depends on natural rainfall. Due to high intensity of natural disasters as well as due to increase in climate change, the intensity of natural disasters has been increased such as cyclones, floods and droughts; additionally there is a shift in rainfall pattern also. In developing countries, such disasters are creating major problems such as poverty and economic inequalities.

The present study focuses on various risks faced by different households who are living in flood affected areas of rural India and it also examines the effectiveness of coping mechanisms which are adopted by the people to help themselves against the risk of such disasters. The relationship between different household specific characteristics has been made through an attempt such as age of head of the family, availability of social network, economic status as well as special coping strategy

1.1. Disaster

United Nations defined disaster as "the occurrence of sudden or major misfortune, which disrupts the basic fabric and normal functioning of the society and community" in 2012.

Indian Government defined disaster as an incident or sequence of events which can make damages, losses of life, properties, livelihood or infrastructure which is more than the normal capacity of the affected community to manage with.

Table 1: World Disaster Events

S.No.	Disaster	Year	Country	No. of People Affected
1	Floods	1931	China	35,00,000
2	Floods	1954	China	40,000
3	Cyclone	1970	Bangladesh	3,00,000
4	Cyclone	1991	Bangladesh	1,39,000
5	Earthquake	1999	Turkey	17,000
6	Tsunami	2004	Indonesia, Srilanka, India, Malaysia, Somalia, Bangladesh and Thailand	2,30,210
7	Hurricane, Katrina	2005	USA	1,836
8	Earthquake	2008	Susichuan, China	87,476
9	Cyclone, Nargis	2008	Myanmar	1,38,000
10	Earthquake	2010	Haiti	3,16,000

Source: CRED – 2013

Ecological imbalances as well as climatic changes are the reason in recent years for the frequent disastrous events such as flood at the world level. It becomes important to comprehend this disaster at every single level.

1.2. Why Flood in Narmada?

According to "State Disaster Management Authority of Madhya Pradesh, 2005", Madhya Pradesh has been divided into 10 different river basins. The names of the river basins of Madhya Pradesh are: Chambal, Sindh, Tapti, Mahi, Betwa, Son, Ken, Wainganga, Tons and Narmada. These river basins are shown in the figure given below:

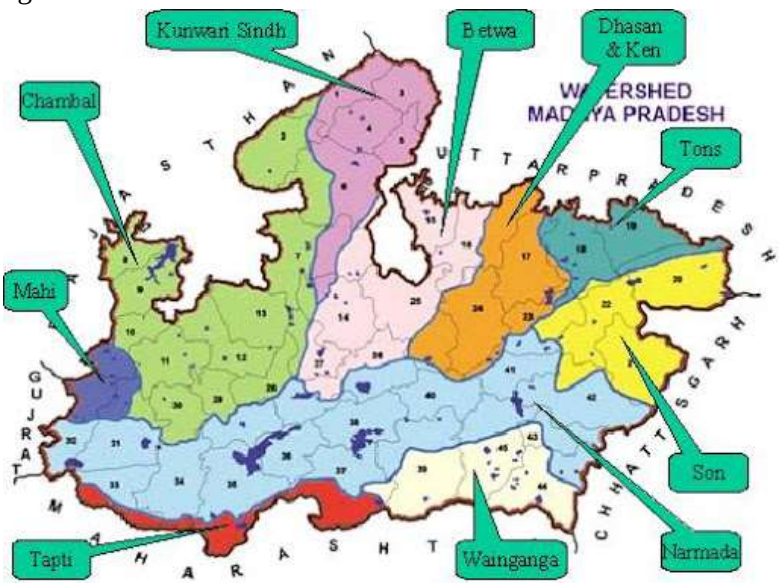

Figure 1: River basins of Madhya Pradesh (2005)
Source: - MPWRD

The challenges caused by rapidly increasing cities' susceptibility to urban flooding rise with susceptibility as the rate at which urban areas develop raises the susceptibility, resulting in a decrease in water penetration and infiltration into the earth. Due to deficiency of management and amalgamation among institutions which are answerable for managing the city, run-off water and solid waste management is aggravated because of the unplanned urbanization and solid waste management by the urban people. For urban planners, urban flooding is now becoming a challenge for making cities stronger to urban floods. Through several planning strategies for the urban development, it is important to address the emerging issues of urban flooding. It is important to understand different features and also to measure the susceptibility of urban areas because of unrealized as well as unplanned development. (Ouma & Tateishi, 2014)

1.3. Why DEA is used in this research?

DEA technique is used for making a model by taking different approaches into consideration to make the improvements upon traditional methods due to DEA approach which do not need any determining weight parameters. The performances of various entities engaged in various activities are evaluated by using DEA modelling which includes education, banks, healthcare, manufacturing and management (Anderson et. al, 2002). But it was also observed that only few studies are performed in the area of DEA field of natural disasters.

DEA model is considered as an excellent and easy used methodology according to the researchers for modelling of operational processes for the performance evaluations on the basis of concept of relative efficiency. The properties of connections inside the regional natural disaster system are considered as the disaster losses which include hazards, exposure units and disaster formative environment. The human society is threatened by hazards which are considered as the physical processes of the earth. The physical environment which reduces the effects of hazards is considered as "disaster formative environment" which includes elevation, vegetation, soil and slopes. All type of human activities is included in exposure units.

When people live along a river with a very low elevation, flood becomes a threat and more dangerous, which can be seen as the behaviour of "disaster formative climate. "Danger and disaster formative environment are the only related conditions for disaster risk since hazard is directly related to individual socioeconomic behaviour. The vulnerable locale will suffer loss only when the human activities & structures are the constitute components. In regional human activities, this variable vulnerability is a unseen distinctive which simply reflects the difference strictness of the disaster loss sustained by various areas under the same "natural hazards scenario".

However, disaster situations are compared with the reflections of same disasters amid different 3-D and time domains. Moreover, the prejudice of comprehensive flood index is overcome by the method by utilizing the prior weighting system which happens in disaster vulnerability approximation of current disasters.

1.4. Objective

- To evaluate the flood vulnerability of the districts in the Narmada river basin
- On the basis of vulnerability index value, the priority level of the districts is determined.
- For policy makers, a scientific approach is provided with the implementation of flood anticipation and mitigation technique.
- The applications of mathematical model are also provided for disaster management issues.

2. LITERATURE REVIEW

Numbers of studies are performed to study the vulnerability of flood disaster. Vulnerability of different regions must be analyzed and different periods are also required for enabling the government to make policies for the distribution of relief funds as well as to help the regions so that they can enhance their capabilities against disasters. For the evaluation of Vulnerability, physical or economic-ecological perspective is needed on the basis of the researchers' concern as per (Li et al., 2013). However, vulnerability is considered as the base for both systems as it involves detailed description of disaster management as well as flood severities. The over-all flood system has been decomposed into several factors which are as follows: disaster environment, disaster driver, disaster bearer as well as disaster intensity. Some factors are mentioned here which are used for demonstrating the flood disaster components such as disaster drivers risk levels, disaster environment stability levels as well as disasters bearer sensitivities.

Charnes, Cooper and Rhodes were the first people who together introduced data Envelopment analysis in 1978 (Kuah et al., 2010). DEA are in wider research as they are used in various fields and domains. Some of the applications are: information technology, agricultural industry, education, power plants, supply chain, stock market, computer industries, sports, banking industry, etc. Moreover, this study also presents the current research trends. On the other hand, various research trends in the field of DEA are also mentioned by (Kamat, 2019). Some of his works are: network DEA model, applications of DEA, fuzzy DEA models and stochastic DEA models. These can be used in future research.

(Huang et.al., 2008) used images of AVHRR 1991, MODIS 2003, and 2007 were used to generate water-inundated region maps, which were then used to estimate the 20-year frequency of water logging by overlaying the maps. A pixel's weight was determined by the frequency of water logging. Every nation and city was ranked according to the weighted score of the area and frequency of water logging danger.

(Purba et.al., 2002) argued in their study that using photos from remote sensing, it is possible to determine how many regions have been damaged by flooding. Before and during the flood, they generated the data using near real-time satellite pictures. Using data from both the pre-flood and during the flood, a flood map was created.

According to the study conducted by (Shi et. al, 2003), water logging was considered as the most serious hazards. The main groups of society were greatly affected by this disaster. A method of scenario simulation had been introduced by the author who is mainly used as a base. Then on the basis of concept structure of vulnerability, for the development of an indicator system representative indicators were selected on the basis of objective weights derived from the Principle Component Analysis. Population vulnerability assessment was performed by using this method which is based on the scenario simulation of rainstorm-induced water logging for 50 years. Several degrees of population vulnerability were observed from the final results.

(Huang et al, 2013**)** as there are many methods to assess the vulnerability of flood, the three methods of assessment disaster loss, the vulnerability index system and the vulnerability curve method but he preferred the vulnerability index system-based method.

3. METHODOLOGY

The "flood vulnerability" is described through DEA model. This study is performed on the plain of Narmada River, India for the reduction of negative effects of expected vulnerability. The study is divided into five important sections as shown in the figure given below:

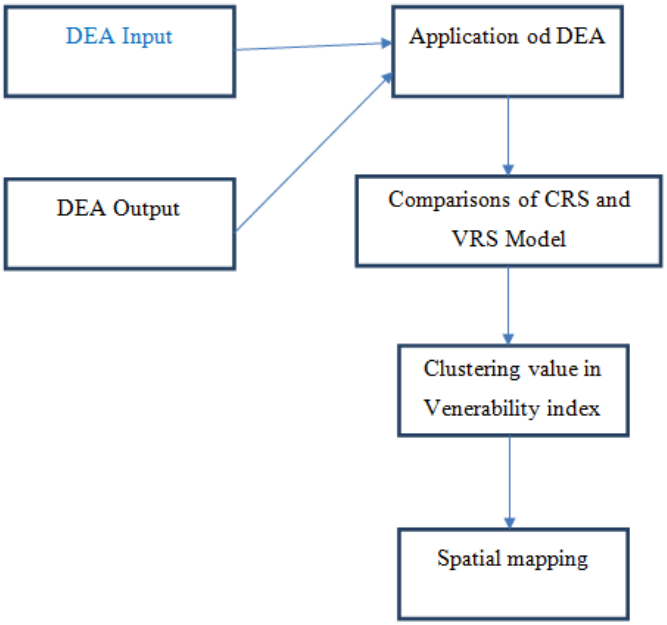

Figure 2: Layout of work

Stage 1

For DMUs, first stage is considered as the determination. Description of the problem, basic evidence about the usability, collection of data, determining tools for the present study as well as determination of the decision-making unit are observed. Evaluation is done through DMUs or decision making units. (Sherman & Zhu, 2006)

Stage 2

The input and output are selected through this second stage. It is considered as the most significant stage because if decision variables are incorrectly selected than incorrect results will be obtained. (Wei et al. 2002) introduced a theoretical framework for flood disaster system which defines flood disaster system as the consequence of comprehensive effect of hazards, vulnerability as well as exposure. Input-output system is the other name given to flood disaster process and efficiency index of the system is used for defining flood vulnerability.

The exposure parameter (Input)is

1. District wise population density per sq. km (2011)
2. District area (sq. km) and
3. The flood frequency since 2005 in that DMU.

The study employs four outputs (disaster loss)

1. No of people affected (2019)
2. Fully damaged kutcha houses (2019)
3. No of animal lost (2019)
4. Total agricultural area of crop loss (in Ha.)2019

Stage 3

This stage considers application of DEA in input-output oriented system and then the flood vulnerability was assessed by scheming efficiency index of different model of DEA. Various DEA models are observed in the literature section. "Constant returns to scale" assumptions are obtained through CCR models and "variable return to scale" assumptions are obtained through BCC models with DMUs demonstrating IRS, CRS as well as DRS.

Stage 4

DEA model construction is the fourth stage in this study. Different models and methods must be applied (CRS and VRS) for the evaluation of its efficiency; results are compared as well as expert's knowledge must be used to figure out the problem before coming to the conclusion.

Stage 5

Grouping of "decision-making units" is the last stage of this study that is done by the Clustering of the obtained Vulnerability Index Value. DMUs are classified on the basis of model results. On the basis of preferential basis, DMUs are being considered as per the classification.

3.1. Data selection and processing

For the present study, data has been collected from 22 districts of three states from where Narmada flows. Madhya Pradesh, Gujarat and Maharashtra are the three states of India from where Narmada River flows. The table mentioned below provides the detailed information about every district. For example, it provides detail about district wise population density that collected from the data book of Census India 2011, the demographic data area of the district collected from the respective states static book, frequency of flood since 2005 to 2019 collected from the Annexure-1 which is in the data book of SDMA (State Disaster Management Authority) of respective States Head department , people affected due to flood in 2019 in each DMUs of the respective states also collected form collected from the Annexure- 6 which is in the data book of SDMA , the data of animals lost due to flood 2019 from Animal husbandry department from Annexure-4, agricultural loss data having details in the Annexure-3 of SDMA , number of people affected in the flood taken from the Annexure-6 of SDMA and data of fully damaged kutcha houses from the Annexure -5 form of SDMA data book.

Table 2: Data selection

DMUS	district wise population density per sq. km (2011)	district area (sq km)	flood frequence since 2005	no of people affected (2019)	no of animal lost (2019)	total agricultral area of crop loss (in Ha.)2019	fully damaged kutcha houses (2019)
Balaghat	184	9299	3	21798	12	1148	95
Betul	157	10043	11	0	26	185971	15
Bharuch	296	5246	11	4977	30	382800	0
Chhindwara	177	11815	10	3030	112	5217	25
Damoh	173	7306	10	0	5	77277	26
Dewas	223	7020	6	3661	11	165628	0
Dhar	268	8153	10	0	12	35106	7
Hosangbad	185	6710	2	4833	25	47862	13
Indore	841	3896	7	0	1	0	28
Jabalpur	473	5211	10	0	12	0	1
Jhabua	285	3600	4	0	8	479	62
Khandwa	178	8304	1	12787	6	130188	13
Khargone	233	8030	1	0	8	170062	9
Mandla	182	5800	11	2344	43	109	102
Narmada	215	2755	11	9300	21	159200	0
Narsinghpur	213	5133	2	0	27	50299	186
Raisen	157	8466	2	6132	32	84282	102
Sagar	232	10252	2	0	36	163880	51
Sehore	199	6578	1	0	41	135066	8
Seoni	157	8758	2	0	33	1690	115
Shahdol	172	6283	2	0	64	0	0
Vadodara	535	7794	11	5700	43	564043	0

4. RESULTS AND DISCUSSION

The presented work is done on VRS and CRS model. On the basis of input parameters and the output parameters of DEA models the efficiency of both CRS and VRS Models are calculated as mentioned below in table 5.1, and the Scale Efficiencies (SE) score obtained by dividing the efficiency of CRS and VRS (Coelli et al, 2005; Coelli, 1996).

Values of FVI range from 0 to 1. 0 indicates less vulnerability and 1 indicates high vulnerability to flood. there are 15 districts having efficiency 1 indicating the flood Vulnerability High and the district that having FVI less than 1 further classify in two category, Medium and Low Vulnerability. The DMUs having scale efficiency 1 means they working within their optimal size and the DMUs having Scale efficiency less than one or more showing that they are very low or too big from the optimal size.

Table 3: Flood vulnerability index based on efficiency of input-oriented DEA model

DMU No.	DMU Name	Input-oriented			
		VRS Efficiency	**CRS Efficiency**	**SE**	**RTS**
1	Balaghat	1	1.00000	1.00000	Constant
2	Betul	1	1.00000	1.00000	Constant
3	Bharuch	1	1.00000	1.00000	Constant
4	Chhindwara	1	1.00000	1.00000	Constant
5	Damoh	0.9766	0.48054	0.49700	Increasing
6	Dewas	0.8994	0.65938	0.73310	Increasing
7	Dhar	0.6775	0.18340	0.27070	Increasing
8	Hosangbad	0.9908	0.73922	0.74608	Increasing
9	Indore	0.8612	0.19833	0.15054	Increasing
10	Jabalpur	0.6361	0.22863	0.35942	Increasing
11	Jhabua	1	0.47528	0.47528	Increasing
12	Khandwa	1	1.00000	1.00000	Constant
13	Khargone	1	1.00000	1.00000	Constant
14	Mandla	1	1.00000	1.00000	Constant
15	Narmada	1	1.00000	1.00000	Constant
16	Narsinghpur	1	1.00000	1.00000	Constant
17	Raisen	1	1.00000	1.00000	Constant
18	Sagar	1	1.00000	1.00000	Constant
19	Sehore	1	1.00000	1.00000	Constant
20	Seoni	1	1.00000	1.00000	Constant
21	Shahdol	1	1.00000	1.00000	Constant
22	Vadodara	1	1.00000	1.00000	Constant

Table 4: Flood vulnerability index based on efficiency of output-oriented DEA model

DMU No.	DMU Name	Output-oriented			
		VRS Efficiency	CRS Efficiency	SE	RTS
1	Balaghat	1	1.00000	1.00000	Constant
2	Betul	1	1.00000	1.00000	Constant
3	Bharuch	1	1.00000	1.00000	Constant
4	Chhindwara	1	1.00000	1.00000	Constant
5	Damoh	0.5865	0.48054	0.81930	Increasing
6	Dewas	0.7146	0.65938	0.92270	Increasing
7	Dhar	0.1851	0.18340	0.99080	Decreasing
8	Hosangbad	0.8529	0.73922	0.86671	Increasing
9	Indore	0.3119	0.19833	0.63587	Increasing
10	Jabalpur	0.2375	0.22863	0.83368	Increasing
11	Jhabua	1	0.47528	0.22863	Increasing
12	Khandwa	1	1.00000	1.00000	Constant
13	Khargone	1	1.00000	1.00000	Constant
14	Mandla	1	1.00000	1.00000	Constant
15	Narmada	1	1.00000	1.00000	Constant
16	Narsinghpur	1	1.00000	1.00000	Constant
17	Raisen	1	1.00000	1.00000	Constant
18	Sagar	1	1.00000	1.00000	Constant
19	Sehore	1	1.00000	1.00000	Constant
20	Seoni	1	1.00000	1.00000	Constant
21	Shahdol	1	1.00000	1.00000	Constant
22	Vadodara	1	1.00000	1.00000	Constant

4.1. Clustering of obtained vulnerability index value

Finally, using the K-means method, cluster analysis was performed on the vulnerability indices in order to group the zones based on similarity in their degrees of vulnerability, and the spatial pattern of the various vulnerability levels was mapped. The cluster analysis is performed on the basis of three parameters such as Low, Medium and High vulnerability. And for these parameters, the results are calculated for no. of districts and cluster centres.

Table 5: Cluster Analysis

Cluster	Number of districts	Cluster Centres
High Vulnerability	15	1
Medium Vulnerability	4	0.588605
Low vulnerability	3	0.203453

.

There are three clusters taken in the present study which are as follows: C1, C2 and C3. These clusters particularly define the zones of Narmada Basin. The values of clusters C1, C2 and C3 are 1, 0.588605 and 0.203453 respectively.

The cluster centre C1 is 1 in which there are 15 districts (Bharuch, Vadodara, Narmada, Khargone, Khandwa, Betul, Sehore, Raisen, Chhindwara, Sagar, Narsinghpur, Senoi, Balaghat, Mandla, Shahdol) are in the zone of High Vulnerability.

The cluster centre C2 is .588605 in which there are 4 districts (Jhabua, Dewas, Hosangabad, Damoh) are in the zone of Medium Vulnerability having efficiency scores .47528, .8994, .9908 and .9766 respectively.

The cluster Centre C3 is .203453 in which there are 3 districts (Dhar, Indore, Jabalpur) are in the zone of Low Vulnerability having efficiency scores .18340, .19833 and .22863 respectively.

Different districts of Narmada Basin are shown in the figure representing different colours. C1, C2 and C3 are the three clusters which indicates orange, green and purple colour respectively. Orange colour indicates high vulnerability, green colour indicates medium vulnerability and purple colour indicates low vulnerability to flood. 15 districts come in C1, 4 districts come in C2 and 3 districts come in C3 cluster as shown in the figure 5.3. Figure 5.4 shows the names of districts of different clusters in Narmada Basin.

Figure 3: K Means Cluster Map with names of the districts

5. CONCLUSION

Floods have a negative effect on the socio-economic status of livelihoods for people living along the Narmada River, as addressed in different sectors and across sectors. This was clear from the above discussion that floods impact households in various ways. Societies should be encouraged to construct homes made of durable materials and away from flood-prone locations as a method of coping with floods. It is imperative that communities be encouraged to expand the area planted on upland via Extension Services in order to enhance their food security position. Farmer input support programmes for farmers with limited resources but high productivity should be addressed. Clearly, greater and more effective flood-preparation measures are required. As a means of reducing flood hazards, increased attention is being paid to limiting the damage caused by floods. Risk management solutions focused on modifying land use and learning to live with floods are known as "resilience flood risk management" strategies. Even though flood maps are typically seen as static, the conditions shown on them are often dependent on assumptions and events that have already taken place. For example, if a location is experiencing moderate or large flooding in a wet or non-rainy environment, the scenario will alter. As a result, flood maps need to be revised to reflect the current state of affairs.

References

1. "EM-DAT". (2013, 1st April 2013). The OFDA/CRED International Disaster Database,
2. Abbas, S. H., Srivastava, R. K., Tiwari, R. P., & Ramudu, P. B. (2009). GIS-based disaster management: A case study for Allahabad Sadar sub-district (India). Management of Environmental Quality: An International Journal, 20(1), 33-51.
3. Abson, D. J., Dougill, A. J., & Stringer, L. C. (2012). Using Principal Component Analysis for information-rich socio-ecological vulnerability mapping in Southern Africa. Applied Geography.
4. Avkiran, N. K. (2001). Investigating technical and scale efficiencies of Australian universities through data envelopment analysis. Socio-Economic Planning Sciences 35(1), 57–80
5. Balica, S. F., Wright, N. G., & Meulen, F. (2012). A flood vulnerability index for coastal cities and its use in assessing climate change impacts. Natural Hazards, 64(1), 73-105
6. Barros, C. P. & Peypoch, N. (2008). Technical efficiency of thermoelectric power plants. Energy Economics 30(6), 3118–3127
7. Chang YC, Yu MM (2014) Measuring production and consumption efficiencies using the slack-based measure network data envelopment analysis approach: the case of low-cost carriers. J Adv Transp 48(1):15–31
8. Cook, W. D. & Zhu, J. (2007). Within-group common weights in DEA: an analysis of power plant efficiency. European Journal of Operational Research 178(1), 7–216

9. Cooper WW, Seiford LM, Zhu J (2011) Data envelopment analysis—history, models and interpretations. In: Cooper WW, Seiford LM, Zhu J (eds) Handbook on data envelopment analysis, 2nd edition, international series in operations research & management science, 2nd edn. Springer, New York, pp 1–39.
10. Dawod, G., Mirza, M., & Al-Ghamdi, K. (2012). GIS-based estimation of flood hazard impacts on road network in Makkah city, Saudi Arabia. Environmental Earth Sciences, 67(8), 2205-2215.
11. Dyckhoff H, Mbock E, Gutgesell S (2014) Distance-based measures of specialization and balance in multicriteria: a DEA-integrated method. J Multi-Crit Decis Anal

Academic Guru Publication House

Research and Development
In Engineering Technology
Volume 1
Year: 2021

AG PH Books

REVIEW ON HYBRID SOLAR AIR HEATER

C.B. Saxena[1*]

[1]*M.Tech Scholar, Department of Mechanical Engineering, RGPV,Bhoppal (M.P.)*

Abstract

The primary component of a solar energy usage system is a solar air heater (SAH). Thermal energy is generated at the absorbing surface of this kind of air heater, which is subsequently transferred to a fluid running through the collector. Because of their intrinsic simplicity, SAHs are the most often utilised collecting devices at a low cost. When it comes to solar-heated air systems, there are three main uses: heating buildings and drying wood and agricultural crops. For example, solar energy may be used for a variety of purposes including generating electricity, heating or cooling a building's interior area, powering air conditioners and heat pumps, and generating chilled water for industrial processes. Due to their versatility and ability to provide considerable environmental advantages, solar energy systems should be used wherever feasible.

Keywords: Solar energy; renewable; air heating; solar collectors; solar air heater.

1. Introduction

There are several ways to use solar energy, such as heating and generating electricity, but the most common is via harnessing solar radiation. Earth's present and future energy needs are dwarfed by the quantity of solar energy available. This widely dispersed energy source, if properly exploited, has the potential to provide all of humanity's future energy demands. With its endless supply and non-polluting quality, solar energy is predicted to become more popular as a renewable energy source in the 21st century. This contrasts with fossil fuels, which are finite. Solar energy has a huge potential since the Earth receives around 200,000 times the world's daily electric-generating capacity in the form of solar energy every day. Despite the fact that solar energy itself is free, the high costs associated with its

* ISBN No. 978-81-953278-9-8

collection, conversion, and storage still restrict its use in many regions. It is simpler to convert solar radiation into thermal energy (heat) than to convert it into electrical energy.

2. INTRODUCTION

There are several ways to use solar energy, such as heating and generating electricity, but the most common is via harnessing solar radiation. Earth's present and future energy needs are dwarfed by the quantity of solar energy available. This widely dispersed energy source, if properly exploited, has the potential to provide all of humanity's future energy demands. With its endless supply and non-polluting quality, solar energy is predicted to become more popular as a renewable energy source in the 21st century. This contrasts with fossil fuels, which are finite. Solar energy has a huge potential since the Earth receives around 200,000 times the world's daily electric-generating capacity in the form of solar energy every day. Despite the fact that solar energy itself is free, the high costs associated with its collection, conversion, and storage still restrict its use in many regions. It is simpler to convert solar radiation into thermal energy (heat) than to convert it into electrical energy.

2.1. Solar Air Heater:

Rather than replacing your heating system, a solar air heater is meant to augment it. An ideal location for a solar air heater is one where warm air may be diffused directly into an area of the house that is often used during daylight hours. Using the well-known scientific theory that warm air rises and cold air sinks, the solar air heater pumps cooled air from the bottom of a room into the solar collector where it absorbs heat before being blown back into the room. The air that travels through a solar air heater is heated using solar collectors positioned on the roof, wall, or window of the heater. Ideally, the solar collector should be placed on a south-facing roof or wall, away from any trees, tall buildings, or other potential sources of shadow. Installing smaller window units under a sunny south-facing window is a viable option. Because it extends through the window, this form of solar air heater eliminates the need for ducts or vents to allow air to circulate. At night or on overcast days, these direct-transfer units won't be able to transmit heat, therefore they can't be used.

Heat sinks are materials that can absorb and store heat for a brief period of time in bigger systems. Excess heat is transported to the heat sink throughout the day and then transmitted to your residence after the sun sets. Adding a heat sink to a retrofit heating system may prolong your usage of solar thermal energy into the night, but the cost is prohibitive. It's also dangerous to your health, so be careful. The development of mould and bacteria on rocks is facilitated by the accumulation of moisture in a heat sink. Your house will be filled with these toxins if you use a blower to draw warm air from a heat sink.

To minimise bulk and enhance total heat transmission, the solar heater mixes parallel and counter flows inside the heater itself. SAHs with complex geometry, such counter flow heaters or parallel flow heaters, cannot be modeled using current methodologies. Experiment and computational fluid dynamics are used to assess the solar air heater. Experiments are used to verify the accuracy of the computer

models. Solar radiation, conduction, convection and turbulence are all taken into consideration by the computer models. A turbulence model screening is carried out. Both the average conversion and the average collector efficiency fall within the range of 23 to 83 percent. Depending on the amount of solar radiation power input, computational models overestimate thermal efficiency by 6.75 percent to 9.01 percent.

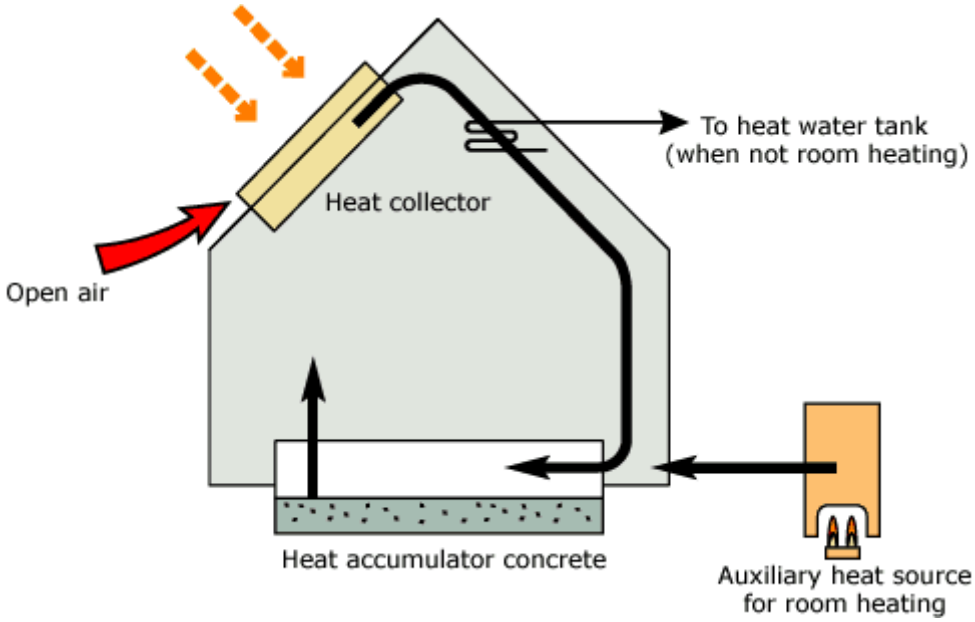

Figure 1: Diagrammatic Representation of Solar Air Heater

2.2. Types of Solar Air Heater

Porous type Solar Air Heater:

Porous absorbers, such as sliced and expanded metal, overlapping glass plate absorber, and transpired honeycomb, are used in the second kind of air heaters. With a porous absorber, sir heaters have the following advantages: The sun's rays penetrate far into the atmosphere and are absorbed by the atmosphere as they travel. As a result, less radiation is lost. The matrix warms up the air stream as it travels through it. Porous materials have a smaller pressure drop than non-porous materials.

However, an incorrect choice of matrix porosity and thickness may result in a decrease in efficiency, since the matrix may not be hot enough to transmit heat to the air stream beyond an ideal thickness. Examples of porous absorbers used in solar air warmers include wire meshes made from shattered bottles, and glass plates that have been overlapped.

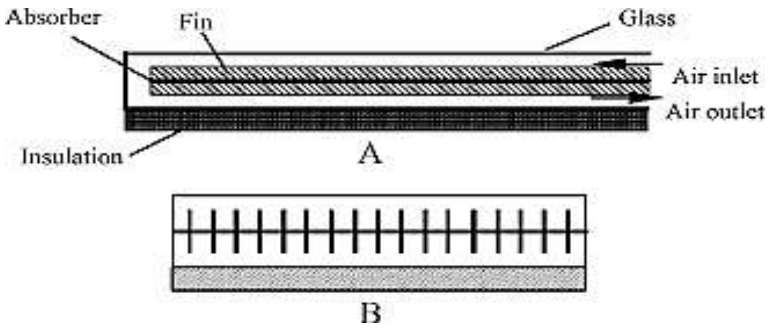

Figure 2: Diagrammatic Representation of Porous Type Solar Air Heater

Non-Porous Type Solar Air Heater:

Non-porous absorber plates do not allow air to flow below the absorber plate, but air may flow above and behind the plate. In the first kind, there is no need for a separate path for the air to move between the absorber plate and the clear cover system. The figure shows (as an example). Flowing hot air above the absorber heats up the cover, which then radiates heat back into the room. A large quantity of heat is lost to the surrounding environment, and so this air heater is not recommended for use. Non-porous absorbers with air passages underneath the absorber are the most prevalent. Between the absorber and the insulation is a plate parallel to the absorber plate, resulting in a passage with a high aspect ratio.

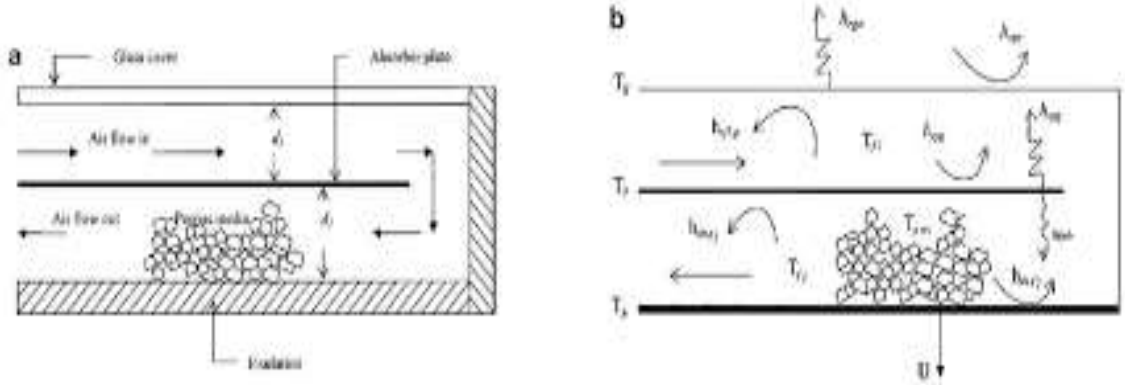

Figure 3: Diagrammatic Representation of Porous Type Solar Air Heater

3. LITERATURE REVIEW

(E.A. Cha´vez-Urbiola, Yu.V. Vorobiev, L.P. Bulat, 2012) (Chávez-Urbiola et al., 2012) In solar hybrid systems, thermoelectric generators have been considered as a potential. A total of four systems were analysed, including a traditional PV/Thermal geometry with TEGs between the solar cells and heat extraction device and three systems that used concentrators, namely: Concentrator – TEG heat extractor, and PV cell – concentrator – TEG heat extractor The power produced has a quadratic temperature dependency due to the linear relationship of current and voltage on temperature.

(Rashid Al Badwawi, Mohammad Abusara ,Tapas Mallick, 2015) (Al Badwawi et al., 2015) If more solar and wind power is included into the electricity grid, it might cause and generate considerable technological hurdles, particularly for weak networks or stand-alone systems without enough and sufficient storage capacity. When solar and wind resources are used together, the volatile nature of solar and wind resources may be alleviated, and the whole system becomes more dependable and affordable to operate. Hybrid solar PV/wind energy integration systems face a variety of problems and possibilities. "Grid-connected and stand-alone systems" are equally vulnerable to voltage and frequency fluctuation and harmonics, which have a greater effect in the event of a weak grid. As long as the hybrid systems are properly designed and implemented, this issue may be greatly alleviated.

(Shuvankar Podder, Raihan Sayeed Khan, ShahMd Ashraful Alam Mohon, 2015) (Podder et al., 2015) In order to fulfil a daily power demand of 276 kWh with a peak load of 40 kW, this research found the optimal size and economic assessment of a solar-wind hybrid RES. The hotels in Patenga, Chittagong, where the load data was gathered, were used. Independent and grid-connected versions of RES have been proposed. Based on "net present cost (NPC)" and energy cost per unit, the best system designs have been identified. An 8 percent yearly capacity shortfall allows for a stand-alone hybrid solar wind battery system to be economically similar to the current cost of diesel-based power plants. Renewable energy sources (RES) account for more than 70% of the total power generated by a grid-tied solar-wind hybrid system. Grid-tied RES also reduces greenhouse gas emissions by more than 60% compared to the traditional grid. This research used sensitivity analysis to examine the impact of changing capital costs or the availability of renewable resources on the system economics. This research will use the programme "Hybrid Optimization of Multiple Energy Resources (HOMER)" as its major simulation tool.

(Sumit Wagh, Dr. P.V.Walke, 2017) (Wagh & Walke, 2017) It is a vital aspect of the country's development and economy. Coal, oil, and natural gas make up the bulk of our energy supply. As we all know, energy is required for industrial, agricultural, commercial, and home purposes, as well as for other purposes. Global energy consumption is rising at an ever-increasing rate. Coal, fossil fuels, oil, and other gases may be used to generate energy. However, all of these sources are hazardous to the environment, thus there are restrictions on their use and they are restricted. For the sake of the environment, we need a source of renewable, pollution-free power. Eco green energy, or creating energy without causing damage to the environment, is the current emphasis in today's globe. Renewable energy sources including sun, wind, small hydro, and biomass, as well as biofuels, are available in this situation. Using renewable energy to meet the world's energy needs has a great deal of promise. The utilisation of renewable energy sources has its drawbacks, and a lot of research is being done to increase their efficiency.

Wenke Fan, Georgios Kokogiannakis, Zhenjun Ma, 2018)(Fan et al., 2018) there is a dearth of guidelines for effective hybrid PVT-SAH system design and a high degree of complexity in its creation; Multi-objective design optimisation will be used to maximise the conflicting outputs of useable thermal energy production and net electricity gains concurrently. ANOVA is used to create the simulation exercises and identify the non-significant system factors in order to lower the optimization size. Multi-objective optimization problem is then created to find the best values of critical design parameters. From

the resulting collection of Pareto fronts, the final optimum design is selected using a decision-making process based on TOPSIS. The sensitivity analysis decreased the number of factors from twelve to seven and found that the material parameter and the thickness of building components are not critical to the performance of the PVT-SAH.. 21.9 percent and 20 percent improvement in useable thermal energy and net electricity gains can be achieved under the parameters of this research by the final determined optimum design, whereas the second selected baseline design can be improved by 24.7 percent and 126 percent.

(M. H. Masud, Raju Ahamed, M. Mourshed, M.Y. Hossan & M. A. Hossain, 2019) (Masud et al., 2019) In recent years, several SAH have been created that have a better efficiency but are more expensive to install in underdeveloped nations. In this case, a more affordable SAH with improved solar energy use and improved efficiency has been designed by combining a fin with the SAH. Air mass flow rate (MFR) was varied from 0.0132 kg/s to 0.02166 kg/s for both the connected and unattached fin configurations. A pyrometer was used to monitor the temperature of the air entering and exiting the heater, and an anemometer was used to measure the flow rate of air leaving the heater. The blower's output was where the anemometer propeller was mounted. Several measurements of speed were made before settling on an average speed for the sake of taking a reading. In the range of 0.0132 Kg/s to 0.02166 Kg/s, the performance of single-pass solar air heaters with and without fins was evaluated, and the mass flow rate was examined.

(Peter Jenkins, Monaem Elmnifi, Abdalfadel Younis, Alzaroog Emhamed, 2019) (Jenkins et al., 2019) Any country's economic and social progress depends on the availability of energy. To reduce reliance on imported fuels, it is necessary to maximise the development of domestic energy resources while also addressing issues of economics, the environment, and society. Research and development in the renewable energy sector have increased as a result, in an effort to find new and better solutions to fulfil the world's energy needs while also reducing reliance on fossil fuels. Wind and solar power are becoming more popular because of their quantity, availability, and simplicity of use in the creation of electricity. This research focuses on a hybrid renewable energy system that includes both wind and solar power. Using maps, we were able to locate areas with great potential for wind and solar energy production in many different sections of Libya. An emphasis of this article is on a wind-solar hybrid power generating system for a specific site.

(Armin Razmjoo, et.al., 2019) (Razmjoo et al., 2019) Fossil fuel emissions of greenhouse gases are the primary sources of air pollution and a grave danger to human health. One of the greatest ways to avoid and decrease this issue in the future is to use a hybrid renewable energy system, as previously discussed. There are a variety of ways to calculate CO2 emissions, and Homer software is one of them. A variety of methods exist for calculating CO2 emissions, however the following equations were developed using the hybrid energy system that combines UN objectives, Urban Themes, and a techno-economic analysis to use solar and wind power in two Iranian cities.

(Ramadoni Syahputra, Indah Soesanti, 2020) (Syahputra & Soesanti, 2020) Central Java in Indonesia is a prime location for a hybrid micro-hydro and solar photovoltaic system. With a strong focus on renewable energy, particularly solar and hydropower, the Indonesian government has invested

heavily. The province of Central Java, situated on the Indonesian island of Java, has a significant potential for both sources of energy. As part of this study, we perform field research to identify the optimum capacity of solar and micro-hydro hybrid power plants, energy load analysis, and the best design of hybrid power plants. It is possible to gather information on the micro-hydrological potential by taking measurements directly on the Ancol Bligo irrigation channel in Indonesia's Central Java province's Bligo village, Ngluwar district, and Magelang regency. NASA's database of solar radiation in Central Java provided information on the region's solar power potential. The length, debit, heads, and power potential of irrigation canals leading from rivers are all included in the statistics on hydropower potential. Using this information, an ideal hybrid power plant may be designed. The examination of capital costs, grid sales, energy expenses, and net present costs is the strategy used to get the best hybrid power plant design.

(M.S.W. Potgieter, C.R. Bester, M. Bhamjee, 2020) (Potgieter et al., 2020) They may be used for room heating, pre-heating for industrial purposes such as drying of different materials and pre-heating for solar water de salinators. A novel solar air heater design is being evaluated for thermal efficiency and temperature distributions inside the solar air heater as part of this study. To minimise bulk and enhance total heat transmission, the solar heater mixes parallel and counter flows inside the heater itself. SAHs with complex geometry, such counter flow heaters or parallel flow heaters, cannot be modeled using current methodologies. Experiment and computational fluid dynamics are used to assess the solar air heater. Experiments are used to verify the accuracy of the computer models.

4. CONCLUSION

Several of the most popular solar collectors are discussed in this article. Flat-plate, compound parabolic, evacuated tube, parabolic trough, Fresnel lens, and parabolic dish collectors are among the different kinds of collectors mentioned. In addition, examples of common uses are provided to demonstrate the reader the breadth of their use. Heating and cooling applications range from water heaters to room heating and cooling, refrigeration to desalination to thermal power systems to solar furnaces. It's important to remember that solar energy collectors don't only have to be used in the places listed above. Other apps that aren't mentioned here are either still in development or haven't matured enough to be included. Using solar collectors in a range of systems may have a substantial environmental and economic impact, and they should be employed wherever practical, according to the application areas specified in this article.

References

1. ADDIN Mendeley Bibliography CSL_BIBLIOGRAPHY Al Badwawi, R., Abusara, M., & Mallick, T. (2015). A review of hybrid solar PV and wind energy system. *Smart Science*, *3*(3), 127–138. https://doi.org/10.6493/SmartSci.2015.324

2. Chávez-Urbiola, E. A., Vorobiev, Y. V., & Bulat, L. P. (2012). Solar hybrid systems with thermoelectric generators. *Solar Energy*, *86*(1), 369–378. https://doi.org/10.1016/j.solener.2011.10.020
3. Fan, W., Kokogiannakis, G., & Ma, Z. (2018). A multi-objective design optimisation strategy for hybrid photovoltaic thermal collector (PVT)-solar air heater (SAH) systems with fins. *Solar Energy*, *163*(September 2017), 315–328. https://doi.org/10.1016/j.solener.2018.02.014
4. Jenkins, P., Elmnifi, M., Younis, A., & Emhamed, A. (2019). Hybrid Power Generation by Using Solar and Wind Energy: Case Study. *World Journal of Mechanics*, *09*(04), 81–93. https://doi.org/10.4236/wjm.2019.94006
5. Masud, M. H., Ahamed, R., Mourshed, M., Hossan, M. Y., & Hossain, M. A. (2019). Development and performance test of a low-cost hybrid solar air heater. *International Journal of Ambient Energy*, *40*(1), 40–48. https://doi.org/10.1080/01430750.2017.1360202
6. Podder, S., Khan, R. S., & Alam Mohon, S. M. A. (2015). The Technical and Economic Study of Solar-Wind Hybrid Energy System in Coastal Area of Chittagong, Bangladesh. *Journal of Renewable Energy*, *2015*, 1–10. https://doi.org/10.1155/2015/482543
7. Potgieter, M. S. W., Bester, C. R., & Bhamjee, M. (2020). Experimental and CFD investigation of a hybrid solar air heater. *Solar Energy*, *195*(August 2019), 413–428. https://doi.org/10.1016/j.solener.2019.11.058
8. Razmjoo, A., Shirmohammadi, R., Davarpanah, A., Pourfayaz, F., & Aslani, A. (2019). Stand-alone hybrid energy systems for remote area power generation. *Energy Reports*, *5*, 231–241. https://doi.org/10.1016/j.egyr.2019.01.010
9. Syahputra, R., & Soesanti, I. (2020). Planning of hybrid micro-hydro and solar photovoltaic systems for rural areas of central Java, Indonesia. *Journal of Electrical and Computer Engineering*, *2020*. https://doi.org/10.1155/2020/5972342
10. Wagh, S., & Walke, P. V. (2017). Review on Wind-Solar Hybrid Power System. *International Journal of Research In Science & Engineering*, *March 2017*.

Research and Development In Engineering Technology
Volume 1
Year: 2021

AG PH Books

PROCESS THE OPTIMIZATIONS BY TAGUCHI METHOD IN DRILLING MACHINE

Prateek Singh[1*]

[1] *Research Scholar, Department of Mechanical Engineering, SIRTE, Bhopal*

Abstract

Material removal and surface roughness response are the primary goals of this research, which investigates and evaluates the effects of various input process parameters (cutting diameter and cutting speed) on these outcomes. Various variables have been taken into account in each experiment. The L9 Orthogonal array was used to design experiments during the milling of aluminium plate (work material). "Cutting diameter (10mm), cutting speed (1000rpm), and feed rate (0.014mm/rev)" are the most important input parameters for material removal rate and surface roughness.

Keywords: Drill; drilling machine; taguchi method; Metal matrix composites; Roughness..

1. Introduction

The basic principles of electromechanical machine tool controls, production standards, and testing instruments' characteristics and uses for checking components or products made in various manufacturing facilities in various countries are all addressed in this study. The study also aims to provide students with a foundational understanding of workshop practises. Diverse hand tools (such as measuring tools and marking instruments) as well as machinery and various techniques of production are described and shown in this section of the book to aid the shaping or moulding of different raw materials into acceptable useable shapes. Ferrous and non-ferrous metals as well as their characteristics and applications are examined as part of the study of industrial environments. Knowledge of basic workshop processes such as bench work and fitting; sheet metal; carpentry; pattern-making; mould-

* ISBN No. 978-81-953278-9-8

making; foundry and smithy; forging and metalworking; welding; fastenings; machine shops; surface finishing; and coatings; assembly inspection; and quality control; should be included in the course curriculum. Composition, characteristics and utilises of raw materials; numerous production processes; replacement or improvement over a large number of old processes; new compact designs; improved accuracy in dimensions; quicker production methods; better surface finishes; more alternatives to the existing materials and tooling systems; automatic and numerical control systems; higher mechanization; greater output are some of the goals of this course.

1.1. Drilling Tool material

Every cutting tool used in drilling may be found in a variety of materials, which determines the qualities of the equipment and the materials for which it is most suited. Hardness, durability, and resistance to wear are included in these characteristics. The following are the most often used materials in the construction of electronic devices:

- High-speed steel (HSS)
- Carbide
- Carbon steel
- Cobalt high speed steel

For example, a machine's material is chosen based on the kind of workpiece, its cost, and its lifespan. A device's life expectancy is an important factor to consider when selecting one, since it has a considerable impact on assembly costs. Having a limited apparatus life will need the purchase of more instruments, as well as the time required to replace the device each time it becomes overly worn.

Figure 1**:** Shapes of turning cutting tool

1.2. Taguchi's Parameter Design Approach

Control factors and noise factors are the two sorts of parameter design parameters that have an impact on a product's functional characteristics. In an injection molding process, control parameters include material selection, cycle duration, and mould temperature. Noise factors are those that are difficult, impossible, or prohibitively costly to manage. Outer noise, internal noise, and product-to-product noise are all examples of different sorts of noise. There are several noise elements that might cause a product's performance to fall short of its desired value. As a result, parameter design aims to establish control factor settings that reduce the product's sensitivity to changes in the noise factors without eradicating their source.

2. LITERATURE REVIEW

(Murthy, Rangappa and Almouns, 2020) [1] The primary goal of this study is to improve the quality of holes drilled throughout the drilling process. A carbon-basalt hybrid composite is a higher performing composite at a lower cost than traditional carbon-based composites. Using the hand layup process, a hybrid composite test specimen was created for this study. The matrix substance is a general purpose polyester resin. During the production process, the composite is prepared by stacking layers of carbon and basalt.. The tests were carried out using the DOE technique of design. Each experiment's combination of parameters was determined using Taguchi's three-level and three-factor array. There are a total of 27 holes bored, each with a distinct process parameter combination. DD1, F1 and S3 combination parameters produce the lowest thrust value according to Taguchi and RSM techniques.

(Manickam and Parthipan, 2020) [2] In manufacturing, the drilling process is critical. To cut the material, several drilling process parameters were used. Material removal and surface roughness are the primary goals of this study. Based on the input parameters of speed, feed, and the chosen drill tool; the different drilled holes in AISISS317L material. After confirming the accuracy of the findings, the output parametric optimization was done in thrust force, torque, material removal rate, and surface finish.

(Krivokapić et al., 2020) [3] For drilling hardening steel EN 42CrMo4 to 28-HRC hardness, using cruciform blade twist drills made of high-speed steel with 64 HRC hardness level, this paper describes development of models for predicting surface roughness using "multiple regression and artificial neural networks (ANN)". The models link an arithmetic mean deviation of surface roughness to torque as an input variable. Input variables (nominal twist drill diameters, speed, feed, and angle of work piece installation) were varied at three levels by Taguchi design of experiment and measured experimental data for torque and arithmetic mean deviation of surface roughness for different values of flank wear on twist drills were used in the model development. According to this comparison, the neural network model outperforms numerous linear and nonlinear regression models when applied to the inputs at the point when wear spans approach a limit value that corresponds to the moment when drills become blunt.

(Siva Prasad and Chaitanya, 2020) [4] Conventional drilling of fiber-reinforced polymer composites suffers from issues such as delamination, chipping of the matrix, heat impacted zone, and low surface

roughness, hence an unusual machining approach was used. When abrasive water jet machining (AWJM) of GFRP/Epoxy composites is used, the effects of hydraulic pressure, stand of distance, abrasive flow rate, fibre orientation, material thickness, and abrasive mesh size on surface quality are studied in this work. The Taguchi L27 orthogonal array is used to design the experiments. The findings of the experiments showed that the abrasive mesh size had the greatest impact on surface roughness.

(Siva Prasad and Chaitanya, 2020) [5] Abrasive ceramic particles in metal matrix composites (MMCs) make the machining process harder. Due to MMCs' potential broad application, the development of a suitable technology is crucial for the effective machining process. Drilling settings for (LM5/ZrO2) utilising Taguchi technique are investigated. “Taguchi's Signal-to-Noise ratio analysis” was used for the investigation. Response graphs are used to examine parametric findings' response properties. The relevant factors were classified and their impact on response characteristics was measured using ANOVA. The most critical input parameters for producing the lowest possible thrust force are the spindle speed and feed rate.

(Shunmugesh and Pratheesh, 2019) [6] For the "Carbon Fiber Reinforced Plastics (CFRP)," the "Taguchi Grey Relational Analysis (TGRA)" was used to optimise micro-drilling settings. Drill bits of various sizes were used to achieve this. The micro drilling test's process parameters are feed rate, drill diameter, and spindle speed. This study used Taguchi's L27 orthogonal array as the basis for its design. "Tool wear rate," "delamination factor," "material removal rate," and "machining conditions" are the primary goals of the experiments. The Taguchi Grey Relation Analysis is used to identify the optimal values for the lowest delamination factor, the highest material removal rate, and the lowest tool wear rate. The S/N ratio is also subjected to an ANOVA in order to determine the relative importance of the various variables.

3. RESEARCH METHODOLOGY

3.1. Steps of working

1. M1TR machine is selected for drilling operation.
2. Material selection for manufacturing of specimen.
3. Feed rate and other parameter are selected for drilling operation.
4. Drilling bit material and type was selected.
5. Operation is performed on M1TR machine.
6. Surface roughness is checks by surface roughness tester.
7. Taguchi method was performed on MINITAB software.
8. Different data implemented in taguchi analysis process.
9. s/n ratio graphs are drawn in MINITAB software.
10. Results are analyzed and compared.

3.2. Work piece preparation

Aluminum was selected as the work piece material of Plate of 50mm x 50mm x 20mm, then drilling operation were performed on that work piece on M1TR milling machine. [7] [8] [9]

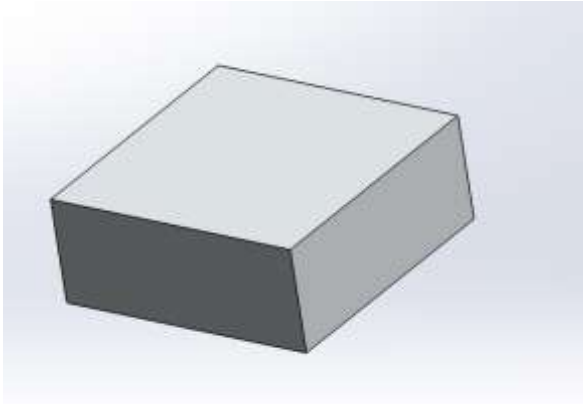

Figure 2**:** Workpiece

Table 1: Parameters used in drilling operation

Factors	**Parameters**	**Level**		
		1	2	3
A	Cutting dia (mm)	5	10	15
B	Cutting speed (rpm)	500	1000	1500
C	Feed rate (mm/rev)	0.012	0.014	0.016

4. RESULTS AND DISCUSSION

4.1. Experimental result

For three different drill diameters of 5mm, 10mm and 15mm, optimization results were obtained for different combinations of the feed rate and cutting speeds. Material Removal Rate, Surface roughness, Single to noise ratio and the means for each combination of the characteristics parameters are noted down in table below. [10]

Table 2: Experiment result

S.No.	Drill Dia(mm)	Cutting Speed(rpm)	Feed Rate	MRR	Surface Roughness	S/n ratio	Mean
1	5	500	0.012	117.804	0.35	-38.3871	59.077
2	5	1000	0.014	276.846	0.75	-45.8109	138.798
3	5	1500	0.016	471.216	0.97	-50.4362	236.093
4	10	500	0.014	549.733	1.73	-51.7654	275.7315
5	10	1000	0.016	1256.624	2.11	-58.9592	629.367
6	10	1500	0.012	1413.702	3.12	-59.9777	708.411
7	15	500	0.016	1413.712	2.45	-59.9819	708.081
8	15	1000	0.012	2120.568	3.99	-63.5024	1062.279
9	15	1500	0.014	3710.994	4.01	-68.3701	1857.502

Response Table for Signal to Noise Ratios

The table and the graphs below show the response ratios of the different characteristics of the machining process.

Nominal is best (-10×Log10(s^2)) criteria has been used.

Table 3: Response table for s/n ratio

Level	Drill Dia(mm)	Cutting Speed(rpm)	Feed Rate
1	-44.88	-50.04	-53.96
2	-56.90	-56.09	-55.32
3	-63.95	-59.59	-56.46
Delta	19.07	9.55	2.50
Rank	1	2	3

Table 4: Response Table for Means

Level	Drill Dia(mm)	Cutting Speed(rpm)	Feed Rate
1	144.7	347.6	609.9
2	537.8	610.1	757.3
3	1209.3	934.0	524.5
Delta	1064.6	586.4	232.8
Rank	1	2	3

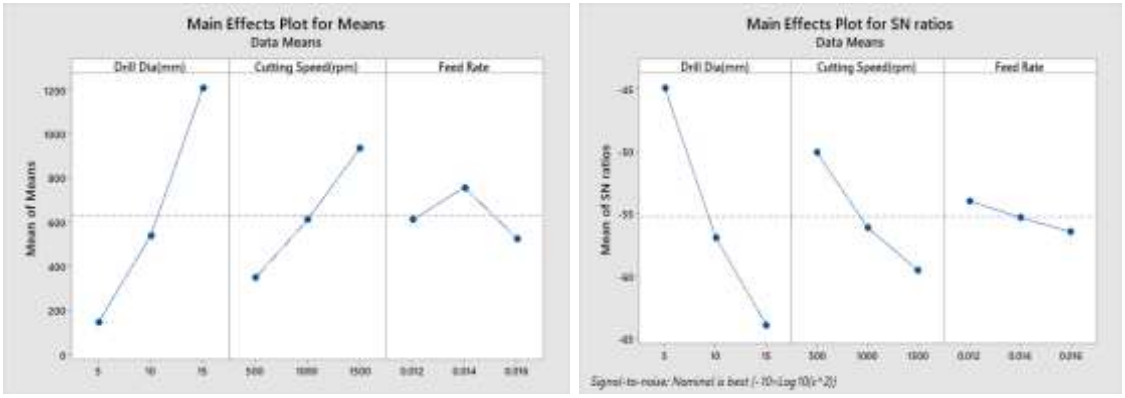

Figure 3**:** main effects plot for (a) means; and (b) SN ratios

The drill diameter is observed to be the most affected parameter in the graphs above with greater response ratio, followed by the cutting speed and the feed rate. Hence, the drill diameter is ranked no. 1 parameter, to be considered during the drilling process and that would affect the surface roughness and the S/N ratio the most. According to that analysis it is obtained that drill diameter should be at 10 mm cutting speed at 1000 rpm and feed rate should be at 0.014 mm/rev for obtained better results with less damage of work piece surface.

4.2. Result validation

The results have been validated from the paper of **C. Manickam.**

Table 5: result comparison

Base Paper value (C. Manickam)		**Experiment value**	
MRR	**Surface roughness**	**MRR**	**Surface roughness**
169.460	0.7566	117.804	0.35
402.123	1.86	276.846	0.75
785.398	1.61	471.216	0.97
170.421	1.63	549.733	1.73
326.230	1.25	1256.624	2.11
800.235	1.84	1413.702	3.12
155.236	1.44	1413.712	2.45
311.124	1.65	2120.568	3.99
902.101	0.90	3710.994	4.01

5. CONCLUSION

Drilling test is performed on an aluminium slab on M1TR milling machine. Surface roughness is tested and taguchi method is used to analysis the quality of drill and which parameters are better for drilling.

- According to that analysis it is obtained that drill diameter should be at 10 mm cutting speed at 1000 rpm and feed rate should be at 0.014 mm/rev for obtained better results with less damage of work piece surface.
- According to response table it can be observed that drilling diameters found on rank 1 which means diameter of drill is a most important factor which should be analysed appropriately according to drill requirement.
- Cutting speed is at rank 2 in response table which affects surface roughness a lot. And for better finishing of work piece surface, it should be maintained according to the requirements.
- Optimum MRR and surface roughness is attained because of using 'nominal is best' criteria.

References

[1] B. R. N. Murthy, R. Rangappa, and M. O. Almouns, "Optimization of thrust force in drilling of carbon-basalt hybrid composites through Taguchi and RSM," *Mater. Today Proc.*, no. xxxx, 2020, doi: 10.1016/j.matpr.2020.05.043.

[2] C. Manickam and N. Parthipan, "Optimization of drilling parameters in AISI SS317L stainless steel material using Taguchi methodology," *Mater. Today Proc.*, vol. 21, no. xxxx, pp. 837–842, 2020, doi: 10.1016/j.matpr.2019.07.589.

[3] Z. Krivokapić, R. Vučurević, D. Kramar, and J. Š. Jovanović, "Modelling surface roughness in the function of torque when drilling," *Metals (Basel).*, vol. 10, no. 3, pp. 1–15, 2020, doi: 10.3390/met10030337.

[4] K. Siva Prasad and G. Chaitanya, "Optimization of process parameters on surface roughness during drilling of GFRP composites using taguchi technique," *Mater. Today Proc.*, vol. 39, no. xxxx, pp. 1553–1558, 2020, doi: 10.1016/j.matpr.2020.05.562.

[5] S. Jebarose Juliyana and J. Udaya Prakash, "Drilling parameter optimization of metal matrix composites (LM5/ZrO2) using Taguchi Technique," *Mater. Today Proc.*, vol. 33, no. xxxx, pp. 3046–3050, 2020, doi: 10.1016/j.matpr.2020.03.211.

[6] K. Shunmugesh and A. Pratheesh, "Taguchi Grey Relational Analysis based Optimization of Micro-Drilling Parameters on Carbon Fiber Reinforced Plastics," *Mater. Today Proc.*, vol. 24, pp. 1994–2003, 2019, doi: 10.1016/j.matpr.2020.03.628.

[7] K. S. Prasad and G. Chaitanya, "Analysis of delamination in drilling of GFRP composites using Taguchi Technique," *Mater. Today Proc.*, vol. 18, pp. 3252–3261, 2019, doi: 10.1016/j.matpr.2019.07.201.

[8] M. K. Bharti, P. Girwal, and P. Patidar, "Improving Productivity and Maintainace Efficiency of an Automobile Industry Through Lean - Production Cum Maintance System," *Int. J. Eng. Res. Gen. Sci.*, vol. 6, no. 6, pp. 6–18, 2018.

[9] D. Geng, D. Zhang, Y. Teng, and X. Jiang, "An experimental investigation on hole exit geometric error in orbital drilling process," *Procedia CIRP*, vol. 71, pp. 128–133, 2018, doi: 10.1016/j.procir.2018.05.084.

[10] K. S. Prasad and G. Chaitanya, "Selection of optimal process parameters by Taguchi method for Drilling GFRP composites using Abrasive Water jet machining Technique," *Mater. Today Proc.*, vol. 5, no. 9, pp. 19714–19722, 2018, doi: 10.1016/j.matpr.2018.06.333.

Academic Guru Publication House

Research and Development
In Engineering Technology
Volume 1
Year: 2021

AG PH Books

An Empirical Study and simulation analysis of MAC layer model using AWGN channel of WiMAX technology

Mukesh Patidar[1*], Ankit Jain[2]

[1,2]*Department of Electronics and Communication Engineering, Indore Institute of Science and Technology Indore (Madhya Pradesh), India, 4520011,*

[1]*mukesh.patidar@indoreinstitute.com, ORCID: 0000-0002-4401-8777,*

[2]*ankit.jain@indoreinstitute.com 2*

Abstract

The IEEE 802.16 specification defines WiMAX, a wireless broadband data transmission technology. It enables high-speed data transmission over a wide range and remains inexpensive. This is a point-to-multipoint wireless network technology that can also be used in other network applications such as wireless sensor networks. In this article, we will use MATLAB Simulink to analyze the MAC tier model on WiMAX. This MAC tier model can be used to evaluate WiMAX performance in multiple scenarios such as high data rates, modulation schemes, and channel conditions. The proposed simulation model has reduced simulation time and performance. In this analysis, various modulation techniques such as QPSK and QAM were used on the AWGN channel and the simulation results were compared by SNR and BER.

Keywords: WiMAX, LLC, MAC, quality of service, AWGN, IEEE 802.16, Matlab Simulink.

1. INTRODUCTION

Using IEEE 802.16 and IEEE 802.11e, WiMAX provides fixed, mobile, portable, and mobile wireless broadband without requiring a direct line of sight (LOS) to the base station. It allows for the

* ISBN No. 978-81-953278-9-8

establishment of connections, and also in charge of providing the globe with an alternative to wired internet, namely, broadband wireless access (BWA). IEEE Wireless MAN (IEEE 802.16) (Metropolitan Area Network) [12], is the standard for wireless networks. We investigated both licensed and unlicensed bandwidth of 266GHz used in fixed broadband wireless and mobile applications. It can provide internet connectivity up to 50km with a transmission rate of 75 Mbit/s. The IEEE 802.16 standard covers only the physical level and MAC (Media Access Control) level of the air interface, and does not change the upper layer. The IEEE802.16 standard suite (IEEE802.162004 and IEEE80216e2005) [3] outlines the four physical layers that can be used in combination with the MAC layer to create wireless broadband systems. To improve performance in a blind (NLOS) environment, the IEEE 802.16e air interface [56] uses Orthogonal Frequency Division Multiple Access (OFDMA). The IEEE divides the data link layer into two sub-layers. The terms "media access control" (MAC) and "logical link control" (LLC) are interchangeable (MAC). This form of wireless channel degradation can be addressed with MIMO (Multiple Input Multiple Output) technology [7].

The remainder of the paper is structured as follows: The WiMAX MAC Layer Simulink model blocks have been presented in section II. In part III, the modulation methods are explained, in section IV, the experimental simulation findings are presented, and in section V, the conclusion is presented.

2. WIMAX MAC LAYER SIMULATION MODEL

This paper shows a Matlab implementation of a WiMAX MAC layer simulation model. The operational phase of the model was designed using the Simulink version of Matlab 7.11.0 (R2010b), Simulink 7, and Communication Block Set 3. Independent autonomous MAC tiers, dynamic network topology adaptations, multi-hop networks, and dynamic network settings are all features of the MAC tier [8]. The sender, channel, and receiver are WiMAX-MAC layer models [6]. The WiMAX configuration (MACLAY and PHYLAY) is shown in Figure 1. The data that the MAC layer receives from the upper layer is called the service data unit (SUD). The data received from the channel is then input to OFDM demodulation. This includes removing cyclic prefixes, performing fast Fourier transforms, and decomposing OFDM frames.

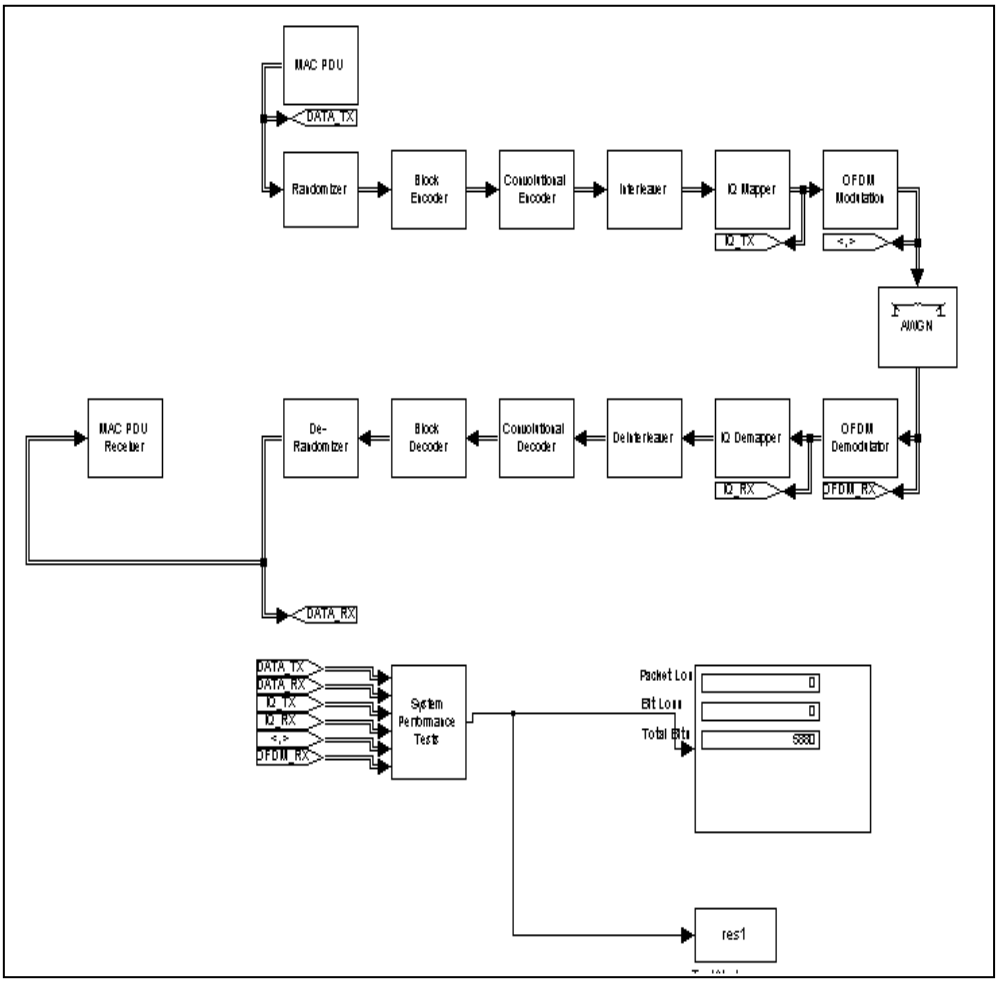

Fig. 1: WiMAX Model in Matlab Simulink

Table 1: Characteristics of WiMAX Simulation Model [6]

Standard	802.16e
Data Rate	70Mbps
Carrier Frequency	10GHz
Channel Size (Bandwidth)	1.5 MHz to 20 MHz
Modulation	QPSK, QAM
Topology	Mesh
Radio Technology	OFDM and OFDMA

2.1. MAC Layer of WIMA

The WiMAX MAC layer acts as a link between the upper transport layer and the physical layer. The convergence sub-layer is included in the IEEE802.162004 and IEEE802.16e2005 [3] MAC designs. It can be associated with various upper layer protocols such as ATM, IP and Ethernet. Packet header suppression is also supported to reduce MSDU overhead. The WiMAX MAC layer supports very high peak bit rates while providing quality of service comparable to ATMs. The Generic MAC Header (GMH) is placed before each MAC frame and contains the frame length, connection identifier (CID), CRC existence quality bits, sub-headers, secure keys, and encryption flags. ARQ (Automatic Repeat Request) [4] is also supported by WiMAX MAC to request a retransmission. MAC is further divided into three layers:

a. Convergence Sub-layer (CS),
b. Common Part Sub-layer (CPS),
c. Security Sub-layer (SS).

2.2. Quality of service

There are several applications for which the WiMAX MAC layer may be used, including voice and multimedia services. Non-real-time traffic, variable bit rate and greatest efficiency are all supported by the system. Multi-user and per-device connections are supported. Each connection has its own identification, which is used to control the quality of service. Traffic priority, burst and acceptable rate limits, ARQ type and delay limits, data unit type and size, and other QoS parameters are all part of this set of specifications.

2.3. OFDM

OFDM is based on the Multi-Carrier Modulation (MCM) transmission technology [4]. The MCM principle describes splitting one input bitstream into multiple parallel bitstreams, subsequently utilized to modulate various subcarriers. Each sub-carrier is separated from the others by a guard band to prevent them from overlapping. Bandpass filters are used on the receiver side to separate the spectra of different sub-carriers. OFDM is a spectrally efficient MCM technology that uses closely spaced orthogonal subcarriers with overlapping ranges. By executing FFT on the input stream, orthogonality is attained. A high data rate is achieved by merging numerous low data rate subcarriers into a single carrier. In multipath situations with short symbol durations, Inter-Symbol Interference (ISI), a common issue, may be minimised or eliminated, depending on the coherence time.

2.4. Communication Channel

Data is sent via a wireless channel with a specific bandwidth to obtain a greater data rate and preserve service quality. When delivering data over the air, it must contend with environmental challenges such as unexpected noise. Because of this, multipath delay spread, fading, path loss, Doppler spread and co-

channel interference, among other things, are all factors that affect data transmissions. WiMAX technology has significant environmental impacts.

2.5. Additive White Gaussian Noise (AWGN)

There has been substantial modelling of the optical wireless channel, and the ideal modulation scheme for a particular channel is well established. This channel is called the AWGN (noise). This noise channel model works well for satellite and deep space communication, but not for terrestrial transmission because to multipath, terrain obstruction, and interference. AWGN is used to mimic channel noise. The mathematical statement r(t)=s(t)+ n is the same as in the received signal (t). This went through the AWGN channel, where s (t) represents the sent signal and n (t) means the background noise. The AWGN Channel block replaces a real or complex input signal with white Gaussian noise. The AWGN channel capacity equation 1 is if the average received power is P'[W] and the noise power spectral density is N0 [W/Hz].

$$c_{awgn} = W \log_2 \left(1 + \frac{p'}{N_0 W}\right) {}^{Bit}/_{Hz}. \quad (1)$$

Where $\frac{p'}{N_0 W}$ is the received signal-to-noise ratio (SNR)

Shannon–Hartley theorem equation 2 is used to calculate the channel capacity of an additive white Gaussian noise channel with a bandwidth of B Hz and a signal-to-noise ratio of S/N.

$$C = B \log \left(1 + \frac{S}{N}\right). \quad (2)$$

2.6. Channel Coding

This enhances communication performance by altering signals and making them more resistant to interference, fading, and other channel defects. In order to encode a channel, randomization, FEC, and interleaving are all necessary steps.

3. MODULATION TECHNIQUES

Quadrature Amplitude Modulation (QAM) is a unique modulation method used by WiMAX that combines ASK and PSK (QAM). In QAM, a signal's amplitude and phase change at the same time. WiMAX networks provide a variety of QAM options, depending on the network's speed and range. For example, 64 QAM has a higher throughput, but it is limited in its range, whereas 16 QAM is more expansive, but it has less bandwidth. Quadrature Phase Shift Keying (QPSK) and Quadrature Amplitude Modulation (QAM) are WiMAX modulation methods.

3.1. Binary Phase Shift Keying (BPSK)

Because it uses two phases separated by 180o to represent binary digits, it's also known as two-level PSK (0, 1). This phase modulation is very effective and resistant to disturbances, especially in low data rate applications—the basic equation 3—because it can only alter one bit/symbol at a time.

$$s(t) = \begin{cases} A\cos(2\pi f_c t) & \text{for binary 1} \\ A\cos(2\pi f_c t + \pi) & \text{for binary 0} \\ A\cos(2\pi f_c t) & \text{for binary 1} \\ -A\cos(2\pi f_c t) & \text{for binary 0} \end{cases} \quad (3)$$

3.2. Quadrature Amplitude Modulation (QAM)

Wireless protocols use QAM modulation technology extensively. Two independent signals may be sent simultaneously using ASK and PSK, but one of them has to be 90 degrees offset from the other. The fundamental equation 4 is:

$$s(t) = d_1(t)\cos 2\pi f_c t + d_2(t)\sin 2\pi f_c t\,. \quad (4)$$

3.3. Quadrature Phase Shift Keying (QPSK)

This is also referred to as four-level PSK since each piece represents several bits. Each symbol has two bits and employs a phase shift of /2, which shifts the phase 90 degrees rather than 180 degrees. The fundamental equation is 5.

$$s(t) = \begin{cases} A\cos\left(2\pi f_c t + \frac{\pi}{4}\right) & \text{for binary 11} \\ A\cos\left(2\pi f_c t + \frac{3\pi}{4}\right) & \text{for binary 01} \\ A\cos\left(2\pi f_c t - \frac{3\pi}{4}\right) & \text{for binary 00} \\ A\cos\left(2\pi f_c t - \frac{\pi}{4}\right) & \text{for binary 10} \end{cases} \quad (5)$$

4. EXPERIMENTAL SIMULATION RESULTS

Emergency communications, military communications, 4G / 5G wide area coverage, and ultra-dense network scenarios can all benefit from mobile ad hoc networks [13]. Figure 1 shows a Simulink model of the WiMAX MAC layer (medium access control). This model uses AWGN (Additive White Gaussian Noise) and various modulation schemes such as QPSK (Quadrature Phase Shift Keying) and QAM (Quadrature Amplitude Modulation) (Quadrature Amplitude Modulation). Figures 2, 3, and 4 show the performance of the WiMAX MAC layer based on the simulation results. Table 2 shows the parameters used in this study.

Table 2: Performance of IEEE 802.16e MAC layers Parameters

Parameters	Value
Channel	AWGN
Modulation Techniques	QPSK and QAM
IFFT (Input port size)	256
CC Code Rate	1/2
Channel Size (Bandwidth)	10 MHz
Radio Technology	OFDM
RS Encoding (Codeword length N)	255
RS Encoding (Message length K)	239
Input Signal Power	0.01 ohm(Watts)
Simulation Mode	Normal
Simulation time	10 Sec
Trellis structure	poly2trellis(7, [171 133])
Generator polynomial input bit by PN- sequence	[1 0 0 0 0 0 0 0 0 0 0 0 0 0 1 1]

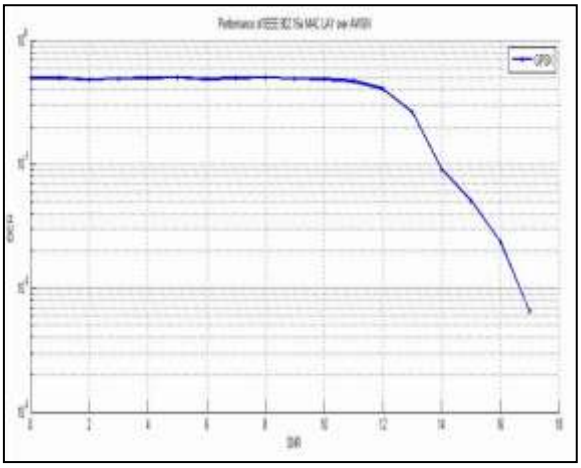

Fig.2: IEEE 802.16e MAC Layer Performance over AWGN with QPSK Modulation Scheme

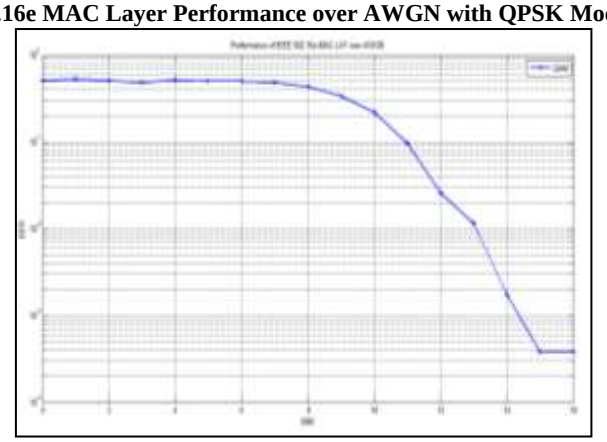

Fig.3: IEEE 802.16e MAC Layer Performance over AWGN with QAM Modulation Scheme

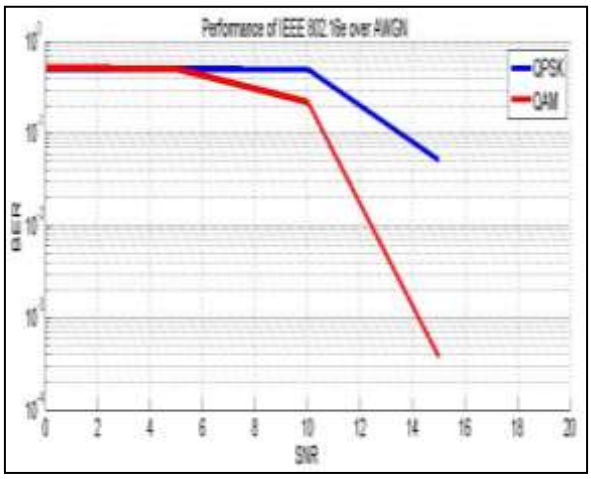

Fig.4: Performance of the MAC Layer over an AWGN Channel compared to QPSK Modulation and QAM

5. CONCLUSION

This study shows the performance of the MAC layer of an AWGN channel for various modulation schemes. BER vs. SNR is an important performance metric for wireless communication systems. The performance of the QAM system for BER is lower than the performance of the QPSK system at a particular SNR level for a particular signal power.

References

[1] S. M. Lalan Chowdhury, P. Venkateswaran "Performance Analysis of WiMAX PHY" by, IEEE CASCOM Post Graduate Student Paper Conference 2010 Jadavpur University, Kolkata, India. Nov. 27, 2010; pp 13-16

[2] M. Patidar, R. Dubey, N. Kumar Jain and S. Kulpariya, "Performance analysis of WiMAX 802.16e physical layer model," 2012 Ninth International Conference on Wireless and Optical Communications Networks (WOCN), 2012, pp. 1-4, doi: 10.1109/WOCN.2012.6335540.

[3] Muhammad Nadeem Khan, Sabir Ghauri "The WiMAX 802.16e Physical Layer Model" by, the University of West of England, United Kingdom,

[4] Neha Rathore "Simulation of WiMAX 802.16 MAC Layer Model: Experimental Results", IJECT Vol. 3 Issue 1, Jan.- March 2012, R.K.D.F. Institute of Technology & Science, Bhopal, MP, India

[5] Pavani Sanghoi, Lavish Kansal " Analysis of WIMAX Physical Layer using Spatial Diversity under Different Fading Channels", International Journal of Computer Applications (0975 – 8887) Volume 45– No.20, May 2012

[6] M.A. Mohamed, M.S Abou-El-Sound, and H.M. Abdel-Atty "Performance and Efficiency of WiMAX-MAC-Layer: IEEE-802-16e", IJCSNS International Journal of Computer Science and Network Security, VOL.10 No.12, December 2010

[7] Jang, J., Natarajan, B. "Performance analysis of an enhanced cooperative MAC protocol in mobile ad hoc networks." J Wireless Com Network 2018, 76 (2018). https://doi.org/10.1186/s13638-018-1088-3.

[8] Yaohua Chen, Waixi Liu, "MAC Layer Energy Consumption and Routing Protocol Optimization Algorithm for Mobile Ad Hoc Networks", Complexity, vol. 2021, Article ID 6687189, 12 pages, 2021. https://doi.org/10.1155/2021/6687189.

[9] Jian Li, Guoqing Liu, and Georgios B. Giannakis, Fellow, IEEE, "Carrier Frequency Offset Estimation for OFDM-Based WLANs", IEEE SIGNAL PROCESSING LETTERS, VOL. 8, NO. 3 MARCH 2001.

[10] IEEE 802.162004, "IEEE Standard for Local and Metropolitan Area Networks Part 16: Air Interface for Fixed Broadband Wireless Access Systems", 1 October 2004

[11] William Stallings, "Wireless: Communications and Networks", Page 139-146, Pearson Education, 2002.

[12] WiMAX Forum, "Mobile WiMAX – Part 1: A Technical Overview and Performance Evaluation", August 2006.

[13] Yutao Liu, Yue Li, Yimeng Zhao, Chunhui Zhang, "Research on MAC Protocols in Cluster-Based Ad Hoc Networks", Wireless Communications and Mobile Computing, vol. 2021, Article ID 5513469, 12 pages, 2021. https://doi.org/10.1155/2021/5513469.

[14] H. Chun et al., "Optimum Device and Modulation Scheme Selection for Optical Wireless Communications," in Journal of Lightwave Technology, vol. 39, no. 8, pp. 2281-2287, 15 April15, 2021, doi: 10.1109/JLT.2021.3051379.

Academic Guru Publication House

Research and Development
In Engineering Technology
Volume 1
Year: 2021

AG PH Books

HEAT TRANSFER IN SOLAR THERMOCHEMICAL REACTOR USING TAGUCHI'S METHOD

Vikram Kumar[1*]

[1]*Research Scholar, Department of Mechanical Engineering, Sagar Institute of Research and Technology, Bhopal*

Abstract

Solar-driven thermochemical reaction systems utilising concentrated solar radiation for the synthesis of syngas and hydrogen (primarily CO and H_2) are now widely regarded as a viable alternative to conventional fossil fuels in solving energy and climate change issues. Thermal analysis of a thermochemical reactor system is the subject of this study. During the study, several situations of porosity, fluid medium entry velocity, and solar irradiation intensity are taken into account. In order to discover the optimal configuration for porosity, intake velocity, and solar irradiance for the full reactor system, the Taguchi L27 orthogonal approach was used.

Keywords: Solar energy, hydrogen, Thermochemical reactor, Porous media, Taguchi technique, CFD.

1. Introduction

As nations aim to reduce their dependence on oil, engineers and scientists are searching for new ways to meet their ever-increasing energy demands. It is possible to satisfy these demands using a renewable energy source such as concentrated solar thermochemical technology (CST). Liquid fuels produced by concentrating solar power and thermochemistry may be easily incorporated into the existing energy grid. A solar thermochemical reactor has a capacity to do exactly that; however, such reactors are still in their developmental stage. Because of the cost and time needed to fabricate such reactors, it is of great benefit

* ISBN No. 978-81-953278-9-8

to evaluate and modify reactor designs computationally before a final design is chosen. First though, solar energy engineering is considered from the very beginning of its development.

1.1. Thermochemical Reactor

A wide variety of reactors have been developed over the years, using different concepts and cycles. The common denominator between all these reactors is that they were designed to be solar reactors that produce some kind of fuel by means of thermochemical cycling. It is typical for a research group to design a reactor and develop more reactor prototypes improving upon that design. Most of the reactor models presented here, however, is unrelated and developed by separate research groups. In other words they are not being presented as a design progression. In general, each reactor and its corresponding results, computational modeling, and design development is complex and to go into such detail would go beyond the focus of this section. The purpose here is to lay a basic foundation for the reactors that have been developed.

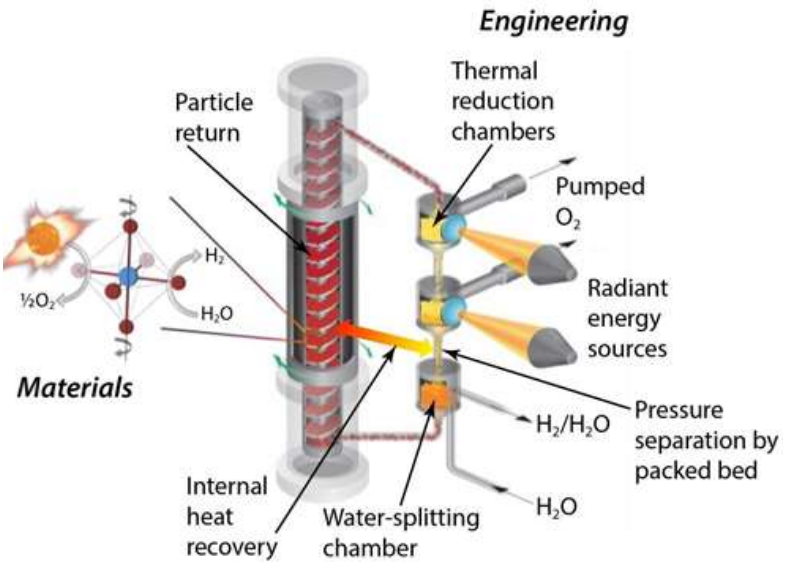

Figure 1: Thermochemical Reactor

Types of Thermochemical reactor

- High Temperature Particle Reactor
- Zinc Oxide Tubular and Windowed Reactors with Carbon reduction
- Honey comb Solar Reactor
- Rotary-type solar reactor
- Two-cavity solar reactor
- Zinc Oxide Particle Reactor
- Gravity-Fed solar-thermochemical reactor
- Counter-Rotating-Ring Receiver/ Reactor/ Recuperate (CR5)

1.2. Objectives of the Study

The following objectives are proposed in the present work,

1. The simulation is carried out on the LTNE model of the solar thermochemical reactor.
2. Factor of solar irradiance is considered during analysis.
3. Three different cases of porosity, intensity of solar irradiance and fluid inlet velocity is considered in the analysis.
4. In order to identify the most optimum configuration values of porosity, solar irradiance and fluid inlet velocity; Taguchi L27 optimization technique is used via MINITABS software.
5. Validation of CFD results with existing constraints as per the base paper.

2. Literature Review

Yan et al., 2019 [1] Hydrogen, gas hydrocarbons, as well as liquid biofuels may all be produced using the "solar thermal electrochemical process (STEP)". Methane, n-pentane, and other light hydrocarbons in the gaseous stage were highly congested as a result of the thermal electrolysis process. The chemistry of the STEP is explained in this publication, which shows how the biomass is transformed into biofuels and hydrogen. The presentations of the thermo/electro iatrogenic radical reactions are presented in a simplified form with the help of series manner. To rework the solar biomass towards biofuels as well as hydrogen, the systems are designed from the power of solar also with the chemical reactions as an option of ideal, in the form of green, along with property, as well as reclaimable operation.

Moser, Pecchi and Fend, 2019[2] Analysis and additionally the techno-economic are evaluating the designated path of solar hydrogen production supported thermochemical cycles. The study of solar energy is focused on the concentrated solar power (CSP) solar power is employed so that the two-step thermochemical cycle can run or work easily and supported 2 completely different red-ox materials, particularly "nickel-ferrite and metal oxide (ceria)". The first step was initiated to activate as well as style the system with the enforcement of the versatile mathematical model. There is a temporal delay between the activation of one reactor in parallel and another reactor in a "nickel-ferrite-associated ceria cycle", according to a technical comparison of these cycles.

Jarimi et al., 2019[3] THS systems provide a number of advantages over conventional heat storage systems because of their high energy density and minimal heat loss when they are hermetically sealed. THS is the subject of a number of review publications. THS technology, materials, reactor design and THS thermal batteries are all covered in this paper. There we tend to combine the various reactor styles, coupled with hybrid THS systems, towards the development of improved reactor construction, numerical studies of heat and mass transfer in the style of reactor, and the implementation of thermal batteries. THS technological advancements need further study and development before they can become commercially viable, according to our extensive assessment. Information regarding the numerous studies and gaps in research will be provided by this literature.

Guene Lougou et al., 2018[4] Solar thermochemical reactor was used as an experimental check on the basis of the laboratory-scale. The impact is seen at the time of transfer of heat also with the flow of fluids and the results are bought on the structural parameters that are in the expression of intensity in delicate irradiance, the flow of mass rate, stability rate of heat transfer, emissivity of quartz and inner wall surface, the porosity as well as extinction stability that is investigated on the basis of planned solar cavity receiver. Temperatures dropped significantly as a result of thermal losses via radiation, convection and semi-conductive heat transfer. The comparison between experimental and numerical findings is undertaken for model validation.

Huang et al., 2018 [5] Industrial gas-to-liquid conversion technology relies heavily on the conversion of methane to syngas, a process that requires a significant amount of energy. Here we tend to present an extremely selective and long-lasting iron-based La0.6Sr0.4Fe0.8Al0.2O3-δ. Using a solar-driven thermochemical process, oxygen carriers are employed to produce syngas. During redox cycling, a dynamic structural transition occurs between the perovskite section and a FeO oxides core–shell composite. As a micro-membrane, the compound shell inhibits coke deposition by preventing methane from directly coming into touch with new iron (0). Avoiding direct contact with methane and fresh iron, the micro-membranes of oxides form a micro-membrane.

Falter and Pitz-Paal, 2018 [6] It is investigated that, the fuel production by a solar thermochemical process is a good choice for de-carbonization of the transport sector. victimization ceria because of the material that is reactive in nature and hence, the latest data reveals that the demand of inert gas as well as the demand of energy for “vacuum pumping from the fiction”, there is a balance in the energy of thermo-setup is analyzed for “vacuum pumping and inert gas sweeping”, and therefore the required method parameters for reaching high efficiencies are mentioned. As the temperature drops below 1900 K, the thermochemical energy conversion efficiency increases by 20%, the pump efficiency is increased by 50%, the volume-quantity relation increases by 5000 solar units, and the energy recovery efficiency from the gases and therefore the solid component increases by 70%.

3. METHODOLOGY

3.1. Steps of working

1. A solar thermochemical reactor with porous media was designed and modelled in CATIA V5 using the specified base paper.
2. Import the CATIA V5 file into the ANSYS Fluent workbench by converting it to .STEP format.
3. Allocating names to the thermo - chemical reactors model's many components.
4. Thermochemical reactor model meshing for simulation purposes.
5. Assisting in the selection of appropriate boundary conditions for the chosen base paper.
6. Assigning the model's material characteristics.
7. Configuring your computer so that CFD analysis may be performed properly.

8. After completing the simulation, it's time to evaluate the findings.
9. Using the Taguchi L27 approach, the most optimal results may be achieved.

3.2. Design of Experiment

Experimental design tactics have been intensively explored by statisticians since the early twentieth century, but they were difficult for practitioners to implement. By making it easy for users with little statistical data, Taguchi's technique of experimentation has been widely accepted in the engineering and scientific communities. Taguchi is fond of the following three items:

- "Larger the better (for example, agricultural yield)";
- "Smaller the better (for example, carbon dioxide emissions)"; and
- "On-target, minimum-variation (for example, a mating part in an assembly)".

Table 3.1 Level selection

Level	1	2	3
Porosity	0.6	0.7	0.9
Radiation	1400	1500	1700
Velocity	0.003	0.004	0.006

4. RESULT AND DISCUSSION

4.1. Results

After geometry definition and mesh generation model analyzed by the FLUENT software based on the above assumptions.

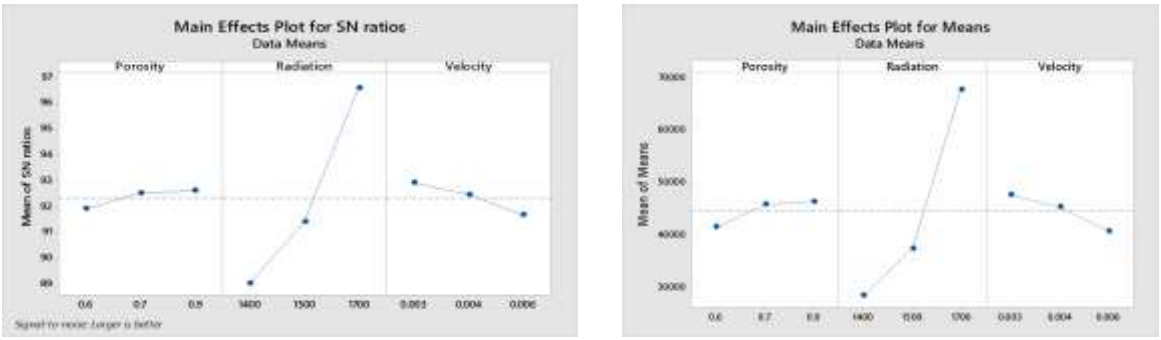

Figure 2: (a) Plots for SN Ratio; (b) Main affect Plot for Mean Ratio

Table 4.1 S/N Ratio and mean calculation

Porosity	Radiation	Velocity	Total Heat Transfer	S/N Ratio
0.6	1400	0.003	28916.33	89.22286
0.6	1400	0.004	31057.98	89.84346
0.6	1400	0.005	27493.87	88.78472
0.6	1500	0.003	36373.45	91.21569
0.6	1500	0.004	35167.88	90.92292
0.6	1500	0.006	35396.1	90.97911
0.6	1700	0.003	70885.86	97.01119
0.6	1700	0.004	67227.43	96.55093
0.6	1700	0.006	60006.48	95.56396
0.7	1400	0.003	31003.54	89.82823
0.7	1400	0.004	29582.7	89.42076
0.7	1400	0.006	26915.8	88.60015
0.7	1500	0.003	41578.54	92.37738
0.7	1500	0.004	39531	91.93876
0.7	1500	0.006	35316.64	90.95959
0.7	1700	0.003	70890.29	97.01174
0.7	1700	0.004	67209.11	96.54856
0.7	1700	0.006	60373.05	95.61686
0.9	1400	0.003	31003.54	89.82823
0.9	1400	0.004	29582.7	89.42076
0.9	1400	0.006	26915.8	88.60015
0.9	1500	0.003	41578.54	92.37738
0.9	1500	0.004	39531	91.93876
0.9	1500	0.006	35316.64	90.95959
0.9	1700	0.003	70890.29	97.01174
0.9	1700	0.004	67209.11	96.54856
0.9	1700	0.006	60373.05	95.61686

Table 4.2 Response Table for Signal to Noise Ratios

Level	Porosity	Radiation	Velocity
1	91.90	89.04	92.91
2	92.52	91.41	92.45
3	92.61	96.59	91.67
Delta	0.71	7.55	1.25
Rank	3	1	2

Table 4.3 Response Table for Means

Level	Porosity	Radiation	Velocity
1	41364	28341	47515
2	45713	37291	45226
3	46280	67725	40616
Delta	4917	39383	6899
Rank	3	1	2

4.2. ANOVA

It is possible to use an applied math approach called ANOVA to see whether two or more groups' methods are significantly different from each other. Using a variety of samples, an analysis of variance examines the influence of one or more variables.

Table 4.4 ANOVA Contribution table of parameters

Source	DF	Seq. SS	Contribution	Adj. SS	Adj. MS	F-Value	P-Value
Porosity	2	0.488	0.19%	0.488	0.244	2.42	0.155
Radiation	2	242.303	96.29%	242.303	121.151	1200.50	0.000
Velocity	2	6.820	2.71%	6.820	3.410	33.79	0.000
Error	20	2.018	0.80%	2.018	0.101		
Total	26	251.629	100%				

4.3. Result Validation

"When porosity is 0.9 radiation is 1700 K and velocity is 0.003 m/s"

Table 4.5 Predicted Values

Porosity	Radiation	Velocity
0.9	1700	0.003

And the predicted values of SN curve and mean ratio are,

Table 4.6 Predicted value of S/N Ratio

SN Ratio
97.17546

4.4. Comparison result of base paper

Table 4.7 Comparison result base paper and present work

Base Paper	Present Work
The base paper is focus to determine the temperature, velocity and pressure distribution by using CFD analysis.	In present work the study is focus to optimize the temperature, velocity, pressure and heat transfer rate using TAGUCHI'S method to after that determine the temperature, velocity and pressure distribution by using CFD analysis.
In base paper single model is simulate in 0.8 porosity limit.	In present work porosity is vary at the value 0.6, 0.7 and 0.9 porosity limit is used and compare the performance of solar thermochemical reactor.
In base paper the value of velocity is used to flowing fluid is 0.005 m/s, and inlet air temperature is used 600K and solar radiation temperature is 1600K.	In present work three different velocity is consider which are 0.003, 0.004 and 0.006 m/s, and three different solar radiation temperature 1400, 1500, 1700 K.

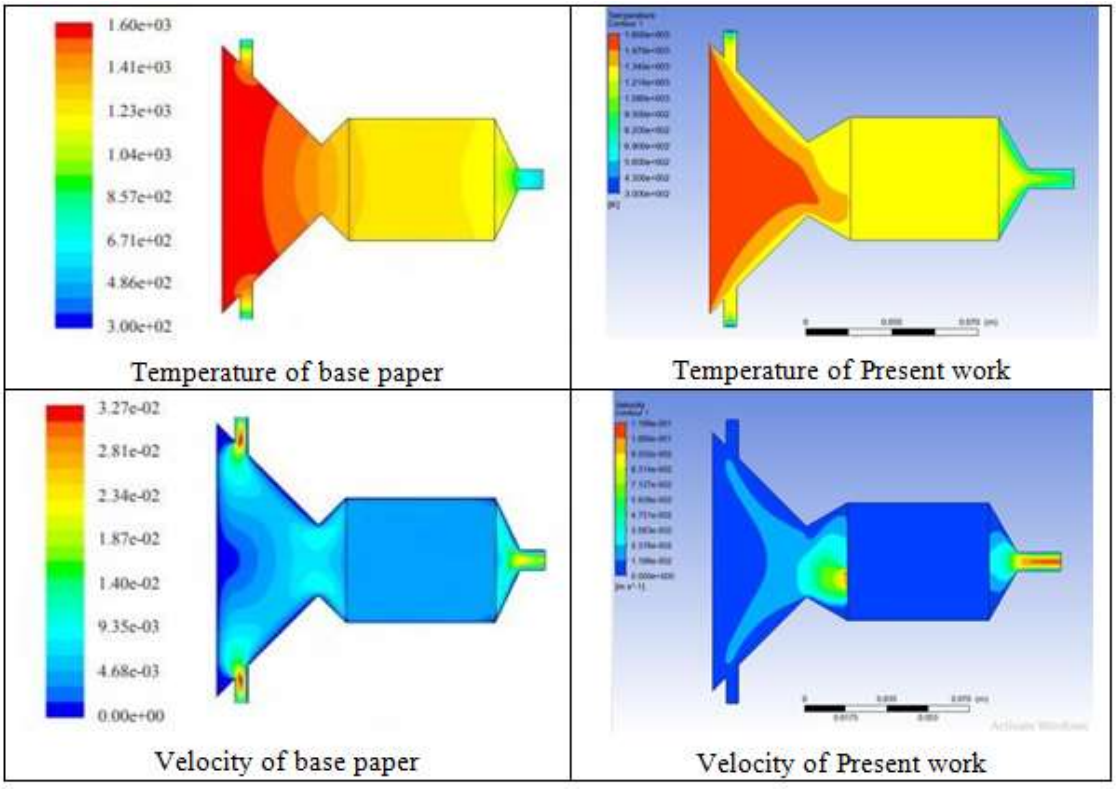

All the base paper condition is considered in present thesis work, the work is including to determine better heat exchange between inlet to outlet by determining Maximum heat transfer rate. After performing analysis, it is seen that every condition which is used in analysis (Inlet Velocity, Inlet temperature porosity and solar radiation temperature) are play major role which affect the heat transfer rate. The most optimize value is determine by using Taguchi and ANOVA method which is not used base paper.

5. CONCLUSION

There are a various type of reactors available. And many researches are on-going on the development of reactors efficiency, improved solar irradiance, heat transfer rate etc. These all parameters can be improved by changing design, material, velocity etc. In this research study, 3D model of solar thermochemical reactor is designed in CATIA and the simulations are performed with varying various parameters in Ansys. Following are the conclusion from the above study is obtained:

- When the porosity is 0.9, the greatest results are shown for overall heat transfer rate.
- The resulting sun irradiance is 1700 K.
- Moreover, the inlet velocity is 0.003 m/s.
- A total heat transfer rate is computed when the Taguchi technique is used to verify new input parameters in ANSYS for CFD analysis.
- Porosity of 0.9, sun intensity of 1700 K, and intake velocity of 0.003 m/s were used to calculate the maximum heat transfer rate of 72239.19 W.

References

1. C. Yan et al., “Solar Thermal Electrochemical Process (STEP) action to biomass: Solar thermo-coupled electrochemical synergy for efficient breaking of biomass to biofuels and hydrogen,” Energy Conver. Manag., vol. 180, no. August 2018, pp. 1247–1259, 2019.
2. M. Moser, M. Pecchi, and T. Fend, “Techno-economic assessment of solar hydrogen production by means of thermo-chemical cycles,” Energies, vol. 12, no. 3, 2019.
3. H. Jarimi, D. Aydin, Z. Yanan, G. Ozankaya, X. Chen, and S. Riffat, “Review on the recent progress of thermochemical materials and processes for solar thermal energy storage and industrial waste heat recovery,” Int. J. Low-Carbon Technol., vol. 14, no. 1, pp. 44–69, 2019.
4. B. Guene Lougou, Y. Shuai, R. Pan, G. Chaffa, and H. Tan, “Heat transfer and fluid flow analysis of porous medium solar thermochemical reactor with quartz glass cover,” Int. J. Heat Mass Transf., vol. 127, pp. 61–74, 2018.
5. C. Huang et al., “In situ encapsulation of iron(0) for solar thermochemical syngas production over iron-based perovskite material,” Commun. Chem., vol. 1, no. 1, p. 55, 2018.

6. C. Falter and R. Pitz-Paal, “Energy analysis of solar thermochemical fuel production pathway with a focus on waste heat recuperation and vacuum generation,” Sol. Energy, vol. 176, no. September, pp. 230–240, 2018.
7. H. Zhang et al., “Analysis of thermal transport and fluid flow in high-temperature porous media solar thermochemical reactor,” Sol. Energy, vol. 173, no. July, pp. 814– 824, 2018.
8. H. Wu, G. Xie, Z. Jie, X. Hui, D. Yang, and C. Du, “Research progress about chemical energy storage of solar energy,” IOP Conf. Ser. Earth Environ. Sci., vol. 108, no. 5, 2018.
9. M. M. Salvatore Boccardi, Francesco Ciampa, “Ac ce us p,” J. Alloys Compd., 2018.
10. T. Kodama, S. Bellan, N. Gokon, and H. S. Cho, “Particle reactors for solar thermochemical processes,” Sol. Energy, vol. 156, pp. 113–132, 2017.
11. C. N. R. Rao and S. Dey, “Solar thermochemical splitting of water to generate hydrogen,” Proc. Natl. Acad. Sci., vol. 2017, p. 201700104, 2017.
12. H. Xing, Y. Yuan, Z. Huiyuan, S. Yong, L. Bingxi, and T. Heping, “Solar thermochemical hydrogen production using metallic oxides,” Energy Sources, Part A Recover. Util. Environ. Eff., vol. 39, no. 3, pp. 257–263, 2017.
13. H. I. Villafán-Vidales, C. A. Arancibia-Bulnes, D. Riveros-Rosas, H. Romero-Paredes, and C. A. Estrada, “An overview of the solar thermochemical processes for hydrogen and syngas production: Reactors, and facilities,” Renew. Sustain. Energy Rev., vol. 75, no. November, pp. 894–908, 2017.
14. X. Huang et al., “Exergy distribution characteristics of solar-thermal dissociation of NiFe2O4 in a solar reactor,” Energy, vol. 123, pp. 131–138, 2017.
15. B. Guene Lougou, Y. Shuai, X. Chen, Y. Yuan, H. Tan, and H. Xing, “Analysis of radiation heat transfer and temperature distributions of solar thermochemical reactor for syngas production,” Front. Energy, vol. 11, no. 4, pp. 480–492, 2017.

Academic Guru Publication House

Research and Development
In Engineering Technology
Volume 1
Year: 2021

AG PH Books

A REVIEW ON DESIGN ANALYSIS AND OPTIMIZATION OF FRONT AXLE FOR COMMERCIAL VEHICLE

Tarun Kumar Yadav[1*], Anshul Gangele[2]

[1]*Research Scholar, Mechanical Engineering, Shree Jagdishprasad Jhabarmal Tibrewala University, Vidhyanagari Jhunjhunu*

[2] *Principal,Adina Institute of Science & Technology, Sagar*

Abstract

To remain competitive in today's market, it is critical for manufacturers to provide new products to consumers at a lower cost and quicker than their competitors. The Front axle beam accounts for up to 40% of the vehicle's load-carrying capability. The existing measuring system shows quite a poor acceptability for the proposed design of the cross pin, except for the micrometer. A review is presented here on design analysis and optimization of cross pin. Literature is also studied of researchers and presented here on the same topic.

Keywords: Front Axle Beam,Cross pin; .Lean manufacturing; Design for manuifacturing.

1. INTRODUCTION

When it comes to manufacturing, there is a vast range of disciplines and skills involved, and a large range of gear, tools and equipment with a variety of automation levels like computers and robots. There are a variety of demands and advances that must be taken into consideration when it comes to manufacturing.[1]

* ISBN No. 978-81-953278-9-8

Apart from that, future technicians must be familiar with the fundamental requirements of workshop routines, such as the number of people, tools and materials needed to do the job properly as well as the various methods, revenue streams, and other infrastructure conveniences that must be properly positioned for optimal shop or plant layouts and other support solutions in the field or industry within a "properly planned manufacturing firm".[2]

1.1. Machining

Machined products are made by cutting material (typically metal) into a specific form and dimension by using a controlled material-removal process. Subtractive manufacturing refers to procedures that use controlled material removal as a common theme, whereas additive manufacturing refers to methods that use controlled material addition. Although the exact meaning of the word "controlled" in the term is up to interpretation, it usually invariably connotes the use of machine tools (in addition to just power tools and hand tools).[3]

In addition to metal items, machining may also be used to create products from materials such as wood and plastic as well as ceramic and composites. A machinist is someone who specialise in machining. The term "machine shop" refers to a space, a facility, or an organisation where machining is carried out. "Computer numerical control (CNC)" is used to control the movement and functioning of mills, lathes, and other cutting equipment in most contemporary machining operations. Machine businesses save money on labour expenses by using a CNC machine that works without a human operator. [4]

1.2. Front axle

The front axle bears the weight of the vehicle's front end, as well as providing steering assistance and absorbing road shocks. Even though they're considered "dead axles", tiny automobiles with compact designs and four-wheel drive have "live front axles".

This axle, located in the front of the car, helps with steering and absorbs road stress. The beam, swivel pin, track rod, and stub axle are the four primary components. Carbon steel and nickel steel are the most common materials for front axles since they are both very durable.[5]

Figure 1: Front Axle Shaft

Front axle are responsible for ascending vehicles of the front wheels [6]:

a) Posterior part of the vehicle is supported by front axle.
b) It provides steering facility.
c) Due to the irregular road surface, shock is absorbed by front axle.
d) While applying brake on vehicles torque is applied.

There are two types of front axles:

i. Dead front axle:

The term “dead axle” refers to an axle that solely serves to keep the wheels on the ground. Neither power nor torque is transferred to the wheels. There are two ways to operate a vehicle: front wheel or rear wheel. In both cases, the rear axle is considered dead, while the front axle is considered precious. The dead front axle bears a great amount of weight, yet it does not spin. Its ends are shaped so that they fit snugly over the stub axles on each side. [7]

ii. Line front axle:

Line axles are used to transmit power from gear box to front wheels. Line front axles although, front wheels. Line front axles although resemble rear axles but they are different at the ends where wheels are mounted.

1.3. Design for Manufacturing (dfm)

A part's or product's design may be optimised to make it easier and more cost-effective to manufacture, known as “Design for Manufacturing (DFM) or Design for Manufacturability (DFM)”. “Design for manufacturing (DFM)” is the process of reducing manufacturing costs by designing or engineering an item more effectively at the product design stage. This enables a manufacturer to detect and avoid errors or anomalies.

Five principles are examined during a DFM. They are:

1. Process
2. Design
3. Material
4. Environment
5. Compliance/Testing

Ideally, DFM should take place from the beginning of the design phase, before any tooling has ever been made. All the players, from engineers to designers to contract manufacturers to moldbuilders to material suppliers must be included in a successfully implemented DFM. "Cross-functional" DFM is designed to question the design, examining the design at all levels, from components to systems to the whole. This is done to guarantee that the design is optimised and does not include superfluous costs.[8]

1.4. Lean manufacturing

To improve production efficiency and total customer value while simultaneously reducing waste, many industrial organisations and enterprises have adopted a set of ideas, tools, and procedures known as Lean, sometimes known as “Lean Manufacturing (LM), Lean Enterprise, or Lean Production”.

Lean is a theory that may be applied to any industrial organisation, not only manufacturing and supply chain management. The major goal of LM is to make higher-quality goods more affordable to a wider range of customers. As a result, it finally leads to a better quality of life for everyone (Melton, 2004). An LM-based manufacturing system is critical to the success of a company. The most important aspects of LM are as follows:

i. Reduce production-line waste.

ii. Lower production costs by integrating quality into the manufacturing process.

iii. Develop and create tools that improve the operational performance of the company.

As a result of lean's emphasis on constant improvement, there are five distinct stages to implementing it in the workplace:

i. Analysing and documenting the existing process and evaluating its efficiency and effectiveness.

ii. Determining the value and the network of the value stream with precision.

iii. A third part of the process is identifying and proposing modifications to remove the causes of undesired impacts.

iv. Achieved performance is measured

v. Applying the suggested improvements

1.5. Principles of lean manufacturing

When it comes to lean manufacturing, the aim is to reduce waste—the non-value-added components in any process. There is always some waste in a process that hasn't gone through lean several times. Lean has the potential to reduce costs and increase competitiveness by reducing waste, increasing productivity, reducing cycle time, and reducing the amount of material used in the production process. Consider the fact that lean is not just applicable to manufacturing. There are a number of ways it may enhance teamwork, inventory management, and customer relations.

Figure 2: Process of lean manufacturing

1.6. Standardization of product and processes

It is the purpose of standardisation to guarantee that certain industrial practises are consistent. As a result of standardisation, the production of products, corporate operations, technology, and particular mandatory procedures are all standardised. Even in the car business there has been a dramatic increase of product varieties over the last several years, according to Ulrich [9]. Customization is the only way businesses can meet the many and diverse needs of their consumers. According to Ulrich (1995), modularization is a way for increasing product diversity. It is possible to standardise components and to use the same ports in several products if they perform the same purpose [10]. The use of modular design improves the likelihood that components can be used in a variety of products. In terms of cost, performance, and product development, product standardisation is a tremendous benefit in the manufacturing sector. It is also possible for production processes to be standardised, which is the largest facilitator of consistent performance when it comes to standardised goods [11].

Standardization also aids in the security, interoperability, and compatibility of manufactured items. Involved parties include end-users, government agencies and companies, as well as standards bodies.

2. LITERATURE REVIEW

(Soyusinmez et al., 2021) [12] In this study, the kingpin parts are examined with optical microscopy, Scanning Electron Microscopy (SEM), hardness tests and %C potential analysis in order to determine the potential causes of the crack formations. By the help of the analysis, the presence of cracks became clear. There are no signs of hydrogen embrittlement. The exact outcome of the fracture could not be determined. It is seen that heat treatment of the parts is not homogeneously obtained throughout their surfaces or desired volume, and therefore fractures occur. With the present structure, it can be expected that even a low dynamic load can lead to breakage. As a result, the investigations suggest that the parts were exposed to inappropriate heat treatment parameters.

(S. H. Kim & Shin, 2020) [13] An examination of the steering pull's sensitivity is presented in this research. As part of the process of creating a steering pull model, many types of pulling forces on the tyres must be taken into consideration. These include plysteer and conicity forces as well as lateral forces resulting from slip angle and cast and kingpin lifting forces. Steering systems are also modeled since the resultant pulling forces are dampened as they are passed via the steering systems. Steering components are modeled and then assembled into a system that includes the lower body linkage and the rack and pinion gear, universal joint and the steering column with electric power steering (EPS) system. Once these two models have been combined, the final steering pull model is created. A vehicle's steering pull is approximated using a model and then compared to experimental data to ensure accuracy. We may examine the impact of several parameters, including kingpin and rack friction force and anti-rattle spring (ARS) stiffness, on steering pull using the steering pull model.

(Marcomini et al., 2016) [14] When the kingpin was installed in a fifth wheel of an off-road vehicle, it was found to be defective at the outset of use. The truck was utilised in a quarry for three months until the kingpin failed. Due to overheating, burning, and cavitation, poor grain structure may result in hot forged products. SEM investigation of the failing component revealed the presence of cavitation, which was detected by the method. Even while cavitation was shown to be a contributing factor, failure analysis findings showed that it was not the primary factor in the fracture.

(Vargas-Arista et al., 2013) [15] Fatigue Crack Propagation in AISI 4140 Steel Shielded Metal Arc Weldings is the focus of this article. Normalizing at 1200 °C for 5 and 10 hours after welding produced different austenitic grain sizes. A decrease in fracture toughness and critical crack length, as well as a transgranular brittle final fracture with an area fraction of dimple zones linking cleavage facets, were seen in three-point bending fatigue testing on pre-cracked specimens along the HAZ. The fracture length reduced as the normalization time rose, according to a fractographical examination. Zone II fatigue crack propagation was also shown to be affected by river patterns, and the ultimate brittle fracture was seen due to “transgranular quasicleavage”. The fatigue resistance of the HAZ was reduced as a result of larger grains.

(Triantafyllidis et al., 2009) [16] There are two instances of steel pin joint failures that are discussed here. There were 90 mm pins, and the failures resulted in long repair wait times. An impact fatigue fracture developed after the initial failure, which was produced by “a combination of bending and twisting fatigue”. Optical metallography and scanning electron microscopy/ electron dispersive x-ray analysis (SEM/EDS) analysis provided a better understanding of the failure mechanism of the two steel pins, since these particular components exhibited excellent fatigue characteristics in both mating fracture surfaces.

(D. H. Kim et al., 2007) [17] The static friction torque of the tyres, which is impacted by tyre loads, kingpin axis geometry, such as camber, caster, and kingpin offset, is the most critical component in estimating steering effort. Effort and rack-bar force are calculated as a function of tyre contact patch friction torque in this study. There is a good connection between calculated rack-bar force and steering effort and the observed results from a vehicle test.

3. CONCLUSION

After studying the literature review, it was observed that the existing measuring system shows quite a poor acceptability for the proposed design of the cross pin, except for the micrometer. As such, there may be need for purchasing new more sophisticated and precise measuring equipments. While, the process capability indexes of the system are within the acceptable limits for most of the characteristics of the cross pin for which the process is capable of manufacturing parts within the specified tolerance limits with very few defects, for certain characteristics it shows a poor capability.

References

[1] J. Kral, M. Palko, M. Palko, and L. Pavlikova, "Design and development of ultra-light front and rear axle of experimental vehicle," *Open Eng.*, vol. 10, no. 1, pp. 232–237, 2020, doi: 10.1515/eng-2020-0032.

[2] L. Jin, D. Tian, Q. Zhang, and J. Wang, "Optimal torque distribution control of multi-axle electric vehicles with in-wheel motors based on DDPG algorithm," *Energies*, vol. 16, no. 3, 2020, doi: 10.3390/en13061331.

[3] V. Murali, A. M. Ramananda, H. Nitin, and S. Pandit, "Design and Development of Four-Wheel Steering for All Terrain Vehicle (A . T . V)," *Int. Res. J. Eng. Technol.*, pp. 1660–1668, 2020.

[4] M. Zhileykin and A. Eranosyan, "Method of torque distribution between the axles and the wheels of the rear axle to improve the manageability of two-axle all-wheel drive vehicles," *IOP Conf. Ser. Mater. Sci. Eng.*, vol. 820, no. 1, 2020, doi: 10.1088/1757-899X/820/1/012008.

[5] W. Wang, J. Li, G. Liu, and Z. Zhang, "Simulation study on ride comfort of three-axle heavy vehicle spatial model based on rigid-elastic model and pseudo-excitation method," *J. Adv. Mech. Des. Syst. Manuf.*, vol. 14, no. 1, pp. 1–16, 2020, doi: 10.1299/jamdsm.2020jamdsm0016.

[6] BIPINWANKHEDE, "Failure Analysis of Automotive Front Wheel Drive Shaft," *J. INFORMATION, Knowl. Res. Mech. Eng.*, vol. 4, no. 1, pp. 707–713, 2016.

[7] S. Nilkanth, I. Poonawala, and M. Ramgir, "Design Optimisation of Four Wheel Drive Tractor Front Axle Housing," *Int. J. Eng. Res.*, vol. V4, no. 08, 2015, doi: 10.17577/ijertv4is080114.

[8] V. Helminen, M. Tiitu, L. Kosonen, and M. Ristimäki, "Identifying the areas of walking, transit and automobile urban fabrics in Finnish intermediate cities," *Transp. Res. Interdiscip. Perspect.*, vol. 8, no. January 2019, p. 100257, 2020, doi: 10.1016/j.trip.2020.100257.

[9] K. Ulrich, "The role of product architecture in the manufacturing firm," *Res. Policy*, vol. 24, no. 3, pp. 419–440, 1995, doi: 10.1016/0048-7333(94)00775-3.

[10] L. R. Buckendale, Detroit, and Mich., "VEHICLE DRIVE AXLE," 1997.

[11] C. Singh, L. Kumar, B. kumar Dewangan, Prakash kumar sen, and K. Shailendra Bohidar, "A Study on Vehicle Differential system," *Int. J. Sci. Res. Manag.*, vol. 2, no. 11, pp. 1680–1683, 2014.

[12] T. Soyusinmez, O. Güzelipek, T. Palandüz, and O. Ertuğrul, "Fracture Analysis of a Case-Hardened Kingpin," vol. 5, pp. 92–98, 2021.

[13] S. H. Kim and M. C. Shin, "Steering pull model and its sensitivity analysis," *Appl. Sci.*, vol. 10, no. 22, pp. 1–17, 2020, doi: 10.3390/app10228072.

[14] J. B. Marcomini, C. A. R. P. Baptista, J. P. Pascon, R. L. Teixeira, and P. C. Medina, "Failure Analysis of a Hot Forged SAE 4140 Steel Kingpin," *Int. J. Eng. Res. Sci.*, vol. 2, no. 6, pp. 102–109, 2016.

[15] B. Vargas-Arista, J. Teran-Guillen, J. Solis, G. Garcia-Cerecero, and M. Martinez-Madrid, "Normalizing effect on fatigue crack propagation at the heat-affected zone of AISI 4140 steel shielded metal arc weldings," *Mater. Res.*, vol. 16, no. 4, pp. 772–778, 2013, doi: 10.1590/S1516-14392013005000047.

[16] G. K. Triantafyllidis, A. V. Kazantzis, E. K. Drambi, E. A. Sami, and A. I. Kalantzis, "Fracture characteristics of torsion-bending fatigue and impact fatigue failure of two steel pins in a crawler excavator," *J. Fail. Anal. Prev.*, vol. 9, no. 1, pp. 23–27, 2009, doi: 10.1007/s11668-008-9196-8.

[17] D. H. Kim *et al.*, "Evaluation and experimental validation of steering efforts considering tire static friction torque and suspension and steering systems characteristics," *SAE Tech. Pap.*, no. 724, 2007, doi: 10.4271/2007-01-3641.

Academic Guru Publication House

Research and Development
In Engineering Technology
Volume 1
Year: 2021

AG PH Books

ANALYSIS OF PIPELINE EROSION BY CFD SIMULATION UNDER THE EFFECT OF SAND PARTICLES OF WATER AND ETHYLENE GLYCOL

Sandeep Gaur[1*]

[1]*Design Engineer, Design and Development, Zenith, Indore*

Abstract

Sand productions include a variety of main essential difficulties for gas and oil productions, as sand managements are increasingly becoming crucial to manage wells with high rates of sand accumulation. Approximately 70 percent of the world's gas and oil reserves are found in sand deposits. Sand erosion over a pipe bend is studied in this research, which examines and analyses many aspects to determine the sand's severity and quantity of erosion. For this work, computational fluid dynamics (CFD) was employed to analyse the fluid flow phenomenon. The sand particle sizes of 160m and 370m will be compared in this experiment to see how different percentages of water and EG may affect the results. The three primary impacts that will be investigated further are erosive rate, skin friction coefficient, and swirl velocity. Through the investigation, it can be concluded that the character of the material and the flow velocity are the most important elements influencing the rate of sand erosion in pipelines.

Keywords: Ethylene Glycol, CFD, ANSYS, Erosion rate, Skin friction coefficientsand erosion.

* ISBN No. 978-81-953278-9-8

1. INTRODUCTION

In pipeline engineering, pipe fitting deterioration and associated problems are the most common problem. Various sand control frameworks have been established throughout time to limit sand at the bottom of the well's pit. In order to prevent sand from getting into the pipeline, these methods use gravel packing at the wellhead or a screen to keep sand out. Because of their effectiveness in significantly decreasing the flow of sand into pipeline lines, these sand exclusion systems are often found in gas and oil wells as well as improved sand observation and control systems. The combination of components generated by hydrocarbons wells will lead to pipeline erosion, which will result in pipeline damage.. Demolitions such as erosion-corrosions and cavitation are only a few examples of what might go wrong. Multi-phase particle modelling focuses on the oil and gas pipeline's transportation. Concerns such as transportation of sand, vibration induced of flow, corrosion, erosion, wax, hydrates and slugging have huge impacts over the assurance of the flow. The common cause of erosion is particulates (sand and prop pants). Particulate erosion is a function of density, viscosity and velocity. For modelling the process of erosion in the pipes of oil and gas, the use of ANSYS software is made in this experimental work; thus, estimating the mechanical and pitting strength estimation. The testing of the design and configuration of the pipe over flow assurance will be done and the effects of damages caused due to erosion will be observed.

1.1. Sand impact Erosion

Particularly in small, deposited sandstone reservoirs during oil and gas abstraction, sand production is a common problem. The sand particles can be extracted from the reservoir and are formed during oil, water or gas production. Sand output will occur at the very starting of the flow or afterwards when the pressure of the reservoir or water breakout has dropped. Based on its degree of magnitude, not all sand production needs intervention, or sometimes constant sand production is admitted. Sand development is regarded as one of the hardest challenges associated with oil and gas production, and is the primary cause of several flow assurance issues, including sand effect erosion. Erosion is characterized as the loss of material from the surface of the metal that is affected by a moving fluid that with a series of mechanical acts carries small solid particles. Erosion can cause significant damage to pipelines, crippling manufacturing and facilities on the surface. Many cases were earlier reported about sand impact erosion which becomes the cause of catastrophic accidents. Some examples are shown in figure given below:

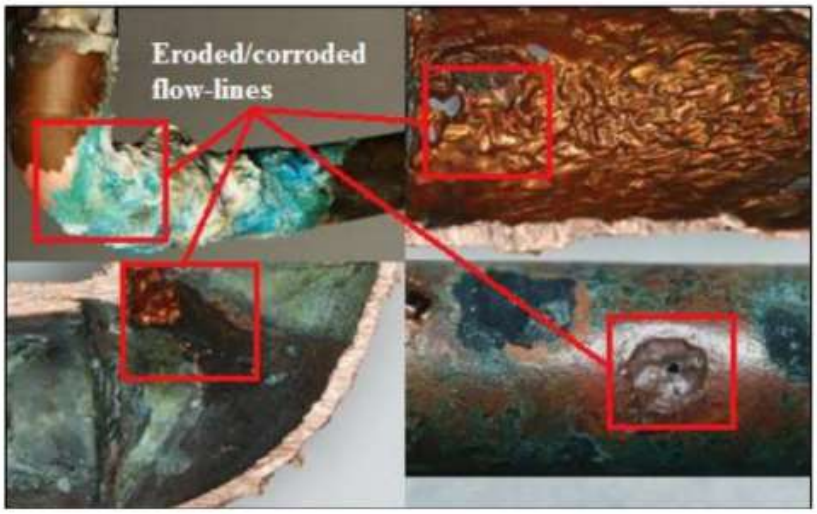

Figure 1: Illustration of severely damaged flow-lines caused by erosion

1.2. Ethylene Glycol and Deionized Water

The formula of Ethylene glycol is $(CH_2OH)_2$. The major use of ethylene glycol is for two purposes which are for antifreeze formulations as well as for the manufacturing of polyester fibers as a raw material. The properties of ethylene glycol are that it is sweet-tasting, colorless, viscous liquid and odorless.

The freezing point of EG is -36.8 °C and is mixed 50:50 by the volume with water. It should be kept in mind that fluid temperature is less cold than the evaporator surface where the cooling takes place. It might be at or below the liquid's freezing temperature. The decrease of glycol/water temperature also increases the viscosity, decreasing the flow rate inside a bath from the pump and/or the mixture. A boundary layer that holds to the much colder evaporator and protects it from the rest of the fluid could also create this higher viscosity, restricting how low a temperature can be reached and decreasing cooling power. [1]

Distilled water and deionized water both are the forms of pure water but still they are not same. As mineral ions are removed in the deionization process for producing high purity water; however, those organic molecules, which are uncharged, will not be removed because of it. The fact that it is being used in cooling has been one of the applications. Dissolved impurities like minerals are contained in varying level in the normal tap water. This contributes to electrical conductivity in it which will not be preferred for various cooling applications. The build-up of size, corrosion and erosion would also lead to these dissolved minerals. Consequently, in these applications, deionized water is favored as it has very low level of electrical conductivity and also, it won't lead to building up of unwanted scale. [2]

1.3. Objective

Pipeline is one of the most common methods of transporting fluids from one location to another in the industrial sector. From the study article, it can be observed that water is one of the most prevalent substances that flow and transfer via pipelines. Due to the presence of sand particles in the water, the pipeline deteriorates at a higher pace than normal.

- Pipeline erosion is increased when it is in continual and continuous contact with water. Further, it can be observed by employing two additional common materials that go through pipelines, ethylene glycol and water, to achieve this effect.
- As part of the CFD analysis, sand particles from Water and Ethylene Glycol are being used to simulate pipeline erosion (Used in Different Percent ratio). Comparing the rate of pipeline deterioration under various fluids, an analysis was made.
- Viscosity of the fluid has a significant impact on pipeline erosion. Consequently, the influence of viscosity on pipeline erosion rate is examined and compared.
- Elbow bending angle, flow direction and particle size will also be examined.

2. LITERATURE REVIEW

(Ejeh et al., 2020) [3] For the sake of the aforementioned investigation, this research examines crude oil dynamics in pipeline flow and identifies erosion hotspots for different pipe elbow curvatures. As part of this research, “PTM and Reynolds Averaging Navier–Stokes (RANS)” were used. Fluid dynamics and particle tracking are the primary goals of this research project. The fluid velocity magnitude was much larger in the region with the smallest curvature radius, according to post-processing results. The maximum static pressures and turbulence dissipation levels were found in low-velocity severity zones. At the elbow, erosive wear was substantially more common, and the curvature of the pipe varied with the hotspot.

(Okafor & Ibeneme, 2019) [4] Engineers working with gas and oil pipelines face a big problem: the deterioration of pipe fittings and other concerns. Various sand control frameworks have been established throughout time to limit sand at the bottom of the well's pit. Sand exclusion methods like gravel packing at wellheads and screens are used to keep sand out of pipelines. Aside from increasing visibility and control over sand, these sand exclusion systems are widely employed in oil and gas well production since they reduce sand output in the pipelines by a significant amount. In this work, the results are based on simulations done using a well-known proprietary CFD model. The degree of bending, diameter, and radius of the pipe all have an effect on the rate of erosion, which increases with fluid velocity and decreases with sand particle size. It is also possible to determine the parameter's threshold magnitude from the results.

(Wee & Yap, 2019) [5] Considered the fact that pipeline deterioration, with its safety and financial integrity problems, remains a major issue for the petroleum business The primary goal of this study work is to analyse the sand erosion behaviour in diameters of 76.2mm using CFD. Sand particles smaller than

50 micrometres seem to predict the erosion result, according to the literature; fluid particles affect sand particle movement; even little geometrical changes may have a significant impact on erosion. The Navier-Stokes equations may be solved using CFD analysis using the Eulerian-Lagrangian technique and the particle force balance secondary phase. Together with low "Reynolds number modification", the Reynolds Stress Model depicts the continuous nature of viscous boundary effects and secondary elbow flows in the near wall area for more accurate performance.. According to the study's evidence, assuming that each sand particle has a constant size leads in a wear rate forecast of more than 10%.

(Lospa et al., 2019) [6] For the purpose of determining how quickly the bends of the pipe used in the installation of the technological installation are eroded by solid particles. CFD was used to perform an investigation by the researchers, who reported their findings in this paper. The CFD analysis is used to identify the region where erosion occurred and the rate of erosion. Erosion is concentrated in the extrados of the pipe. As the curvature of the curve increases, the total erosion rate increases, causing the observed differences. The project will continue to construct an experimental test framework for erosion analysis in order to compare CFD and experimental programme results.

(Xian & Che Sidik, 2019) [7] Ethylene glycol and water are the most often utilised coolants in car cooling systems, according to our research. In nano fluids, the thermal conductivity of traditional heat transfer fluids is improved by dispersing solid particles. Using nano fluid as a coolant improves heat transfer in vehicle cooling systems, according to earlier study. After 100 hours of continuous testing, every pump space profile was examined using a 3D imaging microscope. Before and after the testing, exact weight measurements were made to determine the overall amount of material lost. According to the research, the corrosion effect currently seems to be the same whether using a basic coolant or a nano coolant. The "erosion-corrosion effect" has enhanced material loss due to the usage of nano coolant instead of base coolant. Based on the ASTM 2809-09 standard, the impact of corrosion on the impeller was found to be minimal and received a high grade. As a result, it is feasible to consider the use of all coolants in the cooling system as an option.

(N. H. Saeid, 2018) [8] The quantity of sand in the choke valve and the two-phase turbulent flow of crude oil have both been studied using 3D CFD modelling. A discrete phase mathematical model is employed to simulate sand flow and its interaction with the oil flow in the system. Using parametric analysis, the controlling factors for decreasing sand erosion in the given system are uncovered. Measurements and valve geometry may be taken from the industrial oil production project. The study's parameters include the pressure differential between the pipe's intake and output, sand flow rate, and valve opening percentage. The erosion rate fluctuation is shown in the simulation results with regard to sand flow rate, valve opening, and pressure differential. The erosion rate is found to be high for both big and small valve openings. Every instance with a wide range of pressure variations has a minimum erosion rate between 20% and 30% of the valve opening. Areas with the greatest erosion rates are predicted in the models.

3. RESEARCH METHODOLOGY

3.1. Step of working

- For the purpose of creating a pipe elbow, CatiaV5 is used to extract dimensions from a reference document.
- Converting this STP design file to ANSYS fluent workbench for meshing is done.
- The process of selecting a mesh name begins once meshing has been produced.
- With the selection of a name, a set of parameters are established.
- Work is done using a variety of fluids.
- Setting up the CFD analysis technique in the correct manner.
- After completing the simulation task, it is important to evaluate the outcomes.

3.2. Erosion Modeling

Erosion modelling is the ratio of the loss of the inner wall to the particle mass hitting on the wall that was produced by erosion. The vast majorities of erosion prediction equations are based on experimental data and are empirically derived. “Particle impact angle and impact velocity” are two of the most important factors that govern the erosion process. A 90-degree elbow is used to choose the Oka and E/CRC models for the erosion rate analysis. Due to the fact that after the data have been gathered, they will be compared to CFD and experiment results from past work, the findings of the experiment are compared to those of E/CRC and CFD once the experiment is completed.

3.3. Material Properties

This simulation's materials and attributes are detailed in table 1. Water and air are used to compare the effects of different carriers.

Table 1: Fluid Material Properties

Material	**Properties**	
	Viscosity (kg/ms)	**Density (kg/m^3)**
Water	1.003×10^{-3}	998.2
Air	1.8×10^{-5}	1.125

The sand used to investigate the impact of particle size distribution has the following properties:

Size distribution of Oklahoma No. 1 sand is used as a foundation for the Rosin Rammler Equation. Mean, minimum, maximum and spread diameters as well as the cumulative size distribution of particles are measured. There were 50,000 particles in all, which is enough to accurately portray the erosion of the surface of the earth.

4. RESULTS AND DISCUSSION

Results may be examined based on their maximum degradation rate. The simulated erosion results are derived from a range of particle sizes between 160 and 370 micrometers.

4.1. Particle size 160 µm

The study of the distribution of particle size is used to identify the increases in erosion prediction, since various sized particles have varied effects. This sand particle measures 160 m in diameter. By altering the amount of water and EG, several instances have been explored.

Table 2: Case design Particle size 160µm

Cases for particle size 160µm	Percentage of WATER	Percentage of EG
Case 1	100%	0%
Case 2	90%	10%
Case 3	80%	20%
Case 4	70%	30%
Case 5	60%	40%

To accurately anticipate the pace of erosion and identify the most vulnerable pipe places, a detailed knowledge of erosion's nature and brittleness is required. Bends are particularly vulnerable to sand damage.

4.2. Result Comparison of cases with Sand particle size 160 µm

A graph is used to compare the results of all instances. Sand particles have a diameter of 160 nm. The attributes of six examples, including erosion, skin friction coefficient, and swirl velocity, are examined here.

Table 3: Result Comparison of Five cases

Case No.	Erosion (Kg/m^2s)	Skin friction coefficient	Swirl velocity (m/s)
1.	$1.43x10^{-5}$	**$4.75x10^3$**	-41.7m/s
2.	$1.22x10^{-5}$	**$5.36x10^3$**	-41.7m/s
3.	$1.00x10^{-5}$	**$5.78x10^3$**	-41.7m/s
4.	$9.57x10^{-6}$	**$6.13x10^3$**	-41.7m/s
5.	$1.06x10^{-5}$	**$6.42x10^3$**	-41.6m/s

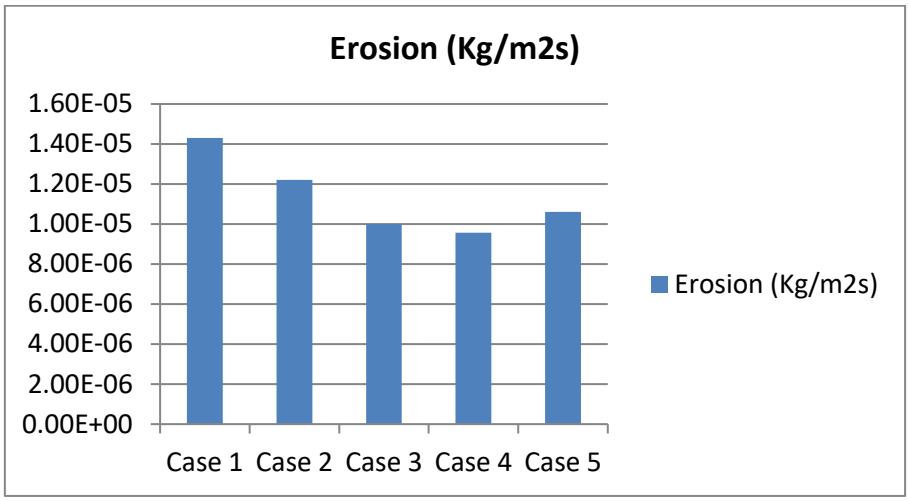

Figure 2: Graph showing the results of Erosion in different cases

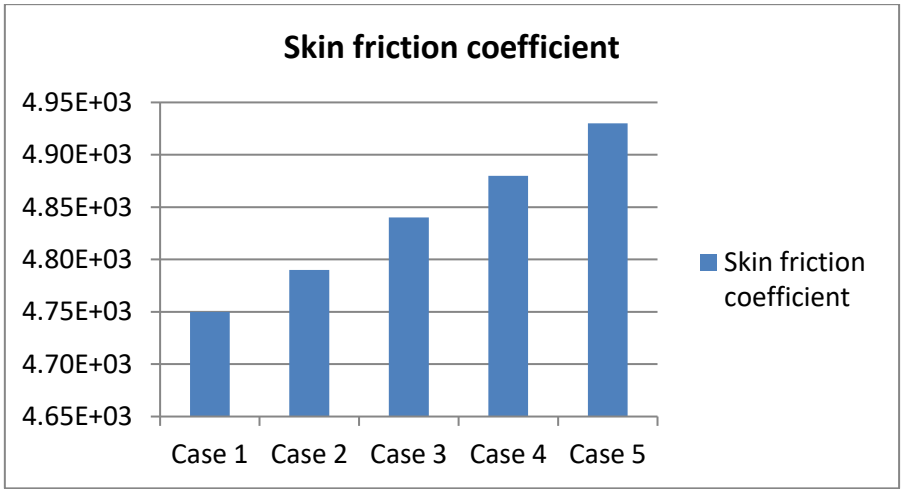

Figure 3: Graph showing the results of Skin friction coefficient in different cases

4.3. Particle size 370 μm

As a result of the examination of particle size distribution, erosion prediction is improved since the effect of particles of different sizes is varied. Here, a sand particle of 370 m in diameter is used. By altering the amount of water and EG, several instances have been explored.

Table 4: Case design for particle size 160 μm

Cases for particle size 160 μm	Percentage of WATER	Percentage of EG
Case 6	100%	0%
Case 7	90%	10%
Case 8	80%	20%
Case 9	70%	30%
Case 10	60%	40%

In order to accurately anticipate erosion rates and identify pipe areas most vulnerable to erosion, it is vital to have a full grasp of erosion's nature and severity. Bends are particularly vulnerable to sand damage.

4.4. Result Comparison of cases with Sand particle size 370 μm

A graph is used to compare the results of all instances. Sand has a particle size of 370 nm. The attributes of six examples, including erosion, skin friction coefficient, and swirl velocity, are examined here.

Table 5: Result Comparisons for particle size 160 μm

Case No.	Erosion (Kg/m^2s)	Skin friction coefficient
6.	$1.53x10^{-5}$	**$4.75x10^3$**
7.	$1.44x10^{-5}$	**$5.36x10^3$**
8.	$1.47x10^{-5}$	**$5.78x10^3$**
9.	$1.46x10^{-5}$	**$6.12x10^3$**
10.	$1.19x10^{-5}$	**$6.42x10^3$**

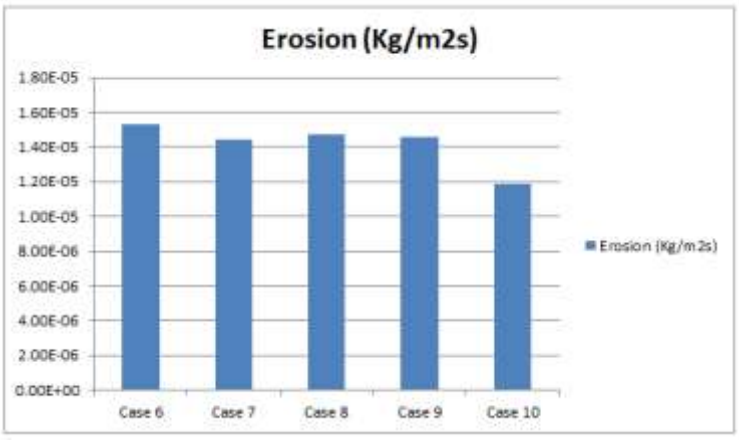

Figure 4: Erosion comparison for particle size 160 μm

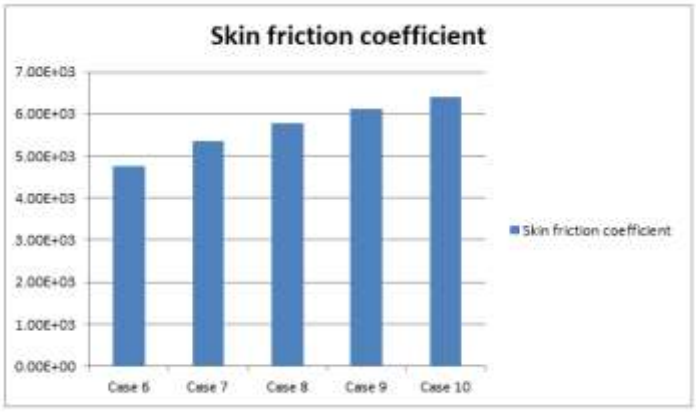

Figure 5: Skin Friction coefficient for particle size 160 µm

5. CONCLUSION

A key challenge in the oil and gas business is that of sand production since it may cause serious damage to the equipment. One of the drawbacks of sand extraction is the erosion of pipelines caused by sand particles. There are certain parametric elements that affect the erosion rate in pipe bends in this research, and the results are studied using a proprietary CFD simulation model. Erosion, skin friction coefficient and swirl velocity were all examined in this study. From this investigation, the following are the findings that emerged:

The highest erosion rate is used to evaluate the results. According to this comparison, the findings are found to be consistent. Particles with a diameter of 160 micrometres and 370 micrometres have been detected in this study. Sand particles (size 160 m) are compared by altering the percentages of water and EG. It may be argued from this that:

- Erosion reduces as EG % increases, however after Case 4, the findings are different in the fifth case. Erosion rates rise as the proportion of EG increases in Case 5 when water is 60 percent and the EG content is 40%.
- It has been shown that when EG concentration rises, so does the skin friction coefficient.
- When the sand particle size is 160 micrometres, there are no noticeable differences in the swirl velocity of the particles.
- Different types of sand particles (with a diameter of 370 microns) may be compared by altering the water and EG content. It may be argued from this that:
- Increasing the EG content reduces erosion rates; from Case 6 through Case 10, erosion rates drop as EG content rises and water content falls.
- It has been shown that when EG concentration rises, so does the skin friction coefficient. When the sand particle size is 370 micrometers, there are no noticeable differences in the swirl velocity of the particles.

References

[1] W. Pao, N. Nur, H. Binti, and N. M. Kamil, "Numerical Analysis of Sand Particles Erosion in Pipeline Flow Assurance-Waxy Crude View project Two-Phase separation in a T-junction View project Numerical Analysis of Sand Particles Erosion in Pipeline," *Researchgate.Net*, no. September, 2016, doi: 10.13140/RG.2.2.27142.16968.

[2] R. E. Vieira, A. Mansouri, B. S. McLaury, and S. A. Shirazi, "Experimental and computational study of erosion in elbows due to sand particles in air flow," *Powder Technol.*, vol. 288, pp. 339–353, 2016, doi: 10.1016/j.powtec.2015.11.028.

[3] C. J. Ejeh, E. A. Boah, G. P. Akhabue, C. C. Onyekperem, J. I. Anachuna, and I. Agyebi, "Computational fluid dynamic analysis for investigating the influence of pipe curvature on erosion rate prediction during crude oil production," *Exp. Comput. Multiph. Flow*, vol. 2, no. 4, pp. 255–272, 2020, doi: 10.1007/s42757-019-0055-5.

[4] E. Okafor and I. O. Ibeneme, "Parametric Analysis of Sand Erosion in Pipe Bends Using Computational Fluid Dynamics," vol. 3, no. 6, pp. 60–65, 2019.

[5] S. K. Wee and Y. J. Yap, "CFD study of sand erosion in pipeline," *J. Pet. Sci. Eng.*, vol. 176, no. October 2018, pp. 269–278, 2019, doi: 10.1016/j.petrol.2019.01.001.

[6] A. M. Lospa, C. Dudu, R. G. Ripeanu, and A. Dinita, "CFD Evaluation of sand erosion wear rate in pipe bends used in technological installations," *IOP Conf. Ser. Mater. Sci. Eng.*, vol. 514, p. 012009, 2019, doi: 10.1088/1757-899x/514/1/012009.

[7] H. W. Xian and N. A. Che Sidik, "Erosion-corrosion effect of nanocoolant on actual car water pump," *IOP Conf. Ser. Mater. Sci. Eng.*, vol. 469, no. 1, 2019, doi: 10.1088/1757-899X/469/1/012039.

[8] N. H. Saeid, "Numerical predictions of sand erosion in a choke valve," *J. Mech. Eng. Sci.*, vol. 12, no. 4, pp. 3988–4000, 2018, doi: 10.1017/CBO9781107415324.004.

Academic Guru Publication House

Research and Development
In Engineering Technology
Volume 1
Year: 2021

AG PH Books

SEISMIC ANALYSIS OF RCC BUILDING WITH AND WITHOUT FLOATING COLUMN USING STAAD PRO V8i

Shail Agrawal[1*]

[1]*Research Scholar, Department of Civil Engineering, Gyan Ganga Institute of Technology and Sciences, Bhopal*

Abstract

Ground vibrations may cause moderate to severe damage to many reinforced concrete structures in metropolitan areas that are located in active seismic zones. Architectural design and the frame drawing of a structure with floating columns are the focus of this project. The consequences of the load distribution on the floating columns are also being examined. The path of action of force is also examined for its significance and impacts. We're comparing the seismic analysis of multistory buildings with and without floating columns in this research. STAAD Pro V8i is being used to do an analogous static analysis on the whole mathematical 3D model of the project and the resulting models are being compared. Floating columns are used in many structures, particularly those above ground level, to provide additional open space for parking and other purposes.

Keywords: Floating Column, Multistorey Buildings, STAAD PRO V8i, seismic.

1. INTRODUCTION

Several structural design rules seem to be concerned with preventing or mitigating progressive collapse. Structures need to be strong enough, flexible enough, and redundant enough to compensate for the danger of disproportional failure.

* ISBN No. 978-81-953278-9-8

Analytical methodologies such as linear static, nonlinear static, and linear dynamic are all options in the alternative load route approach. In linear static analysis, the whole factored load is applied simultaneously to the damaged structure. The damage zone's size may be calculated using the DCR (Demand capacity ratio) after the static analysis. Structure elements and joints connections with DCR values less than 2 are inconvenient if the structure has a lot of fractures and damage, in which case a different solution is better. This approach is simple, quick, and can only be used for buildings with a maximum of ten storeys, making it ideal for smaller projects. To account for the material and geometric nonlinearity, nonlinear static analysis is a time-consuming process that requires iteration. Because of these differences in material and shape, nonlinear dynamic analysis is used to describe the structure's real behaviour while undergoing inelastic deformation, whereas linear dynamic analysis is used to analyse the structure's load history from zero to full factored load put on it.

1.1. Progressive Collapse

When a modest or local structural failure leads to the deterioration and failure of adjacent elements, this is considered a progressive collapse, which may lead to the complete collapse of a structure (or at least an unreasonably significant piece of it). Building structures begin to decompose when one or more vertical load-bearing components, often columns, are lost. To distribute the load after one or more columns have collapsed, an alternate load channel must be devised. Failure will occur if the neighbouring components are not intended to withstand the redistributed loads, resulting in partial or complete collapse of the structure.

Progressive collapse is a highly nonlinear dynamic event that involves the whole structural system, making the process incredibly intricate. Hand-calculations and basic analytical approaches are ineffective in investigating the process, if not impossible. Computational models of progressive building collapse have become the dominant method for investigating this phenomenon because of the high cost, complexity, and danger of conducting practical experiments. More high-quality experimental findings that may be utilised for model validation, on the other hand, are required in order to increase the accuracy and dependability of the computational models.

There are three ways to mitigate progressive collapse in a design strategy for progressive collapse. The following is the progression of this classification:

(a) Specific local resistance;
(b) Alternate load path method;
(c) Prescriptive design rules.

Direct approaches (a and b) and indirect approaches (c) are used interchangeably. The Alternate Load Path Method (APM) involves constructing the structure such that stresses may be reallocated after the loss of a vertical bearing part. Alternate load routes, from static linear to static nonlinear to dynamic linear or nonlinear, may be accounted for in the design process by adopting various degrees of idealization.

Pressure Loads

1. Internal gas explosions

2. Blast
3. Wind over pressure
4. Extreme values of environmental loads

Impact Loads

1. Aircraft impact
2. Vehicular collision
3. Earthquake
4. Overload due to occupant overuse
5. Storage of hazardous materials

1.2. Progressive Collapse Guidelines

Criteria defined by the “American Society of Civil Engineers (ASCE)”, as well as the GSA, DFA, and NIST, have been used to analyse, design, and enhance the structural integrity of both existing structures as well as new construction. Load combinations with anomalous loads and their corresponding probability are provided by ASCE. It also discusses generic methods for ensuring structural integrity if a major load-carrying element is damaged. Following ASCE 7 recommendations, the test building's collapse resistance is tested in this article using suggested load combinations.

Existing structures may be evaluated against progressive collapse using GSA principles, and new structures can be designed using these rules as well. For structures with relatively simple layouts and a maximum of ten floors above ground, a simplified threat independent technique is advised. To perform a linear elastic static analysis of the structure, an immediate removal of a first-story column positioned near the building's corner is needed. The computed demand-to-capacity ratio (DCR) for each structural member is used to analyse the progression of collapse and likely future failure of components. the moment, shear, and axial forces determined after a column's loss and the member's capacity are specified as the DCR ratio.

1.3. Shear Wall in RCC Building

An example of a shear wall would be a vertical element that can withstand a combination of lateral load transfer from another structural part to the wall, as well as the axial load produced by gravity. The typical need for multi-story buildings is RCC walls, including shear walls. When designing a structure, it's preferable if the building's mass centre and its centroid coincide. It is the most effective way to stiffen a building's structural system since the primary purpose of a shear wall is to enhance the building's lateral load resistance. Cross-sections of Shear walls are available in a variety of forms and sizes, including rectangular, T, L, barbell, and box cross-sections. If you're creating a service apartment or office/commercial tower, shear wall structures are becoming more popular. Using a shear wall system for a 30-35-story structure has been shown to be an effective structural technique.

To withstand horizontal earthquake stresses, shear walls must have sufficient lateral strength. These horizontal forces will be transferred to the next segment of the load path below shear walls once they're

strong enough to do so. Other shear walls, floors, foundation walls, slabs, and footings are also included in the load path. To avoid excessive side-sway on the roof or floor above, shear walls provide lateral rigidity. Floor and ceiling framing members will no longer be able to defy the shear walls if they're rigid enough. The non-functional damage to a structure may be reduced if it is sufficiently rigid.

2. LITERATURE REVIEW

Samrat Prakash Khokale (2017) discovered the building's most crucial Shear wall, which will cause the most damage or collapse if it is removed. Studying Shear wall's shear strength is the most important component. After that, the same programme is used to examine the building's collapse pattern. An anomalous loading-induced progressive collapse may be avoided by following current design principles described in the U.S. and European building codes and standards presented in this study. It is difficult to define abnormal loading, thus design provisions focus on ensuring that structures are strong, flexible, and redundant in the event of an abnormal load.

MD Goel et al (2017) A four-story RCC structure with 3 x 3 bays and a longitudinal bay span of 5 metres and a transverse bay span of 4 meters has been investigated by my team. Each storey of the building is 3.5 m high, except for the lowest floor, which is 4 m high. It has been determined that the rapid collapse of a load-bearing part has caused behavioural alterations.

P.P Chandurkar (2013) In order to establish the best placement for the shear wall in a multi-story structure, we used four distinct models to conduct a detailed research. ETAB Nonlinear v 9.5.0 was used to model the buildings. After examining ten-story buildings in seismic zones II, III, IV, and V, researchers discovered that shear walls with short spans at corners (model 4) are more cost-effective than other models in terms of lateral displacement, storey drift, and overall ground-floor costs. Shear walls have been shown to be cost-efficient and effective in high-rise structures, and their placement significantly lowers earthquake displacement. If the shear wall's dimensions are substantial, the shear wall absorbs the majority of horizontal forces.

Meng-Hao Tsai (2011) It was found that three prevalent forms of outside non-structural RC walls have an impact on the RC frame's progressive collapse potential. Static evaluations of the RC frames with and without non-structural walls are performed in three distinct column loss situations using linear and nonlinear methods. It is possible to overestimate beam moment demand without taking into account non-structural walls and underestimate shear demand, particularly for panel-type walls, based on demand-to-capacity ratios. They may improve the building's resistance to collapse if a column is lost, but at the expense of ductility. From a structural standpoint, the wing-type outer wall is superior than the parapet-type and panel-type walls because it has a constant opening rate of 60%. Shear failure of the connecting beam members of the panel-type wall looks to be the worst option.

Leslaw Kwasniewski (2010) provided a case study of a multi-story building's progressive collapse analysis. An 8-story steel-framed building used for fire testing at the Cardington Large Building Test Facility in the UK is the topic of the numerical analysis. Nonlinear dynamic finite element simulations

are used to analyse the issue in accordance with GSA recommendations. Global models with increased vertical loads and the elimination of notional columns will be the focus of this research. Multiprocessor computers were used to create a 3D model with many finite components of the structure, taking use of their parallel processing capabilities. Proposed hierarchical verification and validation procedures are intended to reduce the level of uncertainty associated with the final conclusion (potential for progressive collapse) of the feasibility study.

3. METHODOLOGY

3.1. Design Parameters

In order to design in accordance with IS 13920, a number of parameters are included in the software. It accepts all of the parameters required to design in accordance with IS: 456. In addition, it contains a few extra criteria that are only necessary if the design is carried out in accordance with IS: 13920. We chose the default parameter values based on their frequency of usage in standard standards for traditional design. All accessible parameters and their default values are shown so that they may be customised to meet the needs of the specific design being carried out. Before beginning the concrete design, you must provide the units of length and force as millimetres and newtons, respectively.

3.2. Beam Design

Flexure, shear, and torsion are the primary functions of beams. The axial force may be taken into account if necessary. Pre-scanning of all active beam loadings identifies the critical load instances at various parts of the beams for all of the forces. The width of the member must not be less than 200mm in order for the design to be done in accordance with IS: 13920. The member's width-to-depth ratio should be greater than 0.3.

Design for Flexure:

IS 456's design process is the same as this one. However, according to IS-13920, the following requirements must be met throughout the design process:

1. The minimum concrete grade should be M20 at a minimum.
2. Fe415 or lower steel reinforcements must be utilised.
3. The minimum tension steel ratio on any face, at any section, is determined as follows:

$\rho min = 0.24\sqrt{fck}/fy$

4. Steel ratio max = 0.025 defines the maximum steel ratio on any face, at any section.
5. At a minimum, the positive steel ratio at a joint face must be equal to half the negative steel ratio at that face.
6. There must be a minimum of one-fourth of the maximum negative moment steel supplied at each joint face in the steel given at each section's top and bottom faces, respectively.

Design for Shear

In determining the shear force that vertical hoops must withstand, the IS 13920:1993 version is used. When calculating the shear force, elastic sagging and hogging moments of resistance of the beam section at the ends are taken into account. If the PLASTIC parameter is included in the input file, plastic sagging and hogging moments of resistance may also be considered for shear design. Reinforcement designed to withstand shear and torsion is known as "shear reinforcement".

3.3. Column Design

According to IS 456:2000, columns are intended to withstand axial forces and biaxial moments. Shear forces may also be applied to columns. STAAD's column design has addressed all of the primary criteria for choosing longitudinal and transverse reinforcement outlined in IS: 456. The following conditions, however, must be met in order for IS 13920 to be implemented:

1. M20 is the recommended minimum concrete grade.
2. Fe415 or lower steel reinforcements must be utilised.
3. Column members must not be less than 200 mm in diameter. It is not permitted to have columns with an unsupported length of less than 4 metres.
4. A ratio of not less than 0 is preferred for the shortest cross-sectional to perpendicular dimension.
5. Except if extra restricting reinforcement is supplied, the minimum lateral dimension of the column's hoops cannot be exceeded by more than half.
6. Over a length lo from each joint face toward mid-span and on each side of any section where flexural yielding may occur, special confining reinforcement should be supplied. Lo must not be less than a greater lateral dimension of the member at the section where yielding occurs, b) one-sixth of the clear span of the member, and c) the length of the clear span of the member.
7. Hoops used as specific confining reinforcement must not be less than 75 mm in diameter or more than 100 mm in diameter.

3.4. Design Operations

STAAD provides a wide range of tools for developing structural elements as part of a larger structure that is being analysed. These features allow the user to do many design processes. The design of these facilities might be a concern. A design includes the following steps:

- Identify the components and load scenarios that will be taken into account throughout the design process.
- Code checking or member selection may be selected.
- To customise the default settings, enter the values for the design parameters you want to use.
- Specify whether member selection is to be done via optimization.

These operations may be repeated by the user any number of times depending upon the design requirements.

4. RESULTS AND DISCUSSION

A RCC building is designed according to Indian code. We have considered 4 storey building along having floor height of 3.2 m and the depth of foundation is to be 1.5 m. The combination of both the Loads is considered according to Indian standards code IS 456. Concrete grade considered is M25 and steel grade Fe 415. The exterior column of ground floor is removed one by one in a series to find out the critical columns. Comparative study of various parameters like axial forces on column, node displacement at top nodes of removed column and support reactions in vertical direction of both the frame (with and without shear wall) is carried out

4.1. DETERMINATION OF CRITICAL COLUMN AT GROUND FLOOR OF RCC BUILDING

The numbering of columns on the ground level is shown in the figure. The exterior column of a four-story structure is subjected to a series of column removal scenarios to identify the most crucial columns on the bottom level. STAAD Pro's remove command is used for each external column removal scenario on the bottom level.

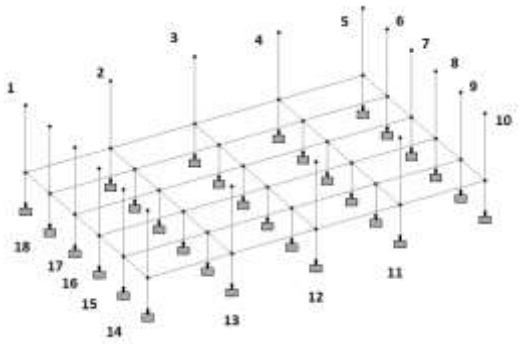

Figure 1: Numbering of columns of ground floor

4.2. When no collapse in column

When no collapse in beam the table shows the forces in each point the maximum axial force is 1299.914 KN and minimum axial force is -141.457. in shear force in y-direction and z-direction case the maximum value is 293.036KN for y-direction and 293.036 is x-direction and minimum value is -293.036 in y-direction and -114.087 is z-direction. In case of banding moment the value in minimum and maximum value in x-direction is 821.869 and -821.868KN, y-direction banding moment maximum and minimum value is 2008.613KN and -1973.064KN respectively and z-direction bending moment maximum and minimum value is 6063.021 and -4920.402KN respectively.

Beam	Node	Axial Force (KN)	Shear force (KN)		Bending moment (KNm)		
		Fx	Fy	Fz	Mx	My	Mz
206	103	1299.914	40.282	2.711	-0.764	1.305	-13.1827
246	131	-141.457	31.156	-0.864	0.195	1.581	22.092
159	62	309.064	293.036	-10.866	1.390	14.419	381.760
158	61	309.064	-293.036	-10.866	-1.390	14.419	-381.760
170	73	260.703	-28.690	114.977	0.825	140.975	36.083
171	74	261.343	-30.073	-114.087	36.083	142.143	
174	77	22.564	97.552	7.812			
184	85	22.564	75.335	-7.812			
170	91	248.971	-28.690	114.977			
171	92	249.610	-30.073	-114.087			
135	61	-115.952	224.304	0.000			
159	80	297.331	293.036	-10.866			

When no collapse in beam the table shows the displacement in each point in x-direction the maximum displacement is 0.059 KN and minimum displacement is -0.059. displacement in y-direction and z-direction case the maximum value is 0.001 for y-direction and 0.017 is z-direction and minimum value is –0.206 in y-direction and -0.001 is z-direction. In case of rotational displacement the value in minimum and maximum value in rx-direction is 0.005 and -0.005, ry-direction rotational displacement maximum and minimum value is 0 and rz-direction rotational displacement maximum and minimum value is 0.040 and -0.040 respectively.

All | Summary

			Horizontal	Vertical	Horizontal	Resultant	Rotational		
	Node	L/C	X in	Y in	Z in	in	rX rad	rY rad	rZ rad
Max X	85	3 Generated	**0.059**	-0.206	0.000	0.214	0.000	-0.000	-0.040
Min X	86	3 Generated	**-0.059**	-0.206	0.000	0.214	0.000	0.000	0.040
Max Y	90	2 LIVE	0.000	**0.001**	-0.016	0.016	-0.000	-0.000	-0.000
Min Y	86	3 Generated	-0.059	**-0.206**	0.000	0.214	0.000	0.000	0.040
Max Z	87	3 Generated	0.004	-0.170	**0.017**	0.171	0.005	-0.000	0.004
Min Z	90	3 Generated	0.000	-0.020	**-0.043**	0.047	-0.001	0.000	-0.000
Max rX	91	3 Generated	-0.004	-0.170	0.017	0.171	**0.005**	0.000	-0.004
Min rX	92	3 Generated	-0.004	-0.167	-0.012	0.168	**-0.005**	-0.000	-0.004
Max rY	77	3 Generated	-0.011	-0.142	-0.001	0.142	-0.001	**0.000**	0.009
Min rY	76	3 Generated	0.011	-0.142	-0.001	0.142	-0.001	**-0.000**	-0.009
Max rZ	80	3 Generated	-0.059	-0.206	0.002	0.214	-0.000	-0.000	**0.040**
Min rZ	79	3 Generated	0.059	-0.206	0.002	0.214	-0.000	0.000	**-0.040**
Max Rs	85	3 Generated	0.059	-0.206	0.000	**0.214**	0.000	-0.000	-0.040

Table 1: Column 1, 4, 8, 12, 16, 18 is removed

Removal of column	Adjacent column	Axial forces before removal	Axial forces after removal
1	2	349.63	529.67
4	3	64.03	71.69
4	5	274.25	539.35
8	7	298.94	435.18
8	9	407.91	543.5
12	11	337.95	401.90
12	13	337.95	362.83
16	15	407.91	556.64
16	17	298.94	1190.94
18	17	407.83	1190.94

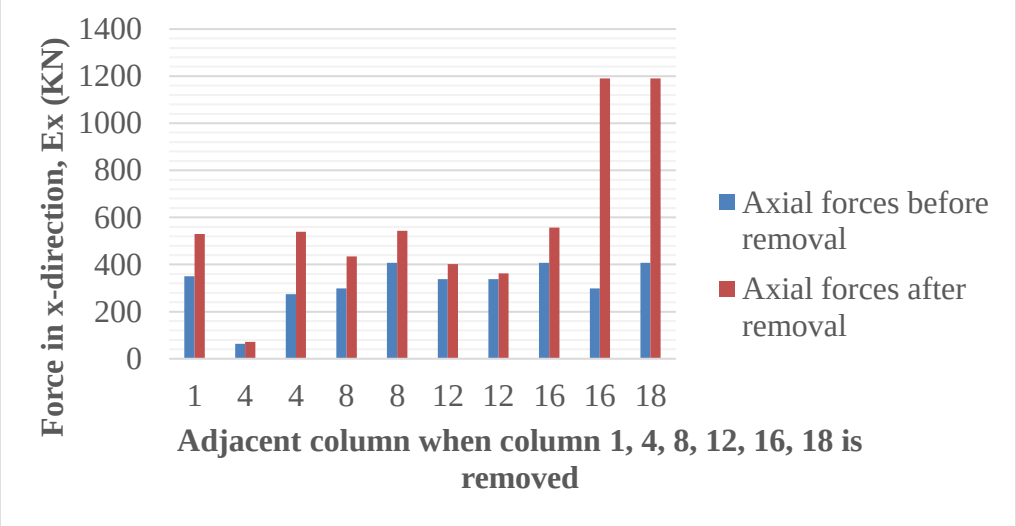

Fig. 2: Comparison of Axial forces in columns of GF

Table 2: Reaction force before column removal and after column removal

Removal of column	Adjacent column	reaction forces before removal	Reaction forces after removal
1	2	382.94	566.62
4	3	69.23	79.96
4	5	288.94	560.28
8	7	323.36	453.15
8	9	430.18	561.09
12	11	360.77	424.2

12	13	109.86	380.16
16	15	430.18	578.13
16	17	323.36	1201.56
18	17	430.02	1201.56

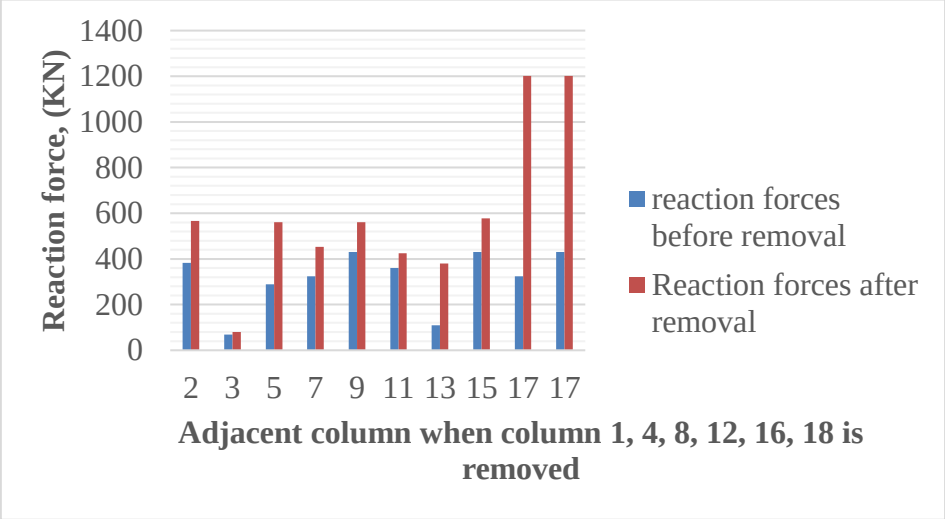

Figure 3: Comparison of reaction force before and after removal

Table 3: Reaction force in y-direction before column removal and after column removal

Removal of column	Adjacent column	Fy before removal	Fy after removal
1	2	0.412	1.773
4	3	0.000	-0.331
4	5	6.050	29.011
8	7	28.34	24.90
8	9	34.09	30.51
12	11	-3.014	-10.78
12	13	3.014	-10.06
16	15	-34.09	-42.54
16	17	-28.34	-39.36
18	17	-3409	-39.36

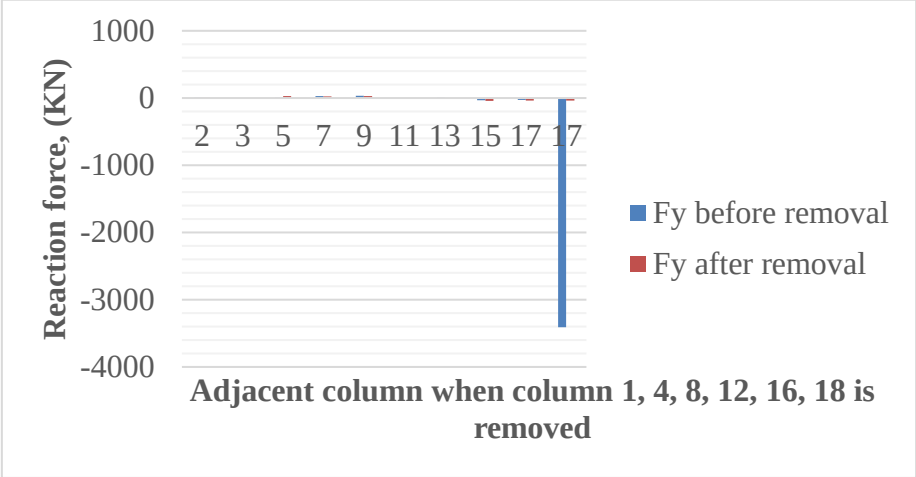

Figure 4: Fy before and after removal

Table 4: Reaction force in z-direction before column removal and after column removal

Removal of column	Adjacent column	Fz before removal	Fz after removal
1	2	12.404	14.43
4	3	2.207	6.741
4	5	2.060	6.776
8	7	-0.309	13.63
8	9	1.013	2.563
12	11	-12.18	-11.14
12	13	-12.18	-9.495
16	15	1.013	-3.786
16	17	-0.309	-24.25
18	17	-0.998	-24.25

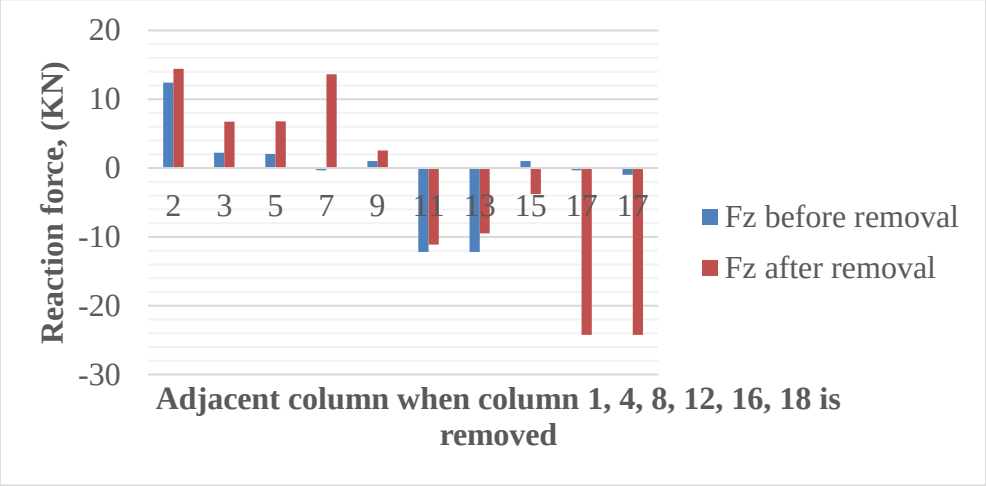

Figure 5: Fz before and after removal

Table 5: Moment force in x-direction before column removal and after column removal

Removal of column	**Adjacent column**	**Mx before removal**	**Mx after removal**
1	2	-1.212	-6.315
4	3	0.000	21.611
4	5	0.231	24.75
8	7	0.135	-0.970
8	9	0.057	3.082
12	11	-0.881	1.488
12	13	0.881	1.057
16	15	-0.057	-3.859
16	17	-0.135	0.437
18	17	0.037	0.437

Table 6: Moment force in y-direction before column removal and after column removal

Removal of column	Adjacent column	My before removal	My after removal
1	2	-84.26	-270.33
4	3	-15.53	-188.012
4	5	-17.70	-124.64
8	7	3.560	-181.89
8	9	-7.551	-108.08
12	11	82.168	-38.78
12	13	82.168	-110.87
16	15	-7.551	-135.74
16	17	3.560	25.81
18	17	7.393	25.81

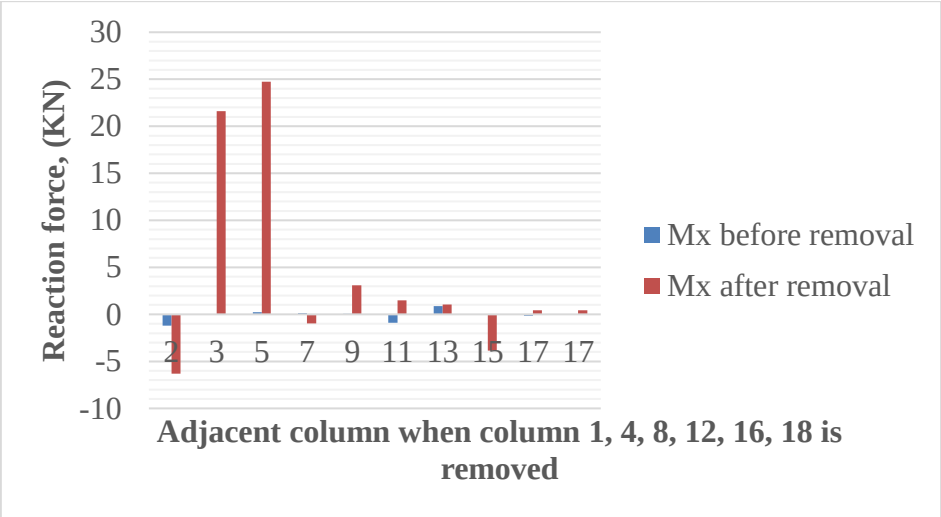

Figure 6: Mx before and after removal

Table 7: Moment force in z-direction before column removal and after column removal

Removal of column	Adjacent column	Mz before removal	Mz after removal
1	2	-21.41	-81.12
4	3	0.000	-19.93
4	5	49.95	157.22
8	7	226.75	108.29
8	9	274.79	166.14
12	11	-25.02	-174.01
12	13	25.02	-166.45
16	15	-274.79	-428.07
16	17	-226.75	-416.68
18	17	-274.23	-416.68

Table 8: Displacement in x-direction before column removal and after column removal

Removal of column	Adjacent column	Node	node displacement in x-direction before removal	node displacement in x-direction after removal
1	2	13	0.000	0.019
4	3	17	0.000	0.003
4	5	4	-0.008	-0.015
8	7	8	0.008	0.001
8	9	12	0.009	-0.008
12	11	20	0.001	-0.027
12	13	14	-0.001	-0.029
16	15	11	-0.009	-0.026
16	17	9	-0.008	-0.014
18	17	5	-0.009	-0.014

Table 9: Displacement in y-direction before column removal and after column removal

Removal of column	Adjacent column	Node	node displacement in y-direction before removal	node displacement in y-direction after removal
1	2	13	-0.01	-0.015
4	3	17	-0.002	-0.002
4	5	4	-0.008	-0.015
8	7	8	-0.008	-0.012
8	9	12	-0.011	-0.015
12	11	20	-0.009	-0.011
12	13	14	-0.009	-0.01
16	15	11	-0.011	-0.015
16	17	9	-0.008	-0.032
18	17	5	-0.011	-0.032

Table 10: Displacement in z-direction before column removal and after column removal

Removal of column	**Adjacent column**	**Node**	**node displacement in z-direction before removal**	**node displacement in z-direction after removal**
1	2	13	-0.002	-0.017
4	3	17	0.000	-0.005
4	5	4	0.000	-0.01
8	7	8	0.000	-0.01
8	9	12	0.000	-0.009
12	11	20	0.002	0.01
12	13	14	0.002	-0.003
16	15	2	0.000	0.000
16	17	9	0.000	0.002
18	17	5	0.000	0.002

Note: displacement in x,y,z direction are in inches convert it into mm when collapse

All | Summary | Envelope

	Beam	L/C	Node	Fx kN	Fy kN	Fz kN	Mx kip-in	My kip-in	Mz kip-in
Max Fx	202	3 Generated	99	**3615.616**	60.858	2.564	11.512	55.778	-174.574
Min Fx	178	3 Generated	81	**-309.785**	230.637	39.315	82.700	-285.415	2211.452
Max Fy	159	3 Generated	62	323.949	**293.667**	3.479	-157.666	-29.426	3333.641
Min Fy	49	3 Generated	27	326.411	**-497.209**	25.150	-373.915	91.725	4670.042
Max Fz	162	3 Generated	65	22.162	-255.259	**130.963**	-129.277	-1616.012	-2840.633
Min Fz	74	3 Generated	25	72.389	-272.181	**-294.590**	-99.051	4819.469	-4491.450
Max Mx	172	3 Generated	75	-2.101	-3.564	62.205	**1062.049**	-832.337	-742.931
Min Mx	184	3 Generated	85	-67.145	199.949	19.927	**-769.486**	49.476	1211.958
Max My	74	3 Generated	25	72.389	-272.181	-294.590	-99.051	**4819.469**	-4491.450
Min My	158	3 Generated	79	30.416	-303.763	-244.295	-175.117	**-3977.905**	5039.723
Max Mz	135	3 Generated	61	-128.716	227.177	-3.315	-41.634	234.135	**6264.044**
Min Mz	159	3 Generated	80	312.217	293.667	3.479	-157.666	69.097	**-4983.654**

			Horizontal	Vertical	Horizontal	Resultant	Rotational		
	Node	L/C	X in	Y in	Z in	in	rX rad	rY rad	rZ rad
Max X	4	3 Generated	**0.071**	-0.044	-0.032	0.090	-0.001	-0.000	-0.003
Min X	78	3 Generated	**-6.318**	-0.266	-1.163	6.430	-0.001	0.003	0.044
Max Y	90	2 LIVE	-1.125	**0.048**	-0.871	1.423	-0.002	-0.003	0.001
Min Y	91	3 Generated	-6.304	**-9.584**	-1.722	11.600	-0.002	-0.003	0.019
Max Z	7	3 Generated	-0.043	-0.095	**0.006**	0.105	0.000	-0.000	0.004
Min Z	75	3 Generated	-6.269	-5.117	**-4.297**	9.162	-0.013	0.003	0.015
Max rX	37	3 Generated	-0.426	-9.579	-0.300	9.594	**0.000**	-0.000	0.019
Min rX	25	3 Generated	-0.622	-3.468	-0.328	3.579	**-0.020**	-0.003	-0.026
Max rY	82	3 Generated	-4.967	-0.205	-1.162	5.105	0.000	**0.009**	0.047
Min rY	90	3 Generated	-3.327	-0.437	-2.475	4.170	-0.008	**-0.007**	0.002
Max rZ	80	3 Generated	-5.780	-0.218	-1.162	5.899	-0.002	0.008	**0.057**
Min rZ	85	3 Generated	-3.549	-0.275	-4.259	5.551	-0.008	0.005	**-0.035**
Max Rs	91	3 Generated	-6.304	-9.584	-1.722	**11.600**	-0.002	-0.003	0.019

5. CONCLUSION

A building with floating columns is structurally inferior than a structure without floating columns. The structure must be able to endure seismic loads if the area of failure is stiffened. There is, however, an increase in the demand for steel and cement.

The fundamental objectives of this study are to improve seismic performance and correctly design floating column-based structures. Open ground floor (stilt floor) in badly damaged or collapsed R.C. buildings generated a "great irregularity of rapid change in stiffness" between ground and upper floors because infilled brick walls increased the lateral stiffness of the frame by a factor of three to four times. An earthquake causes the building to sink roughly one-and-a-half feet in the soft floor due to soil liquefaction. A bulge formed in this road because to the flow of dirt. The raft's base lifted above the water's surface as the structure's rigid body swung to one side. Accordingly, it is recommended that the "soft" floor should fall and do more harm than the upper levels. Buildings on stilts have become more common in order to fulfil the growing need for parking.

References

[1] Leslaw Kwasniewski (2010), Non-linear dynamic simulations of progressive collapse for a multi-story building, Engineering Structures, 32, 1223-1235.
[2] Meng- Hao Tsai (2011), Progressive Collapse Analysis of an RC Building with Exterior Non-Structural Walls, The Twelfth East Asia-Pacific Conference on Structural Engineering and Construction, 14, 377–384, 2011.
[3] P.P Chandurkar, P.S. Pajgade (2013), "Seismic analysis of RCC building with and without shear wall" IJMER, Vol.3, Issue 3, pp- 1805 -1810.
[4] Samrat Prakash Khokale (2017), Progressive Collapse of Shear wall Structure under Accidental Load, 540-549.
[5] MD Goel, D. Agrawal, A. Choubey (2017), collapse behaviour of RCC building under blas load, 11th International Symposium on plasticity and Impact Mechanics, 173, 1943-1950.
[6] IS 1893 (Part1): 2002, "Criteria for earthquake resistant design of structure,"
[7] IS 13920: 1993, "Ductile detailing of reinforced concrete structure subjected to seismic forces".
[8] General Provision and building, New Delhi, India.
[9] Bureau of Indian Standard, IS-456(2000), “Plain and Reinforced Concrete Code of Practice”.

Academic Guru Publication House

Technological Advancements : Research & Reviews
Volume 1
Year: 2021

AG PH Books

BY USING TAGUCHI AND ANOVA METHODS FOR OPTIMIZATION OF STRESS AND DEFORMATION FOR LAP JOINT

Neeraj Upadhyay[1*]

[1]*Research Scholar, Department of Mechanical Engineering, SIRTE, Bhopal*

Abstract

In several industries, welding is significantly used; aviation industry, automotive industry and construction industry are some of the industries which widely use welding. Therefore, for the welding characteristics or responses, optimization of mechanical properties is considered important. For the factorial design of the experiment, Taguchi method is used that is an appropriate statistical method. Moreover, there are several standard methods for evaluating tensile strength of the material, it's necessary to develop new ideas for obtaining tensile strength of welding joints. In this present study, the effective way is used to evaluate and optimise the welding techniques with better tensile strength for Lap Joint. The method opts for analysis of Lap welding joint is Taguchi method. Taguchi method is used for the purpose of result optimization. ANOVA method is used for proper judgement of result along with Taguchi method. The stress and deformation is calculated on the ANSYS software.

Keywords: ANSYS, Joints, Lap joint, Taguchi, Tensile strength, welding.

1. INTRODUCTION

When it comes to securing machine components and structures, welding is the most popular method. Blending occurs when two different materials (metals or thermoplastics) are brought together by welding. With or without filler material, welding is a procedure in which heat or pressure is used to fuse

* ISBN No. 978-81-953278-9-8

two or more metals together. [1] There are several auxiliary materials that may be employed to facilitate the process, such as shielding gases, flux, and pastes. Welding requires an external source of energy. As a permanent connecting procedure without melting the base metal, welding is one of the “well-defined low temperature metal joining methods”, including soldering and brazing.[2]

1.1. Types of material used

S275 Steel: Standard cross-sectional forms (or "sections") are used to create structural steel, a fundamental building material constructed from particular grades of steel. Chemical and mechanical qualities are tailored for particular purposes in structural steel grades. Most of the industrial construction, includes bridges, trains, and ships, uses structural S275 steel plates. Because of this, establishing the S-N curve, which measures the fatigue strength of a material based on the number of cycles it takes to fail and the stress it is subjected to, is critical in industrial building. [3]

Steel structural may be employed in a wide variety of ways and for a wide range of purposes. The unique combination of outstanding welding qualities and guaranteed strength makes them especially valuable. Engineers who want to reduce weight and increase structural strength often turn to structural steel, which has a wide range of applications. [4]

Al6061: Magnesium and silicon are the primary alloying constituents of 6061 (Unified Numbering System (UNS) designation A96061), an aluminium alloy that is precipitation hardened. It was first referred to as "Alloy 61S" in 1935. High mechanical qualities, good weld ability and widespread extrusion make it a popular choice. For general-purpose application, it is one of the most common aluminium alloys Tempered 6061-T6 and 6061-T651 grades are widely available, as are 6061-O (solutionized, stress-relieved stretched and artificially aged).[5]

6061 is commonly used for the following:

- Construction of aircraft structures, such as wings and fuselages, more commonly in homebuilt aircraft than commercial or military aircraft.
- Yacht construction, including small utility boats.
- Automotive parts, such as the chassis of the Audi A8 and the Plymouth Prowler.
- Flashlights
- Aluminum cans for the packaging of food and beverages.
- Scuba tanks and other high pressure gas storage cylinders.

EN8 Steel: Steel having increased strength and through-hardening properties, EN8 carbon steel is a popular medium carbon and medium tensile steel. Additionally, EN8 carbon steel may be machined in any state.[6]

The untreated state of EN8 steels is the most common usage for these metals. However, induction methods allow for further surface hardening of EN8 steels, resulting in components with improved wear resistance. Steel EN8 has excellent homogeneous metallurgical structures in its heat-treated forms, resulting in consistent machining qualities.

All general engineering applications needing a greater strength than mild steel may use EN8 steel, including the following:

i. general-purpose axles
ii. shafts,
iii. gears,
iv. Bolts and studs.
v. spindles,
vi. automotive and general engineering components,
vii. Other general engineering parts etc.

1.2. Objectives of the Study

1. From the above studies, it is observed that different materials like S275, AL6061 and EN8 have not been used in earlier studies. So these materials are used in our study for external welded Lap haunched joints.
2. By varying the length of External welded Lap haunched joints, the design is modified for further studies.
3. In previous studies, the effect of force is not studied. So, investigation can be performed on effect of force in External welded Lap haunched joints.
4. In External welded Lap haunched joints, for analyzing the value of stress and deformation, Finite Element Method will be used.

2. LITERATURE REVIEW

Loureiro et al. [7] A number of academics have recently worked hard to increase their understanding of the behaviour of steel joints. In order to meet the requirements of the EC3, special attention has been paid to acquiring the stiffness of the various components of the joints. However, the component technique has significant limits, hence new methods for determining the stiffness of joints must be developed. An alternate approach for assessing the stiffness of 2D external welded haunched joints is described in the current study. There are four tests in all, each with a finite element model to go along with the findings. The stiffening of the column web has been evaluated with four distinct types of joints. Furthermore, finite element models of the joints have been built and calibrated using the results of the testing.

Daniel Das et al. [8] In his investigation, tool rotational speed was shown to be the most important factor in enhancing the strength of the joint. When it comes to fusion welding, AA 7075 is considered to be an unfabricated metal, and the parent metal can't be weld. When it comes to feeding rates, there are three distinct levels: 162.8, 153.8 and 144.7 mm/min, respectively, for the feed rate. At the feed rate, the delta was about 18.1... As a result, the maximum welding speed (159.8 mm/min) has been increased to level 3 (second place). The tool's rotating speed was measured at 154.6 rpm. Compared to tool speed and

welding speed, feed rate proved to be the most compelling metric in this case. There is no doubt that Feed rate is the most effective parameter among the three that generate efficient weld joints, according to SN ratio values There is a first level of 44.23 mm/min feed rate, followed by 43.73 mm/min and 43.21 mm/min at levels two and three, respectively.

Mandeep Singh et al. [9] Smooth welding is achieved by ionising the supplied gas and creating an arc between the electrode and the workpiece. Welding speed and metal deposition are both boosted when welding is done in continuous mode. A positive polarity filler wire is used, and a negative polarity work piece. R.A. Fisher created the DOE method in 1920. Multiple variables may be analysed concurrently using this method. In order to achieve the needed optimization, DOE's partnership with Taguchi has shown to be effective. For example, combining components at different levels, each with its own range, and yet ensuring little variance around ideal outcomes is also possible using DOR. MIG welding process characteristics include welding current, voltage, gas flow rate; wire feed rate, electrode diameter, and more. Welding voltage and current are the most critical.

H.Li et al. [10] Spot welds are widely utilised in the automotive and aerospace sectors to attach thin metallic sheets. The most common cause of spot weld failure is the formation of fatigue fractures around the weld nugget's edge. Stress intensity factors (SIFs) are used to forecast the fatigue life of spot weld joints, which are critical to the durability of vehicles. The spot weld edges and high fidelity SIFs are consequently essential. When dealing with a real industrial-scale structure including thousands of spot welds, the quantity of welds, the disparity between the structure welds, complicated geometries, and load situations make it even more difficult to do the necessary welding.

Stalin et al. [11] One of the fastest-growing prospects in production engineering is welding technology. Welding is essential in many construction, erecting, ship-building, and body-building projects nowadays. Although welding technology offers numerous advantages, it also has certain drawbacks that must be taken into account when doing this research. If welding technology's flaws could be fixed, many dangers and accidents may be averted. A large number of persons involved in welding projects are unable to determine the precise loading and boundary conditions for the matching weld, which is to be made utilising the “design of experiment (DOE)”.

Asif Ahmad et al. [12] "tungsten inert gas welding" is a popular method for welding "ferrous and non-ferrous" metals. "Stainless steel grade 3HQ (S30430)" is a specialty wire grade in the production of stainless steel. Grades 384 and 305 have been superseded by it for heading use. Consequently, it exhibits outstanding toughness at temperatures even lower than cryogenic. Utilizing Taguchi's design of experiments (DOE), studies were carried out and a mathematical model built using variables such as voltage, depth, current, or speed.

Marcello Lepore et al. [13] Multiple three-dimensional fracture propagation in a welded structure may be modelled numerically using a finite element technique. An AA2024-T3 butt joint subjected to process-induced residual stress develops cracks during friction stir welding. Temperature dependent elastic-plastic material characteristics, softening and isotropic hardening were taken into account in a thermo-mechanical FEM simulation of the process to estimate the residual stress field. After that, fractures are added in the FEM computational domain that enable stress redistribution and fatigue crack

propagation.. Comparison of numerical results obtained by a combined FEM-DBEM process, accessible in literature, has verified the suggested approach.

3. METHODOLOGY

3.1. Step of Method

1. Design of Experiment table by using L9 Orthogonal array table.
2. Further converting the File in .step format for importing it in Ansys Fluent work bench.
3. Assigning the Material property in parts.
4. Meshing for performing the simulation process.
5. Provide the suitable boundary conditions according to the decided objective.
6. Evaluating the results after the finish of simulation work.
7. After simulation the result is analysis in Taguchi method by using Minitab software

3.2. Material Property:

Three different materials as S275 steel, Al6061 aluminum, EN8 steel that are joined by Lap welding. The analytical setup and procedure opted is Lap welding for these material. The joints are designed with the help of Taguchi method and ANSYS software for stress and deformation interpretation.

The materials opted for the work is aluminum and steel. And their density, young modulus, poisson's ratio is taken in account by using the software and the structural frame work of the design is crafted with these characteristics.

Table 1: Table Representing Material Property:

Material	Density Kg/m^3	Young's Modulus (MPa)	Poisson's Ratio
S275	7850	$210x10^3$	0.30
Al6061	2700	$68.9x10^3$	0.33
EN8	7800	$190x10^3$	0.3

3.3. Table showing Orthogonal L9:

Table 2: Table representing Orthogonal L9:

Case	Design	Force (KN)	Material
1	D1	108	S275
2	D1	128	Al6061
3	D1	148	EN8
4	D2	108	Al6061
5	D2	128	EN8
6	D2	148	S275
7	D3	108	EN8

8	D3	128	S275
9	D3	148	Al6061

4. RESULTS AND DISCUSSION

4.1. Calculation of S/N Ratio :

Table 3: Table representing S/N Calculation Ratio:

Case	Design	Force	Material	Stress (MPa)	Deformation	S/N Ratio
1	D1	108	S275	310.95	4.62	-49.8538
2	D1	128	Al6061	362.45	16.87	-51.185
3	D1	148	E8	368.54	6.05	-51.3297
4	D2	108	Al6061	253.48	14.22	-48.0789
5	D2	128	E8	296.28	6.05	-49.434
6	D2	148	S275	342.58	6.33	-50.6952
7	D3	108	E8	283.48	6.54	-49.0504
8	D3	128	S275	335.98	7.02	-50.5263
9	D3	148	Al6061	388.47	8.97	-51.7871

4.2. Response Table:

Table 4: Representing Response Table
(Smaller value is considered better here)

Level	Design	Force	Material
1	-50.79	-48.99	-50.36
2	-49.40	-50.38	-50.35
3	-50.45	-51.27	-49.24
Delta	1.39	2.28	0.42
Rank	2	1	3

4.3. S/N Ratio Graph:

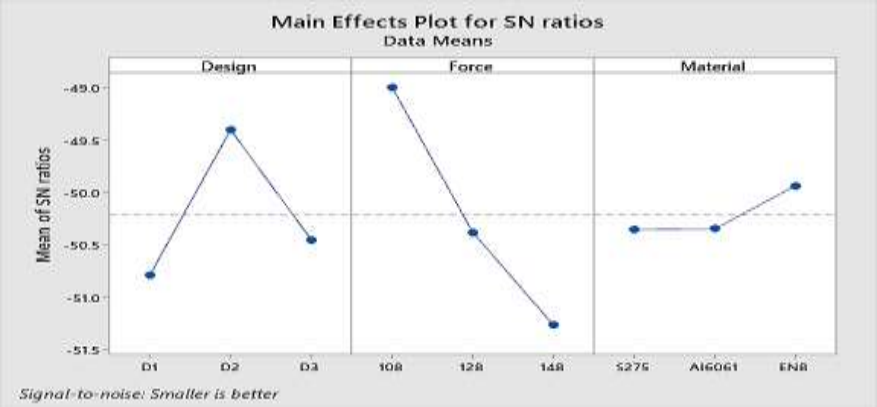

Figure 1: Graphical representation of S/N ratio

4.4. Result Validation:

Equivalent Stress: Using equivalent stress when there is a multiaxial stress condition with numerous stress components working simultaneously in the structure is a common practise. In such cases von-mises stress is considered while drawing the structure of the material component.

In the figure given below, the result of Case 10 is shown. The result shows the maximum 249.99MPa as well as minimum value 0.0019633MPa of equivalent stress.

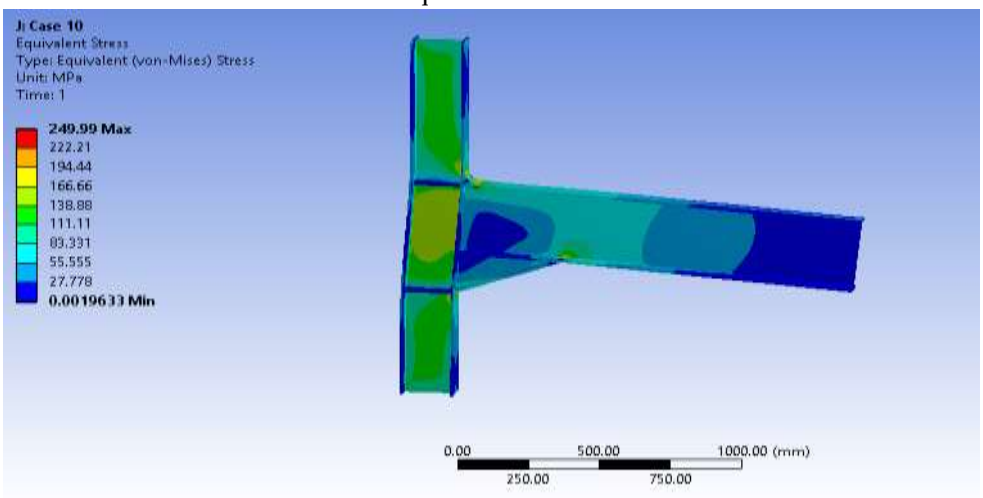

Figure 2: Equivalent stress for Case 10

Total Deformation: In the ANSYS Work Bench, deformation data are often shown as either total or directional deformation. Both of them are used to measure stress-induced displacement.

In the figure given below, the result of Case 10 is shown. The result shows the maximum 5.1108mm as well as minimum “0”mm value of total deformation.

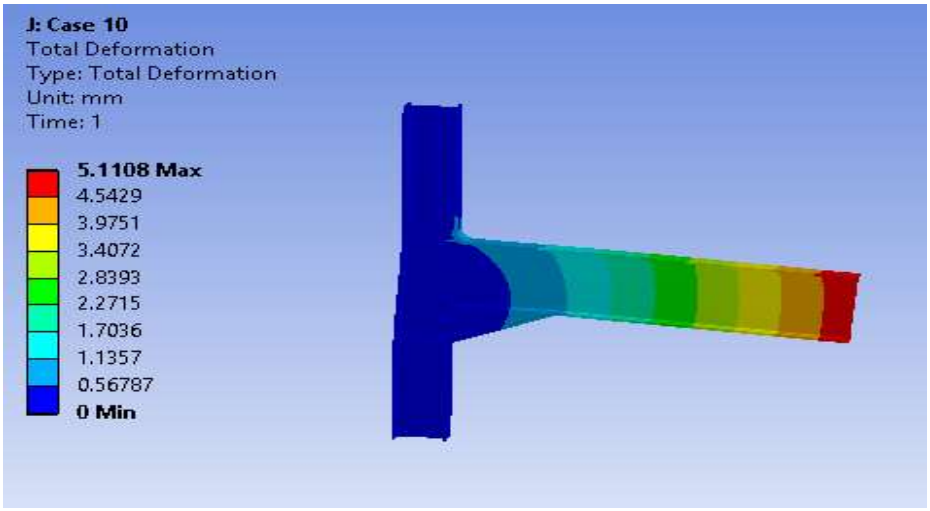

Figure 3: Total deformation for Case 10

4.5. Stress Comparison:

Stresses created during manufacturing operations such as cutting, cold work, welding, grinding, shot peening and so on are known as residual stresses (RS). Residual tensile stress on a surface is generally undesirable, since it reduces fatigue resistance. Therefore, compressive pressures on the surface boost the fatigue strength. Component failure may be attributed to welding-related stresses, which are critical to consider.

Stress v/s Cases:

The graph shown below represents the value of stress in particular cases from Case 1 to Case 10. In case 9, the maximum value of stress is observed and Case 4 shows the minimum value for stress.

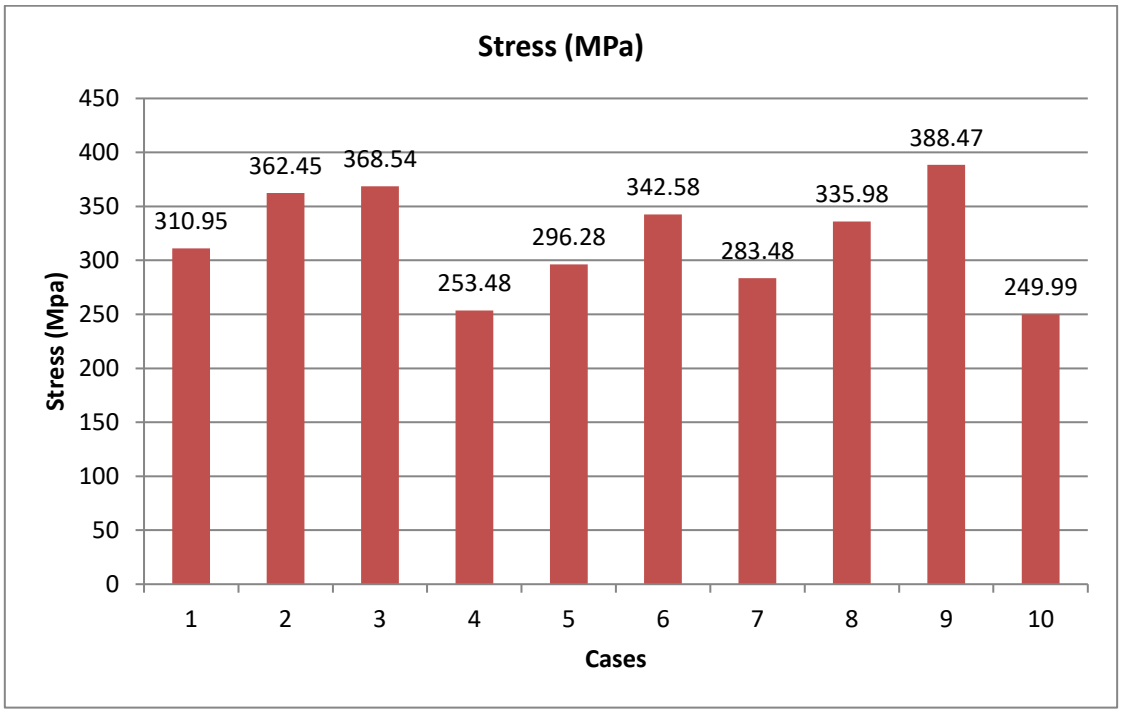

Figure 4: Graphical representation of Stress

Deformation v/s Cases:

The graph shown below represents the value of deformation in particular cases from Case 1 to Case 10. In case 2, the maximum value of deformation is observed and Case 1 shows the minimum value for deformation.

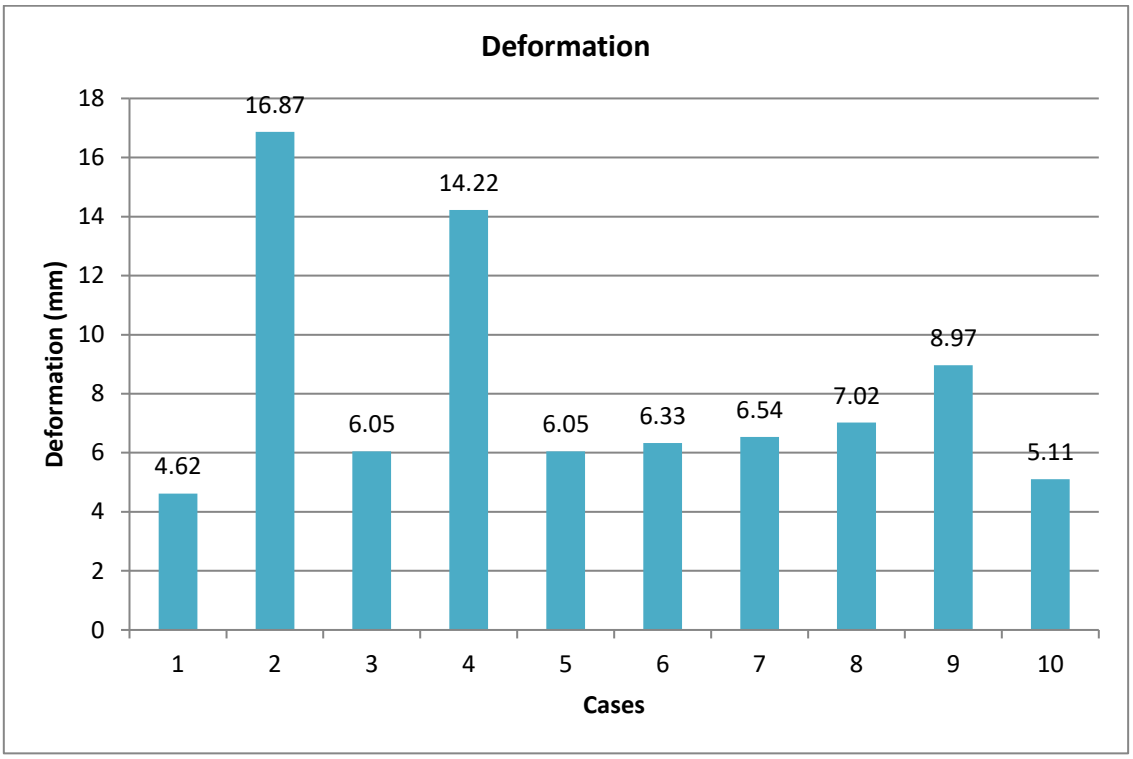

Figure 5: Graphical representation of Deformation v/s Cases

4.6. ANOVA Method for Analysis

In order to determine the relative relevance of different components, the statistical S/N analysis must be followed by an ANOVA analysis. Experiment standard errors or level modifications may have caused the observed response variation, according to ANOVA. Analyzing the outcomes of the studies on reaction is also done using ANOVA, which is a standard statistical technique. Consideration of the chamfer on a vertical plate may also be used in the FE analysis process. When welding Lap-joint weldments with varying throat thickness and gap variation, maximum von-misses stresses are measured, and the corresponding Maximum Breaking Stress is calculated.

Table 5: Table Representing ANOVA Analysis:

Source	DF	Contribution	F-Value	P-Value
Design	2	26.31%	15.35	0.061
Force	2	68.37%	39.89	0.024
Material	2	3.61%	2.11	0.322
Error	2	1.71%	----	----
Total	8	100.00%	-----	----

5. CONCLUSION

A study of the deformation breaking stress of the welding joint is employed in this work to limit the risk of welding failure (using low carbon steel as a base metal and copper filler material). The maximum von-misses stress in the welding under tensile load was determined by doing a static stress study on the welding using ANSYS. Welded lap joint design and analysis has been completed satisfactorily.

1. By applying Finite element analysis (ANSYS), the duration of experimentation can be reduced.
2. The processing quality can be enhanced by using Taguchi method and the processing variations can be reduced.
3. After applying Taguchi method it was observed that Force is placed at first rank, Design at second and Material at third.
4. The efficiency of optimization process can be enhanced by using taguchi method.
5. For obtaining better result, Force of level 1, Design of Level 2 and material of level 3 is taken.
6. The lowest stress value is achieved which is 249.99 Mpa and the corresponding deformation value is 5.11 mm after applying the above shown combinations.
7. ANOVA analysis show that Contribution of Design is 26.31%, contribution of force is 68.37% and contribution of material is 3.61%.

6. References

[1] Y. H. P. Manurung *et al.*, "Welding distortion analysis of multipass joint combination with different sequences using 3D FEM and experiment," *Int. J. Press. Vessel. Pip.*, vol. 111–112, pp. 89–98, 2013, doi: 10.1016/j.ijpvp.2013.05.002.

[2] M. B. Raut and S. N. Shelke, "Optimization of Special Purpose Rotational MIG Welding by Experimental and Taguchi Technique," *Int. J. Innov. Technol. Explor. Eng.*, no. 6, pp. 2278–3075, 2014.

[3] M. Islam, A. Buijk, M. Rais-Rohani, and K. Motoyama, "Process parameter optimization of lap joint fillet weld based on FEM-RSM-GA integration technique," *Adv. Eng. Softw.*, vol. 79, pp. 127–136, 2015, doi: 10.1016/j.advengsoft.2014.09.007.

[4] S. I. Talabi, O. O. Biodun, E. Infrastructure, and Y. Taiwo, "Effect of welding variables on mechanical properties of low carbon steel welded joint," *Adv. Prod. Eng. Manag.*, no. May 2015, 2014, doi: 10.14743/apem2014.4.186.

[5] G. D'Urso, "Thermo-mechanical characterization of friction stir spot welded AA6060 sheets: Experimental and FEM analysis," *J. Manuf. Process.*, vol. 17, pp. 108–119, 2015, doi: 10.1016/j.jmapro.2014.08.004.

[6] G. Buffa, A. Ducato, and L. Fratini, "FEM based prediction of phase transformations during Friction Stir Welding of Ti6Al4V titanium alloy," *Mater. Sci. Eng. A*, vol. 581, pp. 56–65, 2013, doi: 10.1016/j.msea.2013.06.009.

[7] A. Loureiro, M. Lopez, R. Gutierrez, and J. M. Reinosa, "Experimental evaluation , FEM and condensed sti ff ness matrices of 2D external welded haunched joints," *Eng. Struct.*, vol. 205, no. December 2019, p. 110110, 2020, doi: 10.1016/j.engstruct.2019.110110.

[8] A. Daniel Das, S. N. Vijayan, and N. Subramani, "Investigation on welding strength of fsw samples using taguchi optimization technique," *J. Crit. Rev.*, vol. 7, no. 9, pp. 179–182, 2020, doi: 10.31838/jcr.07.09.36.

[9] M. S. D. B. Singh, "A Review on the Parametric Optimization in MIG Welding using Taguchi Method," *Int. J. Sci. Res.*, vol. 8, no. 3, pp. 1782–1784, 2019.

[10] H. Li, P. O'Hara, and C. A. Duarte, "A two-scale generalized FEM for the evaluation of stress intensity factors at spot welds subjected to thermomechanical loads," *Eng. Fract. Mech.*, vol. 213, no. January, pp. 21–52, 2019, doi: 10.1016/j.engfracmech.2019.03.027.

[11] B. Stalin, K. Vadivel, S. Saravanavel, and M. Ravichandran, "Finite element analysis of lap joint through RSM technique," *Int. J. Adv. Technol. Eng. Explor.*, vol. 5, no. 48, pp. 440–444, 2018.

[12] A. Ahmad and S. Alam, "Grey Based Taguchi Method for Optimization of TIG Process Parameter in Improving Tensile Strength of S30430 Stainless Steel," *IOP Conf. Ser. Mater. Sci. Eng.*, vol. 404, no. 1, 2018, doi: 10.1088/1757-899X/404/1/012003.

[13] M. Lepore, P. Carlone, F. Berto, and M. R. Sonne, "A FEM based methodology to simulate multiple crack propagation in friction stir welds," *Eng. Fract. Mech.*, vol. 184, pp. 154–167, 2017, doi: 10.1016/j.engfracmech.2017.08.024.

Academic Guru Publication House

Technological Advancements : Research & Reviews
Volume 1
Year: 2021

AG PH Books

EVALUATION OF SEISMIC PERFORMANCE OF MULTISTOREY BUILDING WITH FLOATING COLUMN

Prateek Kumar[1*]

[1]*Registered Structural consutant, SEP and Associate, Bhopal (M.P.)*

Abstract

The current study deals with utilization of space such as basements, parking areas/recreational hall under building etc. as well as in terms of elevation of building; for this reason, a study of floating columns is necessary for earthquake safety. Finding the influence of floating columns given at various positions on seismic response and determining the optimum placement for floating columns where the structure can resist with the least likelihood of failure for RCC buildings. The primary goal of this research is to use the response spectrum approach to do seismic analysis on an RC building in order to better use the available space.

Keywords: Multi storey buildings; RCC buildings, Earthquake; Floating column; Response Spectrum Method.

1. INTRODUCTION

An open first floor is becoming an inescapable characteristic of many Indian urban multi-story structures. This is often used for the first floor's parking or reception areas. A building's whole base shear during an earthquake relies on its natural quantity, but the peak seismic force distribution is determined by its stiffness and mass distribution. During earthquakes, a building's general shape, scale, and geometry, as well as how the earthquake forces are transmitted to the ground, are key factors in its behaviour. Any variation or discontinuity in the load transfer route from the peak of a structure to the ground results in poor building performance. Vertical setbacks (such the hotel buildings with many floors

* ISBN No. 978-81-953278-9-8

wider than the rest) produce an abrupt increase in earthquake forces. When a building has fewer columns and walls on one floor or an abnormally tall storey, the damage or collapse is more likely to begin there. During the 2001 Bhuj earthquake in Gujarat, many buildings with an open ground floor designated for parking fell or were seriously damaged. Discontinuities in the weight transmission route may be seen in buildings with columns suspended from beams at an intermediary floor level that are not connected to the foundation. (Prasannan & Mathew, 2017)

1.1. RCC Frame

RCC is used extensively in the construction of high-rise buildings. Stress is first transported from a concrete slab to the beams, then to the lower columns, and finally to the foundation, which in turn distributes the load to the earth. Once the structure's frame is ready, the walls are constructed.(Maitra & Serker, 2018)

The compressive strength of cement concrete is high, but its tensile strength is low. Mild steel bars are often used in cement concrete to increase its strength. Cement concrete structures reinforced with steel bars provide a high degree of strength. Occasionally, steel bars are chafed or corrugated to enhance the concrete-steel connection. There should be no joints in steel bars used in RCC construction. Because of this, it's common for RCC steel to be lengthy in length. There should be a suitable overlap in the steel bar if it isn't given in full length. (Udaygowda & Karthik, 2018)

Steel must be kept out of the way when concrete is being poured. Planks or plates for walking should be supplied for steel rods that are not adequately bonded. A minimum of 20 days is required for the curing of all concrete.

A building's structural components are referred to as the following:

Slab: The flat ceiling of a story is called a ‘Slab’.

Columns: The vertical members supporting the beams are called ‘Columns’.

Beam: There are two types of beams: horizontal and vertical. 'Beams' are the horizontal components that hold the slab in place around the perimeter. It resists winding when it is subjected to a certain amount of stress. It is possible to make beams out of a wide range of materials such as metals and woods. RCC is the most used material for a beam.

Foundation: There are two types of reinforced cement concrete foundations: one is a position, and the other is a pedestal. For an RCC construction, "steel" is utilised as a kind of reinforcement in a variety of foundations. When a building is supported by a foundation, it securely conveys its weight to the ground. (Chaudhari & Talikoti, 2017)

1.2. Advantages

- The inclusion of a floating column aids in boosting the building's floor area index (FSI).
- In order to provide a large, unbroken space for people or vehicles to travel through, avoid placing columns in close proximity to each other on the bottom floor.
- The floor has a greater amount of open space.

- The floating column is used for architectural and site-related purposes.
- In addition, open spaces may be used for an assembly hall or parking.
- Cantilever Deflections may be controlled using floating columns.

1.3. Objectives of Study:

1. To perform a comparative study for floating column using "Square Shape Structure, L-Shaped Structure (Regular Columns Placed in L-Shape), Plus (+) Shaped Structure (Regular Columns Placed in Plus (+) Shape, T Shaped Structure (Regular Columns Placed in T-Shape)".
2. To perform the seismic analysis in ZONE-III and ZONE-IV for comparing the performance of all the structures in both the zones.
3. To evaluate and compare the results for "Max. Support Reaction, Max. Bending Moment, Max. Base Shear, Max. Shear Force, Check for Story drift and Check for soft Story". In addition with calculating the quantity of steel and concrete.

2. LITERATURE REVIEW

(Ashwini, 2017) recognised the unique impacts of a building's seismic load-induced structural irregularity caused by a discontinuity in a column. In this work, a multi-story structure with and without floating columns is subjected to static and dynamic analyses using a response variety system. Floating columns may be built in a variety of ways, including on the floor and within the floor. According to the time period, spectral acceleration, the base shear, storey drift and storey displacements of the building models are studied. STAAD Pro V8i software is used to distribute the results of the analysis.

(S.B et al., 2017) A static study of a multi-story structure with and without floating columns has been completed and is available for download. As the position of the floating columns is varied from floor to floor, a variety of architectural scenarios may be examined. Structural response to base shear and level displacements is studied. The software system sap2000v17 is exploited in the study. It has been shown that the base shear of a building with a floating column at the first floor is lower than that of a structure without a floating column. It was also discovered that the base shear would rise from the first storey. In comparison to non-floating column construction, the displacement of each level of floating column building is much greater.

(K & Rajeeva, 2017) A response spectrum analysis is performed on RC and steel-concrete composite structures with floating columns in the middle of the penultimate bay with and without shear walls, and the RC structure's storey displacement, storey drift, and storey shear are compared.

(Kumar, 2016) An examination of a building's structure is incomplete if it does not take into account the existence of a floating column. The irregularity caused by the floating columns has to be reduced by a variety of methods, including balancing the stiffness of the main level and the storey above it. FEM programmes for 2nd multi-story frames with and without floating columns are created to evaluate the structure's reaction to entirely distinct seismic excitations with varying frequency content while

maintaining the PGA and time duration problem constant. All the frames with and without a floating column are analysed for their floor displacement, interstory drift, base shear, and overturning moment.

(Singla, 2015) studied the result of Floating columns that are adopted in soft story and mass irregular building in Zone5 are disclosed. to realize this objective six G+15stories RC clean frame structures that are having 3mt and 4mt column height regular structure are not taking an account within the style as a result of the buildings aren't often subjected to earthquakes, and additionally it takes base shear and displacement with the base shear and displacement of soppy story and additionally mass irregular structure using ETABS 9.7.4.Lateral displacement will increase with the peak of the building. Displacement is a lot of for the floating column buildings compared with the regular building.

(Banerjee & Patro, 2014) The shakiness of the ground may cause damage to floating column buildings because of the rigidity of the infill wall. The nonlinear analysis software IDARC-second is used for modelling and analysis. Damage indices for beams, columns, and levels are calculated using a modified Park model. Building damage indices due to ground tremor are compiled into one comprehensive report. Results are compared to those of standard moment-resisting frame buildings in terms of dynamic response characteristics including lateral floor displacement, level drift, time period, base shear. Analysis determines the formation of fractures, yield, and plastic hinges.

(Engineering & Behera, 2012) The necessity of specifically noting the existence of the floating column in the examination of a structure was examined. Shock-balancing of the basic structure, as well as the structure above, is proposed to mitigate the irregularity induced by the floating columns The PGA of each earthquake has been scaled to 0.2g, and the excitation period is continuous. The dynamic behaviour of a multi-story frame has been studied using a finite component model. The findings obtained using the current finite component algorithms for static and free vibrations are accurate. The column dimension is a variable in the dynamic analysis of the frame. Inter-structure drift values are decreasing as a result of the ground-floor column's rise in displacement; this has been confirmed. Changes in column size affect the base shear and the overturning moment of the structure.

3. METHODOLOGY

Seismic response is utilised to determine the overall position of the structure where it has the least likelihood of failure, and this research mostly includes standard columns set in square shapes, as well as T-shaped, L-shaped, plus-shaped floating columns. Staad Pro is used to generate all of the final findings. Prerna NautiyalA, 2014

Selection of Study Area: For research and investigation, the response spectrum of floating columns on multistory buildings was investigated.

Literature Review: Previous research in the subject of floating columns was investigated and information was gathered based on that study.

Selection of Seismic Zones and Parameters: for this study seismic zones; ZONE III and ZONE IV has been taken. (Banerjee & Patro, 2014)

4. RESULTS AND DISCUSSION

4.1. General

The results of the analyses of instances with square, L, Plus (+) and T-shape structures are presented in this chapter. For each scenario, the results are presented in terms of bending moment, torsional moment, base shearing, maximum shear force, check for storey drift, volume of concrete utilised, and amount of steel used with regard to zones III and IV, respectively.

4.2. Support Reaction

The table below shows the maximum support reaction for cases square shape, L-shape, Plus (+) shape and T-shape structures in Zone III and Zone IV.

Table 1: Max. Support Reaction

Structure Type	Zone III	ZONE IV
Square Shape Structure	2484 KN	2484KN
L-Shaped Structure (Regular Columns Placed in L-Shape)	5168 KN	5168 KN
Plus (+) Shaped Structure (Regular Columns Placed in Plus (+) Shape)	2609 KN	2609 KN
T Shaped Structure (Regular Columns Placed in T-Shape)	3421 KN	3421 KN

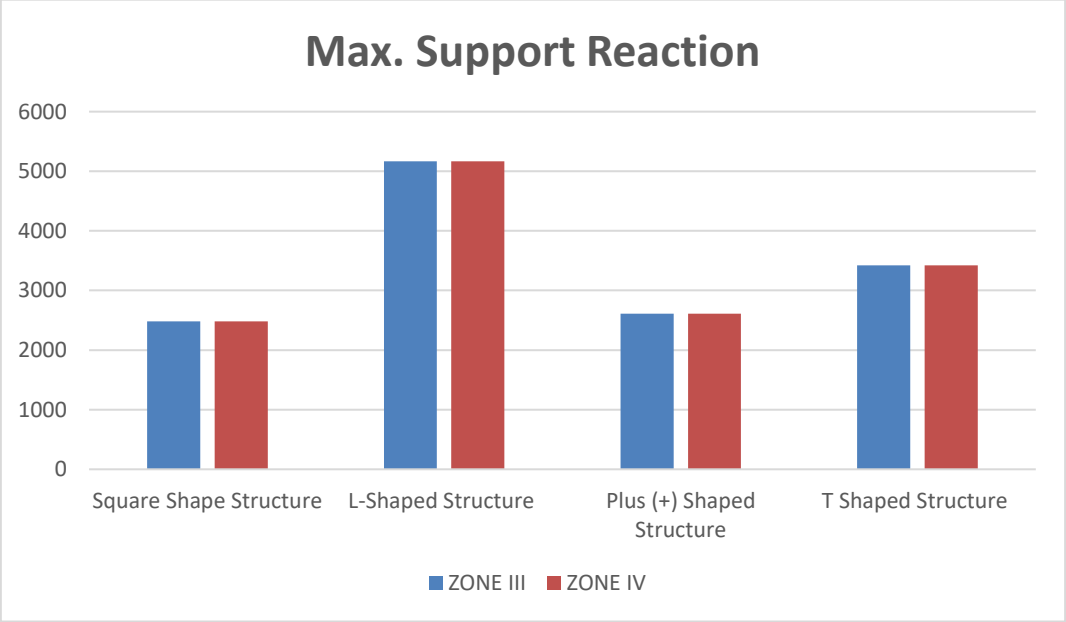

Figure 1: Max. Support Reaction for different structures in Zone III and Zone IV

4.3. Bending Moment

The table below shows the maximum bending moment for cases square shape, L-shape, Plus (+) shape and T-shape structures in Zone III and Zone IV.

Table 2: Max. Bending Moment

Structure Type	Zone III	ZONE IV
Square Shape Structure	238 KN/m	321 KN/m
L-Shaped Structure (Regular Columns Placed in L-Shape)	1288 KN/m	1366 KN/m
Plus (+) Shaped Structure (Regular Columns Placed in Plus (+) Shape)	447 KN/m	499 KN/m
T Shaped Structure (Regular Columns Placed in T-Shape)	702 KN/m	750 KN/m

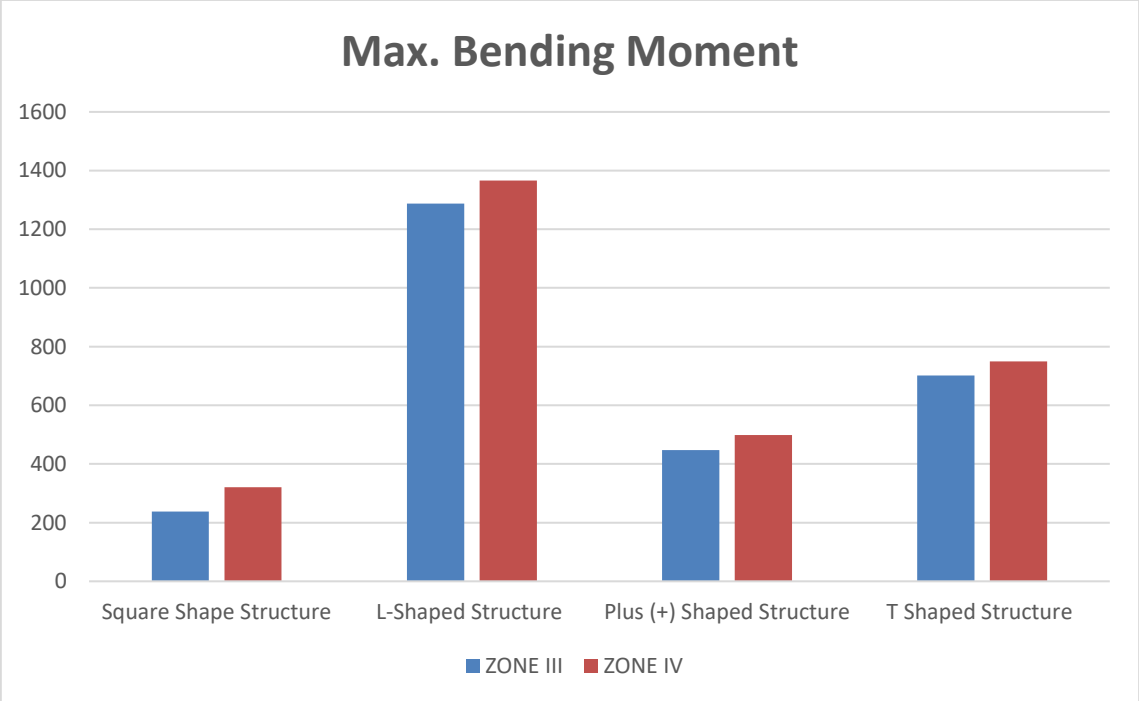

Figure 2: Max. Bending Moment for different structures in Zone III and Zone IV

4.4. Base Shear

The table below shows the maximum base shear for cases square shape, L-shape, Plus (+) shape and T-shape structures in Zone III and Zone IV.

Table 3: Max. Base Shear

Structure Type	Zone III	ZONE IV
Square Shape Structure	238 KN/m	321 KN/m
L-Shaped Structure (Regular Columns Placed in L-Shape)	1288 KN/m	1366 KN/m
Plus (+) Shaped Structure (Regular Columns Placed in Plus (+) Shape)	447 KN/m	499 KN/m
T Shaped Structure (Regular Columns Placed in T-Shape)	702 KN/m	750 KN/m

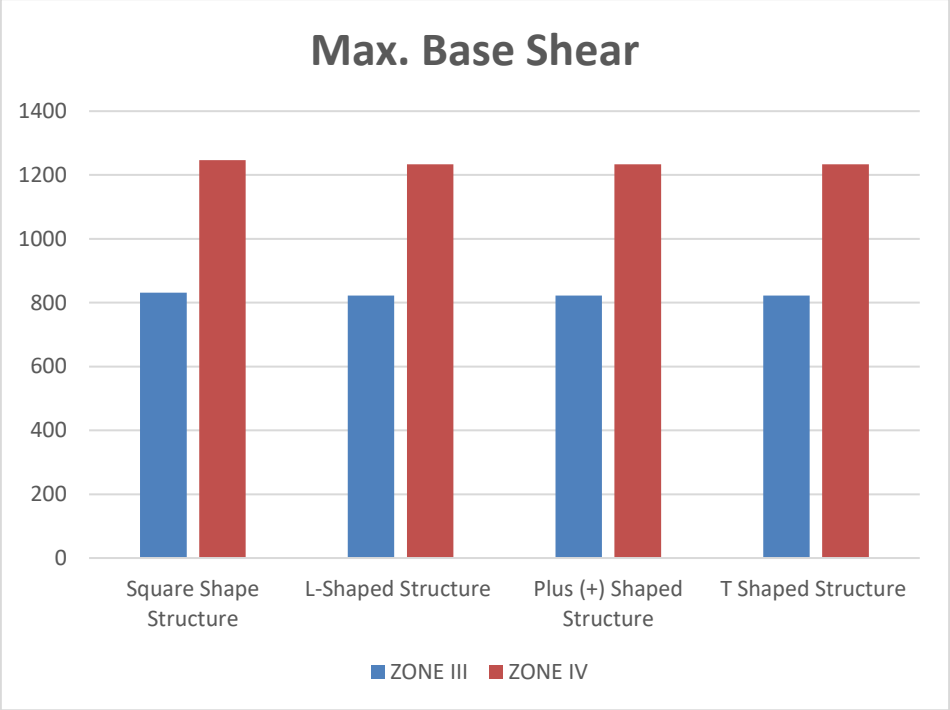

Figure 3: Max. Base Shear for different structures in Zone III and Zone IV

4.5. Shear Force

The table below shows the maximum shear force for cases square shape, L-shape, Plus (+) shape and T-shape structures in Zone III and Zone IV.

Table 4: Max. Shear Force

Structure Type	Zone III	ZONE IV
Square Shape Structure	171 KN	211 KN
L-Shaped Structure (Regular Columns Placed in L-Shape)	644 KN	679 KN
Plus (+) Shaped Structure (Regular Columns Placed in Plus (+) Shape)	268 KN	294 KN
T Shaped Structure (Regular Columns Placed in T-Shape)	394 KN	413 KN

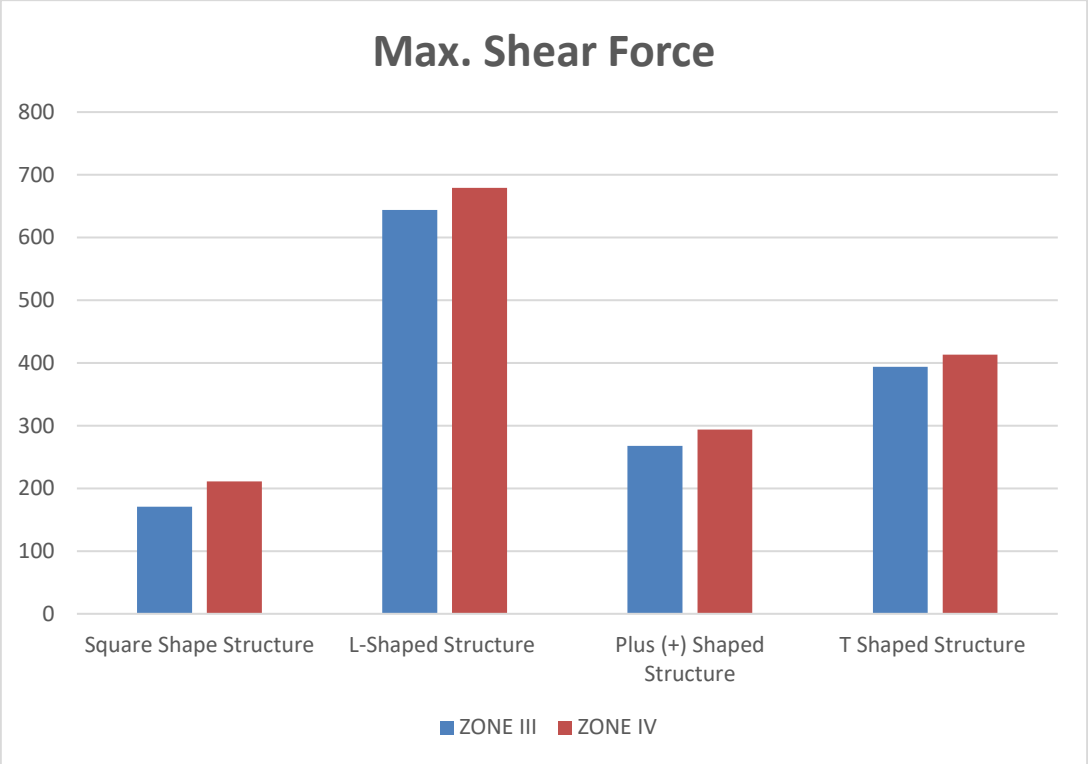

Figure 4: Max. Shear Force for different structures in Zone III and Zone IV

4.6. Volume of Concrete

The table below shows the volume of concrete required in Cum for cases square shape, L-shape, Plus (+) shape and T-shape structures in Zone III and Zone IV.

Table 5: Volume of concrete (Cum)

Structure Type	Zone III	ZONE IV
Square Shape Structure	309.02 Cum	309.02 Cum
L-Shaped Structure (Regular Columns Placed in L-Shape)	296.7 Cum	304.0 Cum
Plus (+) Shaped Structure (Regular Columns Placed in Plus (+) Shape)	304.0 Cum	304.0 Cum
T Shaped Structure (Regular Columns Placed in T-Shape)	304.0 Cum	304.0 Cum

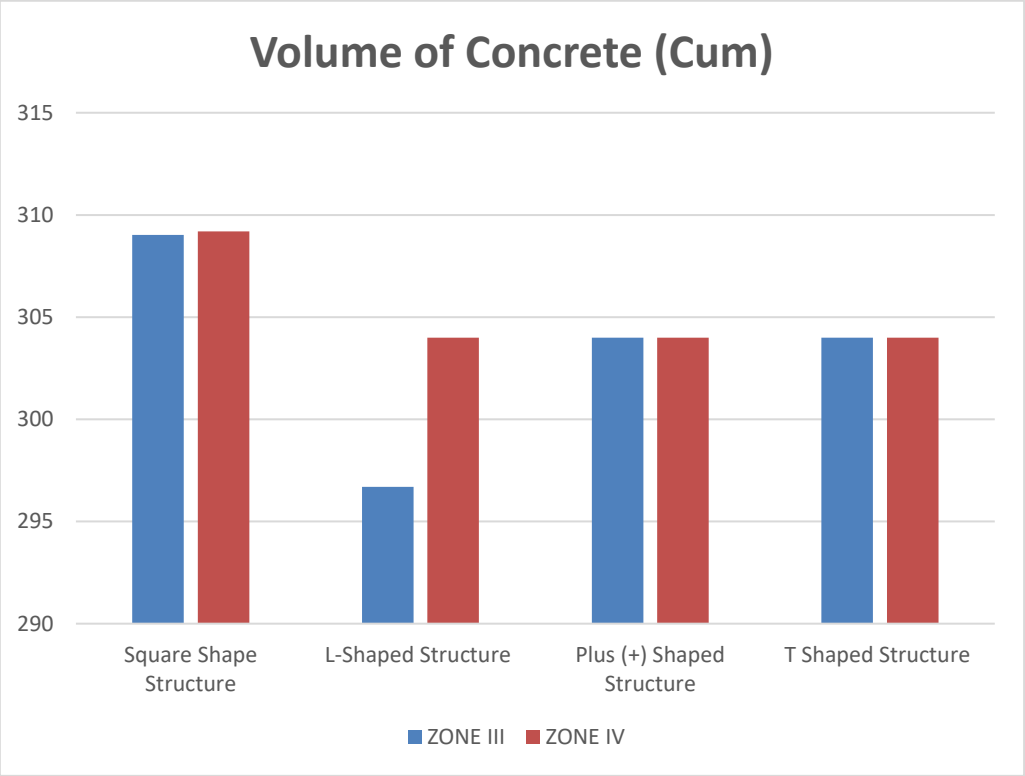

Figure 5: Max. Volume of Concrete for different structures in Zone III and Zone IV

5. CONCLUSION

From the above parameters analyzed in the work; the following set of conclusions are obtained:

1. For the cases discussed base shear is not much affected in Zone III and Zone IV and almost similar values are obtained in **Square Shape structure**, **L-Shaped Structure** (Regular Columns

Placed in L-Shape), **Plus (+) Shaped Structure** (Regular Columns Placed in Plus (+) Shape), **T Shaped Structure** (Regular Columns Placed in T-Shape). In Zone III Max. Support Reaction is obtained for **L-Shaped Structure** (Regular Columns Placed in L-Shape) and Minimum for **Square Shape structure**. In Zone IV Max. Support Reaction is obtained for **L-Shaped Structure** (Regular Columns Placed in L-Shape) and Minimum for **Square Shape structure**. The values of Max. Support Reaction is higher in Asymmetric structures and lower in symmetric structures.

2. The findings of above study discussed values of maximum bending moments in seismic ZONE IV are higher than in seismic ZONE III. Max. Bending stress for Zone III during seismic analysis is obtained for **L-Shaped Structure** (Regular Columns Placed in L-Shape) and Min. for **Square Shape Structure.** Max. Bending stress for Zone IV during seismic analysis is obtained for **L-Shaped Structure** (Regular Columns Placed in L-Shape) and Min. for **Square Shape Structure.** The values of maximum bending moments for the structures without floating columns are lesser than the structures with floating columns.
3. For G+6 Structure Max. Base Shear is obtained in square shape structure. The values of base shear in ZONE IV are approximately 30-40 % higher than in ZONE III. Base shear is not affected by orientation of floating columns weather they are in set in L Shape, Plus Shape or in T Shape.
4. For G+6 Structure Min. Base Shear is obtained in square shape structure. The values of base shear in ZONE IV are comparatively higher than in ZONE III. For G+6 Structure Max. Base Shear is obtained in **L-Shaped Structure** (Regular Columns Placed in L-Shape).
5. All the structures are found to be safe while the check for story drift.
6. All the structures are found with no Soft Story for all the cases and building is stiff in resisting lateral load.
7. The maximum volume of concrete is found in ZONE IV which is little more than ZONE III.
8. The maximum quantity of steel is found in ZONE III which is little more than ZONE IV.

6. References

1. Ashwini, M. (2017). *Comparision Of Buildings With And Without Floating Columns By Using Staad Pro*. *04*(14), 1184–1187.
2. Banerjee, S., & Patro, S. K. (2014). *Estimation of the Park-Ang Damage Index for Floating Column Building with Infill Wall*. *8*(6), 767–770.
3. Chaudhari, A. N., & Talikoti, R. S. (2017). *Study of Seismic Behavior of Building with Different Positions and Types of Floating Column*. *7*(7), 14056–14063.
4. Engineering, S., & Behera, S. (2012). *SEISMIC ANALYSIS OF MULTISTOREY BUILDING WITH FLOATING COLUMN Department of Civil Engineering , National Institute of Technology MAY 2012 " SEISMIC ANALYSIS OF MULTISTOREY BUILDING WITH FLOATING COLUMN " Department of Civil Engineering , National Institut*. *May*.
5. K, V. K., & Rajeeva, S. V. (2017). *SEISMIC BEHAVIOR OF RC AND STEEL-CONCRETE COMPOSITE MULTI-STOREY BUILDING WITH FLOATING COLUMNS WITH AND*

WITHOUT SHEAR WALLS. 104–111.
6. Kumar, G. V. (2016). *SEISMIC ANALYSIS OF MULTISTOREY BUILDING*. *3*(6), 6–10.
7. Maitra, K., & Serker, N. H. M. K. (2018). *Evaluation of Seismic Performance of Floating Column Building*. *6*(2), 55–59. https://doi.org/10.11648/j.ajce.20180602.11
8. Prasannan, P., & Mathew, A. (2017). Seismic Performance of RC Floating Column Considering Different Configurations. *International Journal of Engineering Research & Technology (IJERT)*, *6*(05), 100–108.
9. Prerna NautiyalA*, S. A. and G. B. (2014). *Seismic Response Evaluation of RC frame building with Floating Column considering different Soil Conditions*. *4*(1), 132–138.
10. S.B, M. W. ., Pise, D. C. P., Deshmukh, M. C. M., Pawar, M. . . . ., Kadam, M. S. . ., Mohite, M. . . . ., & Lale, M. S. V. (2017). Comparative Study of floating column of multi storey building by using software. *International Journal of Engineering Research and Applications*, *7*(1), 31–38. https://doi.org/10.9790/9622-0701033138
11. Singla, P. S. (2015). *Effect of Floating Columns on Seismic Response of Multi-Storeyed RC Framed Buildings*. *4*(06), 1131–1136.
12. Udaygowda, M. L., & Karthik, S. (2018). *EFFECT OF FLOATING COLUMN POSITION ON MULTI STORIED RCC STRUCTURE SUBJECTED TO DYNAMIC LOAD*. 162–171. https://doi.org/10.23883/IJRTER.2018.4332.D86TN

Ashwini, M. (2017). *Comparision Of Buildings With And Without Floating Columns By Using Staad Pro*. *04*(14), 1184–1187.

13. Banerjee, S., & Patro, S. K. (2014). *Estimation of the Park-Ang Damage Index for Floating Column Building with Infill Wall*. *8*(6), 767–770.
14. Chaudhari, A. N., & Talikoti, R. S. (2017). *Study of Seismic Behavior of Building with Different Positions and Types of Floating Column*. *7*(7), 14056–14063.
15. Engineering, S., & Behera, S. (2012). *SEISMIC ANALYSIS OF MULTISTOREY BUILDING WITH FLOATING COLUMN Department of Civil Engineering , National Institute of Technology MAY 2012 " SEISMIC ANALYSIS OF MULTISTOREY BUILDING WITH FLOATING COLUMN " Department of Civil Engineering , National Institut*. *May*.
16. K, V. K., & Rajeeva, S. V. (2017). *SEISMIC BEHAVIOR OF RC AND STEEL-CONCRETE COMPOSITE MULTI-STOREY BUILDING WITH FLOATING COLUMNS WITH AND WITHOUT SHEAR WALLS*. 104–111.
17. Kumar, G. V. (2016). *SEISMIC ANALYSIS OF MULTISTOREY BUILDING*. *3*(6), 6–10.
18. Maitra, K., & Serker, N. H. M. K. (2018). *Evaluation of Seismic Performance of Floating Column Building*. *6*(2), 55–59. https://doi.org/10.11648/j.ajce.20180602.11
19. Prasannan, P., & Mathew, A. (2017). Seismic Performance of RC Floating Column Considering Different Configurations. *International Journal of Engineering Research & Technology (IJERT)*, *6*(05), 100–108.
20. Prerna NautiyalA*, S. A. and G. B. (2014). *Seismic Response Evaluation of RC frame building with Floating Column considering different Soil Conditions*. *4*(1), 132–138.
21. S.B, M. W. ., Pise, D. C. P., Deshmukh, M. C. M., Pawar, M. . . . ., Kadam, M. S. . ., Mohite, M. . . . ., & Lale, M. S. V. (2017). Comparative Study of floating column of multi storey building

by using software. *International Journal of Engineering Research and Applications*, *7*(1), 31–38. https://doi.org/10.9790/9622-0701033138

22. Singla, P. S. (2015). *Effect of Floating Columns on Seismic Response of Multi-Storeyed RC Framed Buildings*. *4*(06), 1131–1136.
23. Udaygowda, M. L., & Karthik, S. (2018). *EFFECT OF FLOATING COLUMN POSITION ON MULTI STORIED RCC STRUCTURE SUBJECTED TO DYNAMIC LOAD*. 162–171. https://doi.org/10.23883/IJRTER.2018.4332.D86TN

Academic Guru Publication House

Technological Advancements : Research & Reviews
Volume 1
Year: 2021

AG PH Books

REUSE OF DEMOLITION AND CONSTRUCTION WASTE FOR THE MANUFACTURING OF PAVER BLOCKS

Gourav Raghuwanshi[1*]

[1] *Research Scholar, Department of Civil Engineering, MANIT, Bhopal*

Abstract

With the rising demand for developed areas and the paucity of land, redevelopment projects are becoming more common. The treatment of "construction and demolition (C&D)" waste in India is a matter of concern in the construction industry. C&D garbage accounts for around a third of all municipal solid trash generated in India. Construction, real estate, and the destruction of unlawful structures, among other things, are major sources of trash generation. The importance of C&D waste management in India is highlighted by this. Reuse, recycling, and demolition are used in building and waste management in countries such as the United Kingdom, the United States, France, Denmark, Germany, as well as Japan. 70 percent of the construction sector is unaware of recycling procedures, according to a research commissioned by the "Technology Information, Forecasting, and Assessment Council (TIFAC)".

Keywords: Construction, demolition, concrete, waste management, municipal solid waste..

1. INTRODUCTION

Landfills that take C&D garbage are limited in size. Most of them have already closed or are about to shut down. Nowadays, the majority of C&D waste produced in Connecticut is dumped of in out-of-state landfills, with just around 7% reported as recycled. These data solely reflect waste that travels via Connecticut's permitted solid waste operations and is reported to the "Department of Environmental

* ISBN No. 978-81-953278-9-8

Protection (DEEP)". The reported recycled rate of 7 percent includes most clean fill created as well as recovered and recycled, scrap metal recycled from construction projects, materials immediately transferred from a work site to an out-of-state recycling end market, as well as commodities consumed once more on site.

1.1. Disposal of Construction and Demolition Waste

The generation of waste on a building site is often impossible to avoid. In fact, in 2016, 61 percent of waste produced in the UK would be from the construction, destruction, and excavation industries.

On the other hand, proper management is important for every company if it produces waste. And it should be also observed that the company is following the waste management hierarchy or not, as this hierarchy helps in reduction, reuse and recycling of waste before its disposal. For UK, it is essential for reduction in environmental impacts.

Disposing the C&D wastes is a concern for environment since basically it is great source for wastage and pollution. It is better to recycle the C&D wastes.

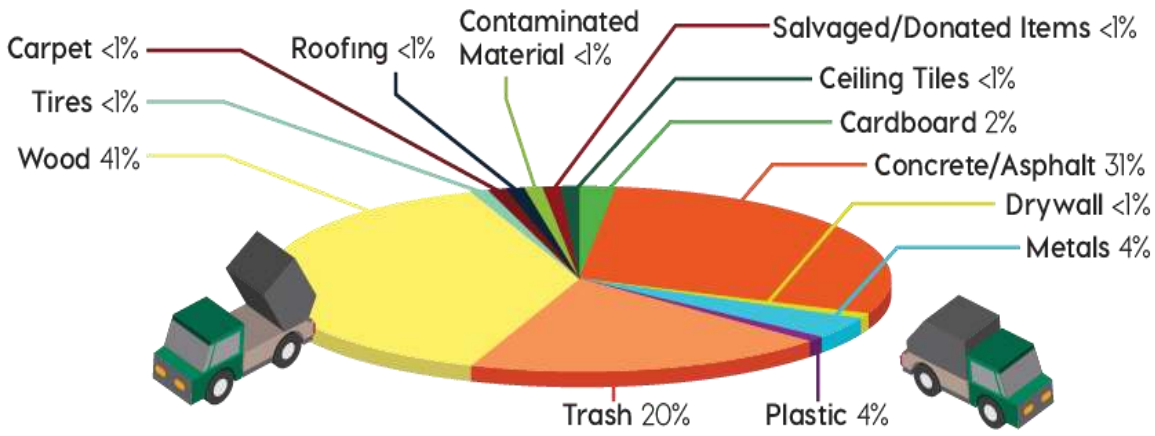

Figure 1: Disposal of waste

1.2. Paver Block

Concrete paver blocks were introduced in the Netherlands in the 1950s as an alternative to paver bricks. Blocks have gone from non-interlocking to partially interlocking to fully interlocking to various interlocking forms in the previous 50 years.. A thin, compressed bedding material is placed over small element, solid unreinforced precast concrete paver blocks that is erected on an appropriately shaped foundation coarse within an interlocking concrete block pavement. Some of the advantages of concrete paving blocks are: versatility, attractiveness, functional as well as cost effective. These blocks require little or no maintenance at all if correctly manufactured and placed. In India, for construction field

"Interlocking concrete paving block technology" has been introduced. In construction this technology is used in parking areas and footpaths.

Figure 2: Different designs of paver blocks

1.3. Benefits of Using C&D Wastes for Making Paver Blocks

The main benefits of using C&D waste for manufacturing paver blocks are:

- To reduce the cost
- To avoid the purchase of new materials
- To avoid going to dumpsite
- To reduce waste going to landfill

Many economic and environmental advantages may be gained by recycling and reusing building materials. Builders and constructors may save money if the materials can be reused. Disposal costs are less expensive than recycling costs. Many environmental advantages may be gained by reducing the amount of garbage that is sent to landfills.

2. LITERATURE REVIEW

(Kedar et al., 2020) Every year, approximately tones of plastic waste are generated in India. Plastic garbage also takes a long time to degrade. The goal of this study is to employ plastic waste in conjunction with fine aggregates to minimise the cost of paver blocks as compared to traditional concrete blocks, as well as to provide better interlocking than other paver blocks. Hence this work is helpful in reducing plastic waste which leads to protect environment from pollution. We used plastic waste in different proportion with the HDPE granules, coarse aggregates, cement, water and fine aggregates. The paver blocks were prepared and tested with reference of IS code. Result of this work indicate that prepared paver block can be used for area varying from non-traffic to light traffic road.

(Maheswari et al., 2020) Due to vast population increase, the use of plastic are in day by day is more. Several researches worked on carrying waste plastic application in construction industry. Every year, roughly lakhs of tonnes of trash plastic are produced in India. The goal of this research is to substitute

cement in paver blocks with waste plastic, lowering the cost of paver blocks in comparison to traditional concrete paver blocks. In this project, researchers mixed waste plastic with sand in various amounts. The paver bocks were made and tested, and the findings were thoroughly reviewed.

(Pabon et al., 2020) Recycled materials are increasingly being used in the construction of new buildings all around the globe. Recycled plastic pavers were compared to hydraulic concrete pavers in terms of economic and financial resilience and effectiveness while adhering to current rules. The study's technical and economic findings were both good.

(Kumar et al., 2020) It is imperative to develop a substitute for NA since natural aggregates are in short supply. Natural coarse aggregates of 10mm have been replaced by coarse recycled concrete aggregates produced from construction and demolition wastes in the production of I-shaped recycled paver blocks. The RPBs were tested for visual inspection, dimension tolerance, strength attributes, water absorption, and impact testing.. CRCA may be substituted for up to 60% of natural aggregates in PBs, and lab-made RPBs beat factory-made RPBs in terms of their performance.

(Sudha et al., 2020) Reduction in the price of paver blocks is the main objective of this study for which cement is also replaced with the ceramic waste after comparing with the conventional concrete paver block. Nowadays, the use of ceramic is increasing in construction works in the form of sanitary fittings, electrical insulations and in the form of tiles. But there are some limitations such as large quantity of ceramic waste material is converted into wastage during the time of transportation, manufacturing and fixation due to its brittle nature. Ordinary Portland cement is used in the present study which is replaced by crushed ceramic tiles. With conventional blocks, the ceramic blocks were compared, casted and tested by analyzing their compressive and flexural strength via experimental investigations. Hardness properties of paver block were investigated through the tests. This experiment demonstrates that waste from the tile industry can be used in paver blocks as a partial replacement for cement.

(Thorat et al., 2019) study regard the properties of the paver block which is manufactured using waste plastic and crushed sand. Waste plastic used to replace cement in the production of pavement block. conventional M20 grade concrete paver block and paver block made of waste plastic and crushed sand of proportion waste plastic to crushed sand: 100:00, 90:10, 80:20,70:30 and 60:40 and tested for weight, water absorption, rebound hammer and compressive strength test. Paver block of proportion 100% plastic and 0% sand gives maximum compressive strength of 23 N/mm2 which is more than conventional M20 grade concrete paver block.

(Nadu & Waste, 2019) From various researches, it was observed that there is a considerable imbalance between the accessibility of building material as well as their demand. However, demolition waste is present in huge amount and also plastic waste is increasing which is affecting the environment. Instead of utilising cement, an attempt was made in this effort to manufacture paver blocks utilising discarded low density polyethylene bags as well as waste material. For sustainability, the obtained plastic paver bocks are used which possess thermal as well as sound insulation properties so that pollution can be controlled. This method is considered to be the best one for avoiding the accumulation of plastic wastes as well as demolition waste in society. Such plastic wastes are naturally available in the environment in surplus quantity so that the cost factor can be reduced.

(Pattnaik et al., 2018) For several years, the problems related with construction sites are known. It is important for the construction industries to support the economic development as well as population growth of the world. In footpaths, gardens and parking areas, interlocking concrete paving bocks are the ideal material used for better look and finish. Hot bituminous mix is used for the conventional construction of pavement as cement concrete technology is not a desirable method. There is a demand of alternating construction techniques due to rising costs of construction materials. For the enhancement in usage of concrete paving blocks, it is important to understand the products manufactured with local materials and indigenously produced mineral admixtures. By using fly ash, aggregates, waste glass powder, concrete paving blocks can be produced in the present study. For variable mix proportions, cement is substituted with fly ash & waste glass powder. According to the findings, fly ash and waste glass powder can be utilised as a cement substitute because their strength is not affected.

(Velumani & Senthilkumar, 2018) In order for industrial wastes to be reused, waste management has a substantial impact. Paper industry wastewater treatment generates sludge. Sludge is formed when hypo sludge and textile effluent treatment plants are combined. It's also difficult to get rid of the muck. There is a need for an environmentally friendly method of producing paver bricks. There are several uses for paver bricks, including pedestrian walkways and municipal roadways. Textile effluent treatment plant sludge and hypo sludge were used to make paver blocks in a first-of-its-kind experiment in this research. Polypropylene fibre and silica fume have been explored in paver blocks.

(Priya & Janani, 2018) Waste materials are a major environmental problem, which is harm to the environment. It is important to reuse the waste materials coming out from construction site. Wastes are like masonry, blocks, tiles, etc. are more. In order to avoid that, the wastes can be crushed and added additional raw materials and it can be converted to paver block (interlocking stones) and can be used in same construction site itself. After recycling, wastes are reused in the construction for making paver blocks. In this paper, a detailed study has been done that paver blocks can be made from construction wastes, and comparison has been done by its quality.

3. METHODOLOGY

The materials and methods which were used in the present study are presented in this chapter for answering the required research questions with the objective of understanding the extent to which the recycling of C&D waste can give their contribution in the manufacturing of paver blocks as these blocks are used in various applications. The following chapter provides a detail study about the materials and methodology used in this research.

The experimental work consists of –

1. Individual material properties
2. Making of a composite material
3. Properties of newly formed composite
    a) Tensile Test

b) Compressive Strength
c) Water absorption Test
d) Breaking load and Flexural test

4. RESULTS AND DISCUSSION

4.1. Results for Compressive strength

Compressive strength, or compression strength, is the ability of any material or the structure of a material to endure stresses such that its size may be decreased. This is employed to counteract tensile strength, which resists elongating stresses. While tensile strength resists tension, compressive strength opposes being squeezed together.

Table 1: Compressive Strength of Paver Block (N/mm^2) AT 7, 14 & 28 DAYS

Days	Compressive Strength (N/mm^2)
7 DAYS	28.56
14 DAYS	30.21
28 DAYS	32.79

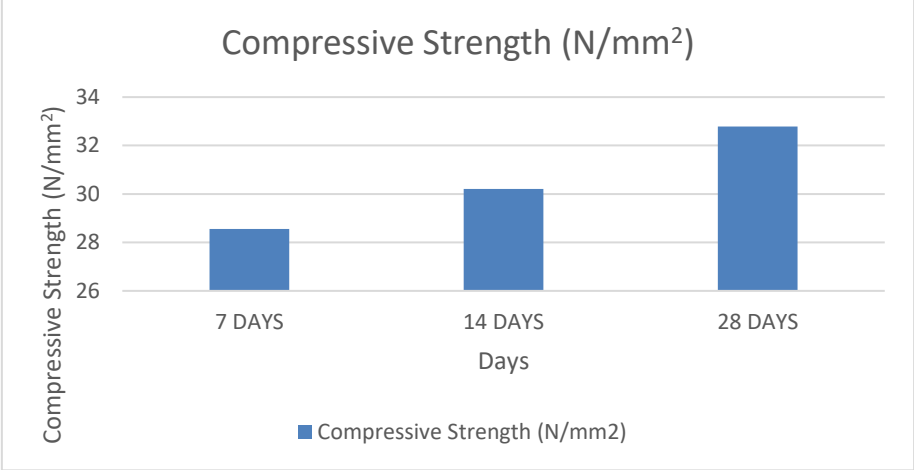

Figure 3: Compressive strength test result graph

The "compressive strength of the paver block" at 7 days was recorded as 28.56 m/mm^2 which increased to 30.21 m/mm^2 and at the final stage i.e. on 28th day, the "compressive strength of the paver block" was 32.79 m/mm^2 which was highest.

4.2. Results for Water Absorption

For determining the amount of water absorbed in particular conditions, water absorption methodology is used. Water absorption is affected by various factors such as: category of plastic, types of additives used, temperature as well as length of the exposure. The light is shed by the data on the performance of material under water or humid environment.

The typical interlocking paving stone does not show permeability, meaning it will not drain water. Flexibility is the benefit of Regular pavers, but not permeability.

Table 2: Water absorption test results

S. No.	Mix Design of Paver Blocks	Water Absorption (%)
1	Trial 1	1.178
2	Trial 2	1.104
3	Trial 3	1.082
4	Trial 4	1.156
5	Trial 5	1.212

A comparison graph between different values of 5 different trials is shown in figure below.

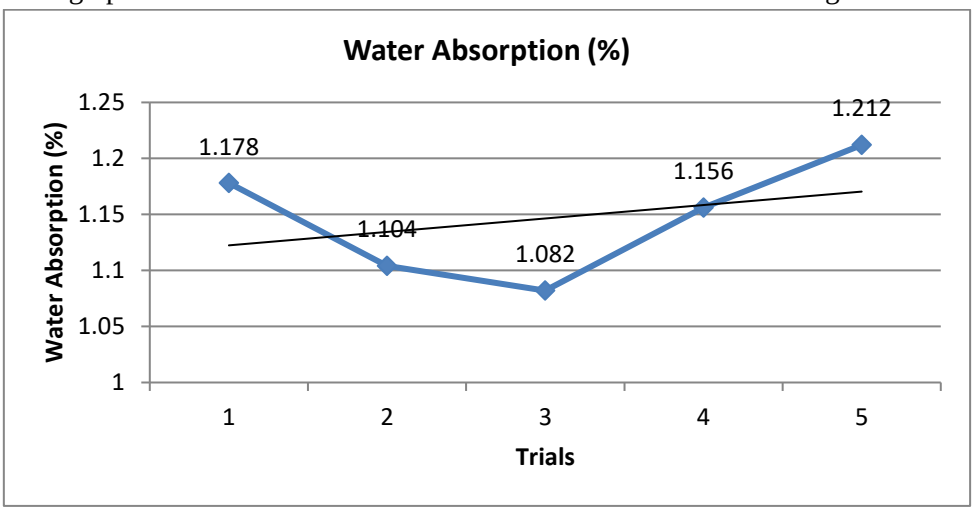

Figure 4: Comparison of Water Absorption values from test.

4.3. Results for tensile splitting strength

For concretes, tensile strength is considered as pone of the most basic and important properties. The designing of concrete structural elements requires knowledge. Pre-stresses concrete structures also need its value. For determining the flexural strength, recourse is also important. Additionally, computation of direct tensile as well as splitting of tensile strength is significant for recourse.

Table 3: Tensile Strength of Paver Block (N/mm2) AT 7, 14 & 28 DAYS

Days	Tensile Strength (N/mm^2)
7 DAYS	1.5
14 DAYS	1.9
28 DAYS	2.21

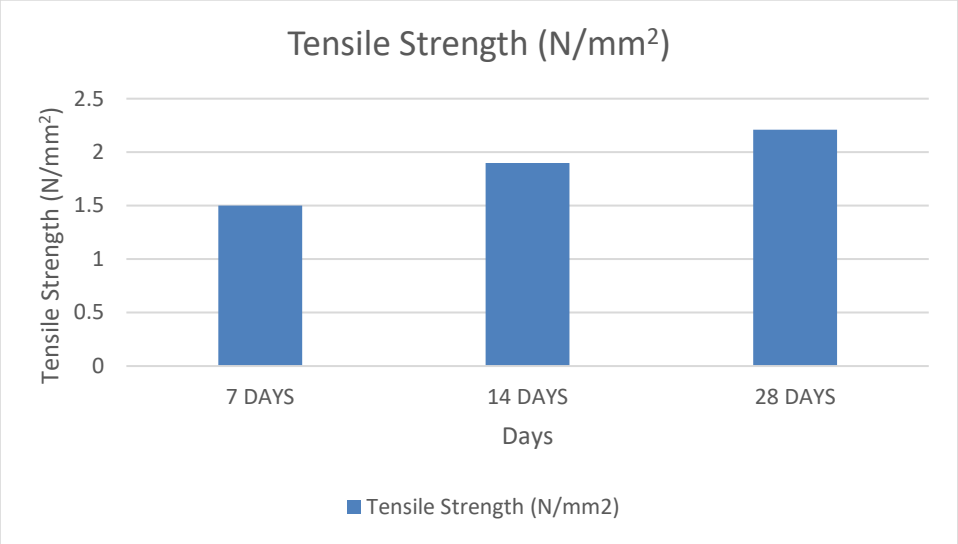

Figure5: Tensile strength test result graph

For tensile splitting test, the tensile strength of paver blocks gives maximum value of strength is 2.12Mpa on the 28th day. However, it was 1.5 MPa on the 7th day and 1.9 MPa on the 14th day.

4.4. Breaking Load and Flexural Strength

As a result, the study's main goal was to see if there were any other test methods that may potentially replace field-cast beam specimens while evaluating the same or similar strength qualities as the flexure test. Because of the inherent issues connected with casting and handling the very large beam specimens required by the test protocol, concrete flexural strength is difficult to evaluate reliably in the field.

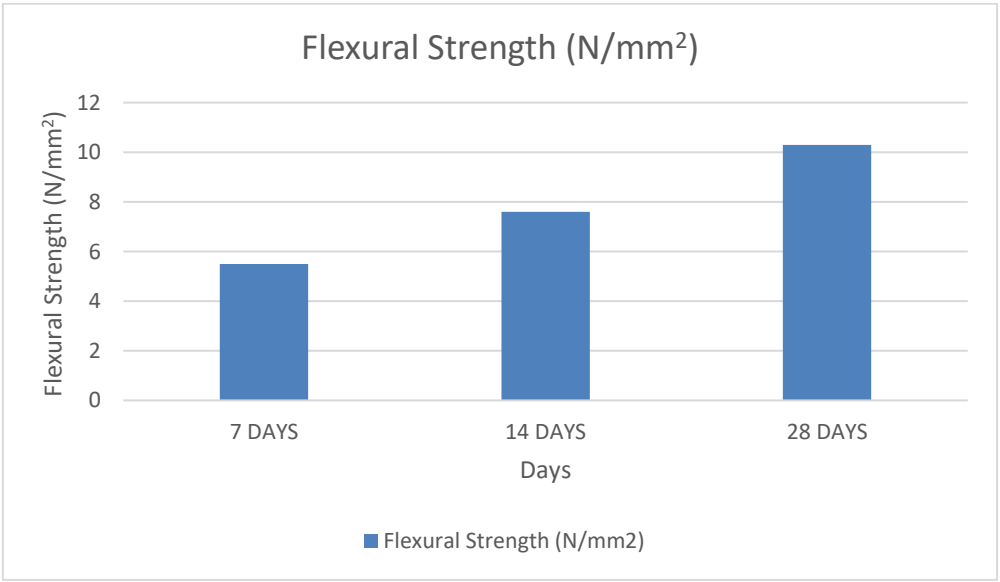

Figure 6: Flexural strength test result graph

Table 5: Flexural Strength of Paver Block (N/mm2) AT 7, 14 & 28 DAYS

Days	Flexural Strength (N/mm^2)
7 DAYS	5.5
14 DAYS	7.6
28 DAYS	10.3

5. CONCLUSION

Despite the existence of a legislative framework, there's been little implementation in the sector of C & D waste management in urban India. All stakeholders have a key role to play in this context for sustainable development, as mentioned in the investigation. On the basis of current construction practices, future challenges are massive with the excessive demand for infrastructure and residential, as well as the resulting growth in the construction industry. For framing and envelop, high rise buildings and in-situ construction are coming up which will be further reconstructed after 40 50 years. There is a big challenge in managing C&D waste, on the basis of situation of scale of these projects and materials in future.

Additionally, manufacturing of concrete paver blocks is cost effective. Through this methodology, the demolition waste is utilized and limits the improper disposal of C&D wastes. This method is more sustainable.

References

1. Kedar, A. A., Birajdar, R. R., Kumbhar, P. J., & Mahajan, N. J. (2020). *UTILIZATION OF PLASTIC WASTE FOR MANUFACTURING OF PAVER BLOCK*. *8*(5), 1006–1012.
2. Kumar, G., Shrivastava, S., & Gupta, R. C. (2020). Paver blocks manufactured from construction & demolition waste. *Materials Today: Proceedings*, *27*, 311–317. https://doi.org/10.1016/j.matpr.2019.11.039
3. Maheswari, A. U., Srinuswamy, L., Mohan, K., Murthy, D., & Rao, V. V. (2020). *Experimental Study on Using Plastic Waste in Manufacturing of Paver Blocks*. *2386*(08), 76–80.
4. Nadu, T., & Waste, D. (2019). Reuse of Waste Plastics and Demolition Waste in the Development of Plastic Paver Block. *Journal of Scientific & Industrial Research*, *78*(4), 248–250.
5. Pabon, C., Saieth, B., Baquero, O., Barrera, M., Carlos, W., García, O., Miguel, A., Godoy, L., & Jaime, O. (2020). Technical and economic comparison between recycled plastic and hydraulic concrete pavers Comparación técnica y económica entre adoquines fabricados con plástico reciclado y con. *Revista Espacios*, *41*(June).

6. Pattnaik, T., Mohanta, N. R., Patel, N., Biswal, P., & Moharana, R. K. (2018). *MANUFACTURE OF INTERLOCKING CONCRETE PAVING BLOCKS WITH FLY ASH AND GLASS POWDER*. *7*(1), 604–612.
7. Priya, R. B., & Janani, R. (2018). *JASC : Journal of Applied Science and Computations ISSN NO : 1076-5131 A STUDY ON PAVER BLOCKS FROM CONSTRUCTION WASTES Page No : 1187*. *V*(1186), 1186–1190.
8. Sudha, N., Sivaranjani, T., Swetha, M., Vaishnavi, S., & Vasuki, P. (2020). *Paver block production from ceramic waste*. *8*(4), 2619–2622.
9. Thorat, P. P. R., Ms, R. D. G., Ms, P. A. S., & Ms, K. M. G. (2019). *An Experimental Investigation of Waste Plastic and Crushed Sand in Paver Block*. *7*(01), 570–573.
10. Velumani, P., & Senthilkumar, S. (2018). Production of sludge-incorporated paver blocks for efficient waste management. *Journal of the Air and Waste Management Association*, *68*(6), 626–636. https://doi.org/10.1080/10962247.2017.1395373

Research And Development In Engineering Technology

(Volume-1)

Dr. Rakesh Kumar Yadav pursed Bachelor of Technology from Uttar Pradesh Technical University, UP, and Master of Technology from Singhaniya University, Rajasthan and Ph.D. from IFTM University, UP. He has worked in many reputed institutes. He is currently working as an Assistant Professor in Department of Computer Science & Engineering, IFTM University, UP. He has published more than 25+ research papers in reputed international journals and conferences. He has been reviewed many research papers of journals and conferences. He has published many Patents. He has guided various M.Tech and PhD students. He has written many books and examination series also. He has also taken many guest lectures. His main research work focuses on Machine Learning, Biometric, Image Processing, Computer Vision, Soft Computing and Artificial Intelligence. He has 14+ years of teaching experience in higher education.

Dr. Shyam Sundar Pawar is currently designated as an Associate professor at Sarvepalli Radhakrishnan University Bhopal (M.P.). With an ambition of enhancing the technical world, he completed his BE from Govt. Engineering college, Ujjain (M.P.) Affiliated from Vikram University, Ujjain (M.P.) and M.Tech from MANIT, Bhopal followed by Ph.D. at RGPV, Bhopal (M.P.). Embedded with his academic skills, Dr. Pawar has reviewed numerous paper and has also made various published researches of his own in several national and international journals. He is also recognized for his amazing teaching skills. He has also supervised various Ph.D. Scholars during his academic Career. There are hundreds of students who were guided by him and completed their M.Tech successfully. He has been guest lecturer at various important events.

Dr. Amit Kumar Mishra earned his PhD from Banasthali Vidyapeeth in Tonk, Rajasthan, and was awarded best paper in COVID-19 by MPCOST Bhopal (Govt Of MP). iNurture Education Solutions Private Limited, Bengaluru, Karnataka, currently employs me as a Senior Faculty, IT Academics. He has attended several international conferences and international workshops worldwide. Several book chapters were published by Taylor & Francis, CRC Press, and John Wiley & Sons, Inc. He has published more than 25 research papers in reputed journals indexed by Scopus and the Web of Science and more than 60 papers at international conferences. Several students have done M.Tech under his guidance. Invited lectures were given at national and international events. He has published one international and three national papers in the fields of machine learning and IOT.

Dr. Rakesh Kumar Bhujade completed Ph.D. in Artificial Intelligence in 2016, cracked UPSC and currently working as Head of the Information Technology Department in Government Polytechnic, Daman. He has published 01 Philippines Patent, 02 Australian Government Patents (Grants), 05 Indian Patents, 03 Books, 02 AWS Global Certifications, 01 Research Grant and more than 30 papers in Scopus Indexed International Journal/Conferences. He also acted as Advisory/Reviewer Board member in many International Journals and Conferences. Dr. Rakesh is expertise in Neural Network, Soft Computing, Artificial Intelligence and Machine Learning.

Price : 1100 INR

AGPH **Books**

9 788195 327898